Aus dem Zentrum für Biomaterialentwicklung, Institut für Polymerforschung,
Helmholtz-Zentrum Geesthacht

Design of Biopolymer-based Networks with Defined Molecular Architecture

Dissertation

**zur Erlangung des akademischen Grades
"doctor rerum naturalium"
(Dr. rer. nat.)
in der Wissenschaftsdisziplin
"Materialen in den Lebenswissenschaften"**

**eingereicht an der
Mathematisch-Naturwissenschaftlichen Fakultät
der Universität Potsdam**

von

Susanna Piluso

aus Terranova da Sibari, Italien

Potsdam, 2011

Published online at the
Institutional Repository of the University of Potsdam:
URL http://opus.kobv.de/ubp/volltexte/2012/5986/
URN urn:nbn:de:kobv:517-opus-59865
http://nbn-resolving.de/urn:nbn:de:kobv:517-opus-59865

Gutachter: Prof. A. Lendlein, Universität Potsdam
Prof. S. Beuermann, Universität Potsdam
Prof. D. Cohn, The Hebrew University of Jerusalem

Tag der Annahme der Dissertation: 15.11.11
Tag der Disputation: 22.05.12

''The important thing in science is not so much to obtain new facts as to discuss new ways of thinking about them.''

Sir William Bragg

Statement of Originality

I, Susanna Piluso, formally submit the dissertation entlited “Design of Biopolymer-based Networks with Defined Molecular Architecture” to the Department of Mathematics and Natural Sciences University of Potsdam, Germany, for the acquirement of the academic degree of Doctor of natural sciences (Dr. rer. nat.) in Materials for life science.

I hereby certify that this submission is entirely my own original work and that, to the best of my knowledge and belief, it contains no material previously published or written by another person, except where due reference is made in the thesis itself. Neither the dissertation, nor any sections thereof, has been previously submitted for a degree or other qualification to any other University or Institution. Any contribution made to the research by other, with whom I worked at HZG or elsewhere, is explicity acknowledged in the thesis.

Susanna Piluso
Potsdam, 15.11.11

Contents

Abstract

In this work, the synthesis of biopolymer-based hydrogel networks with defined architecture is presented. In order to obtain materials with defined properties, the chemoselective copper-catalyzed azide-alkyne cycloaddition (or Click Chemistry) was used for the synthesis of gelatin-based hydrogels. Alkyne-functionalized gelatin was reacted with four different diazide crosslinkers above its sol-gel transition to suppress the formation of triple helices. By variation of the crosslinking density and the crosslinker flexibility, the swelling (*Q:* 150-470 vol.-%;) and the Young's and shear moduli (*E*: 50 kPa - 635 kPa, G': 0.1 kPa - 16 kPa) could be tuned in the kPa range. In order to understand the network structure, a method based on the labelling of free functional groups within the hydrogel was developed. Gelatin-based hydrogels were incubated with alkyne-functionalized fluorescein to detect the free azide groups, resulting from the formation of dangling chains. Gelatin hydrogels were also incubated with azido-functionalized fluorescein to check the presence of alkyne groups available for the attachment of bioactive molecules. By using confocal laser scanning microscopy and fluorescence spectroscopy, the amount of crosslinking, grafting and free alkyne groups could be determined. Dangling chains were observed in samples prepared by using an excess of crosslinker and also when using equimolar amounts of alkyne:azide. In the latter case the amount of dangling chains was affected by the crosslinker structure. Specifically, 0.1% of dangling chains were found using 4,4'-diazido-2,2'-stilbene-disulfonic acid as cosslinker, 0.06% with 1,8-diazidooctane, 0.05% with 1,12-diazidododecane and 0.022 % with PEG-diazide.

This observation could be explained considering the structure of the crosslinkers. During network formation, the movements of the gelatin chains are restricted due to the formation of covalent netpoints. A further crosslinking will be possible only in the case of crosslinker that are flexible and long enough to reach another chain.

The method used to obtain defined gelatin-based hydrogels enabled also the synthesis of hyaluronic acid-based hydrogels with tailorable properties. Alkyne-functionalized hyaluronic acid was crosslinked with three different linkers having two terminal azide functionalities. By variation of the crosslinking density and crosslinker type, hydrogels with elastic moduli in the range of 0.5-3 kPa have been prepared.

The variation of the crosslinking density and crosslinker type had furthermore an influence also on the hydrolytic and enzymatic degradation of gelatin-based hydrogels. Hydrogels with a low crosslinker amount experienced a faster decrease in mass loss and elastic modulus compared to hydrogels with higher crosslinker content. Moreover, the structure of the crosslinker had a strong influence on the enzymatic degradation. Hydrogels containing a crosslinker with a rigid structure were much more resistant to enzymatic degradation than hydrogels containing a flexible crosslinker. During hydrolytic degradation, the hydrogel became softer while maintaining the same outer dimensions. These observations are in agreement with a bulk degradation mechanism, while the decrease in size of the hydrogels during enzymatic degradation suggested a surface erosion mechanism.

Because of the use of small amount of crosslinker (0.002 mol.%→ 0.02 mol.%) the networks synthesized can still be defined as biopolymer-based hydrogels. However, they contain a small percentage of synthetic residues. Alternatively, a possible method to obtain biopolymer-based telechelics, which could be used as crosslinkers, was investigated. Gelatin-based fragments with defined molecular weight were obtained by controlled degradation of gelatin with hydroxylamine, due to its specific

action on asparaginyl-glycine bonds. The reaction of gelatin with hydroxylamine resulted in fragments with molecular weights of 15, 25, 37, and 50 kDa (determined by SDS-PAGE) independently of the reaction time and conditions. Each of these fragments could be potentially used for the synthesis of hydrogels in which all components are biopolymer-based materials.

Zusammenfassung

In dieser Arbeit wird die Synthese Biopolymer-basierter Hydrogelnetzwerke mit definierter Architektur beschrieben. Um Materialien mit definierten und einstellbaren Eigenschaften zu erhalten, wurde die chemoselektive Kupferkatalysierte Azid-Alkin-Cycloadditionsreaktion (auch als Click-Chemie bezeichnet) für die Synthese Gelatine-basierter Netzwerke eingesetzt. Alkin-funktionalisierte Gelatine wurde mit vier verschiedenen Diazid-Quervernetzern oberhalb der Gel-Sol-Übergangstemperatur umgesetzt, um die Formierung tripelhelikaler Bereiche durch Gelatineketten zu unterdrücken. Durch Variation der Menge an Quervernetzer (und damit der Netzdichte) sowie der Länge und Flexibilität der Quervernetzer konnten u.a. die Quellung (*Q:* 150-470 vol.-%) sowie der Young's - und Schermodul im kPa Bereich eingestellt werden (*E*: 50 kPa - 635 kPa, G': 0.1 kPa - 16 kPa).

Um die Netzwerkarchitektur zu verstehen, wurde eine Methode basierend auf dem Labeln unreagierter Azid- und Alkingruppen im Hydrogel entwickelt. Die Gelatine-basierten Hydrogele wurden mit Alkin-funktionalisiertem Fluorescein umgesetzt, um freie Azidgruppen zu detektieren, die bei einem Grafting entstehen. Darüber hinaus wurden die Hydrogele mit Azid-funktionalisiertem Fluorescein reagiert, um die Menge an freien Alkingruppen zu bestimmen, die zudem potentiell für die Anbindung bioaktiver Moleküle geeignet sind. Quervernetzung, Grafting, und die Anzahl freier Alkingruppen konnten dann mit Hilfe der konfokalen Laser Scanning Mikroskopie und der Fluoreszenzmikroskopie qualitativ und quantitativ nachgewiesen werden. Gegraftete Ketten wurden in Systemen nachgewiesen, die mit einem Überschuss an

Quervernetzer hergestellt wurden, entstanden aber auch beim Einsatz äquimolarer Mengen Alkin- und Azidgruppen. Im letzteren Fall wurde in Abhängigkeit von der Struktur des Diazids unterschiedliche Anteile gegrafteter Ketten festgestellt. 0.1 mol-% von gegrafteten Ketten wurden für 4,4'-Diazido-2,2'-stilbendisulfonsäure gefunden, 0.06 mol-% für 1,8-Diazidooktan, 0.05 mol% für 1,12-diazidododecan und 0.022 mol-% für PEG-Diazid. Diese Beobachtung kann durch die unterschiedliche Flexibilität der Vernetzer erklärt werden. Während der Netzwerkbildung werden die Bewegungen der Gelatineketten eingeschränkt, so dass kovalente Netzpunkte nur erhalten werden können, wenn der Vernetzer lang und flexibel genug ist, um eine andere Alkingruppe zu erreichen.

Die Strategie zur Synthese von Biopolymer-basierten Hydrogelen mit einstellbaren Eigenschaften wurde von Gelatine- auf Hyaluronsäure-basierte Gele übertragen. Alkin-funktionalisierte Hyaluronäure wurde mit drei verschiedenen Diaziden quervernetzt, wobei Menge, Länge, und Flexibilität des Quervernetzers variiert wurden. In dieser Weise wurden sehr weiche Hydrogele mit E-Moduli im Bereich von 0.5-3 kPa hergestellt.

Die Variation der Vernetzungsdichte und des Vernetzertyps beeinflusste weiterhin den hydrolytischen und enzymatischen Abbau der Hydrogele. Hydrogele mit einem geringerem Anteil an Quervernetzer wurden schneller abgebaut als solche mit einem höheren Quervernetzeranteil. Darüber hinaus konnte gezeigt werden, dass Hydrogele mit Quervernetzern mit einer rigiden Struktur deutlich langsamer degradierten als Hydrogele mit flexibleren Quervernetzern. Während des hydrolytischen Abbau wurden die Materialien weicher, behielten aber ihre Form bei, was mit einem Bulk-Abbau-Modell übereinstimmt. Während des enzymatischen Abbaus hingegen änderten sich die Materialeigenschaften kaum, jedoch wurden die Proben kleiner. Diese Beobachtung stimmt mit einem

Oberflächenabbaumechanismus überein.

Da in allen vorgestellten Systemen nur eine kleine Menge synthetischer Vernetzer eingesetzt wurde (0.002 – 0.02 mol%), können die Materialien noch als Biopolymer-basierte Materialien klassifiziert werden. Jedoch enthalten die Materialien synthetische Abschnitte. In Zukunft könnte es interessant sein, einen Zugang zu Materialien zu haben, die ausschließlich aus Biopolymeren aufgebaut sind. Daher wurde der Zugang zu Biopolymer basierten Telechelen untersucht, die potentiell als Vernetzer dienen können. Dazu wurden durch die kontrollierte Spaltung von Gelatine mit Hydroxylamin Gelatinefragmente mit definiertem Molekulargewicht hergestellt. Hydroxalamin reagiert unter Spaltung mit der Amidbindung zwischen Asparagin und Glycin, wobei Aspartylhydroxamate und Aminoendgruppen entstehen. Die Reaktion von Gelatine mit Hydroxylamin ergab Fragmente mit Molekulargewichten von 15, 25, 37, und 50 kDa (bestimmt mit SDS-PAGE), und die Formierung dieser Fragmente war unabhängig von den weiteren Reaktionsbedingungen und der Reaktionszeit. Jedes dieser Fragmente kann potentiell für die Synthese von Hydrogelen eingesetzt werden, die ausschließlich aus Biopolymeren bestehen.

List of abbreviations

Asn	Asparagyn
BCNU	Bis-chloroethylnitrosourea
$CaCl_2$	Calcium chloride
CHC	Clostridium hystolyticum collagenase
CLSM	Confocal Laser Scanning Microscopy
$CuSO_4 \cdot 5H_2O$	Copper sulphate pentahydrate
°C	Degree Celsius
DIC	N,N'-Diisopropylcarbodiimide
DMF	N,N-Dimethylformamide
DMSO	Dimethylsulfoxide
DMTA	Dynamic Mechanical Thermal Analysis
DSC	Dynamic scanning Calorimetry
E	Young's Modulus
ECM	Extracellular matrix
EDC	1-Ethyl-3-(3-dimethylaminopropyl)carbodiimide
EDTA	Ethylenediaminetetracetic acid
ε_b	Elongation at break
EtOH	Ethanol
FDA	Food and Drug Administration
FT-IR	Fourier Transform Infrared Spectroscopy
G'	Shear modulus
G''	Viscous modulus
Gly	Glycine
GPC	Gel Permeation Chromatography
H	Water uptake
HA	Hyaluronic acid
Lys	Lysine
Mn	Number Average Molecular Weight
NaN_3	Sodium Azide
NH_2OH	Hydroxylamine
PBS	Phosphate Buffer Solution
PCL	Poly(ε-caprolactone)
PCPP-SA	Poly[1,3-bis(p-carboxyphenoxy)propane-sebacic acid]
PDS	Polydioxanone
PEG	Poly(ethylene glycol)
P3HB	Poly(3-R-hydroxybutyrate)
PVA	Poly(vinyl alcohol)
Q	Degree of swelling
SDS-PAGE	Sodium dodecyl sulphate-poly acrylamide gel electrophoresis
σ_{max}	Maximum tensile strength
T_g	Glass transition temperature
TMDSC	Temperature modulated DSC
TNBS	Trinitrobenzenesulfonic acid
WAXS	Wide Angle X-ray Scattering

List of figures

1. Introduction

The versatility of polymers is based on the fact, that their properties (e.g. mechanical properties, thermal transitions) as well as their functions (e.g. rate of degradation) can be adjusted to the demand of a specific application. First, the monomer composition (type, ratio) and molecular weight have been exploited in the synthesis of tailored polymers, while later when having achieved better control in the synthesis, sequence structure and molecular architecture have been shown to be useful in this respect. In this context the concept of polymer systems is important, which can be defined as families of related polymers in which slight changes in the molecular compositions lead to systematic variations of macroscopic material properties.[1]

1.1 Degradable polymers

One special interesting function of polymers is the degradability. Degradable polymers can be defined as materials containing chemical bonds which can be cleaved e.g. by hydrolytic, enzymatic or redox mechanisms, leading to the formation of small oligomeric fragments.[2] The cleavage of bonds can be in the main or side chains, depending on the monomers and architecture of the polymers.[3] The

degradability of polymers is interesting in terms of reduction of waste in the environments, but is especially important for biomedical applications because it avoids the necessity of a second surgery for removal of an implant.

The most widely investigated polymers for biomedical applications are the polyesters poly(lactic acid), poly(glycolic acid), polydioxanone, poly(ε-caprolactone) and their copolymers, as well as polyanhydrides (Figure 1.1). Polyglycolide, due to its fiber forming ability, was used for developing the first biodegradable synthetic suture, called DEXON approved by the US FDA in 1969.[4]

Polylactides have been used for developing orthopaedic products, including BioScrew, Meniscal Stinge. Copolymers of glycolic acid and lactic acid have been developed as alternative sutures, called Vicryl. Polycaprolactone was investigated as a long term drug or vaccine delivery vehicle. Polydioxanone (PDO) has been investigated for several orthopaedic applications as fixation screws for small bone and osteochondral fragments.

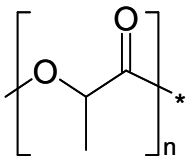

Poly(lactic acid)

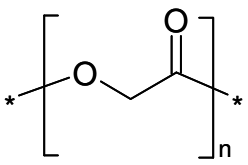

Poly(glycolic acid)

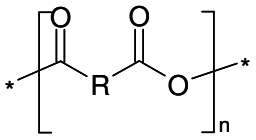

Polyanhydrides

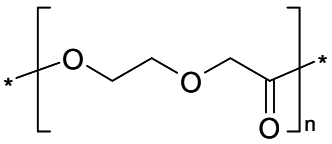

Polydioxanone

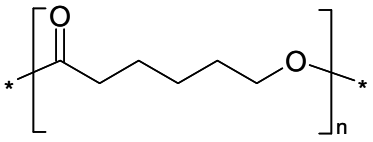

Poly(ε-caprolactone)

Figure 1.1 Chemical structures of the widely investigated degradable polymers.

Polyanhydrides can be considered as the most extensively investigated surface eroding polymers developed for drug delivery applications. The most investigated

anhydride is poly(carboxy phenoxy propane-(sebacic acid) (PCPP-SA). This polymer has been approved by the US FDA as drug delivery system for the controlled release of the chemotherapeutic agent BCNU (bis-chloroethylnitrosourea), used in the treatment of brain cancer.[5] Since degradation plays an important role in the use of polymers for biomedical application, possible degradation mechanisms need to be throroughly investigated.

From a mechanistic point of view polymers can undergo bulk and surface degradation. In bulk degradation the diffusion of water into the polymer is faster than the degradation of polymer bonds and the erosion will occur throughout the entire sample. In surface eroding polymers the degradation of polymer bonds is faster than the rate of water penetration. The implant will decrease in size, but maintain its mechanical integrity during the degradation process (Figure 1.2).[6] In general three types of degradation pathways giving soluble products have been described (Figure 1.3).

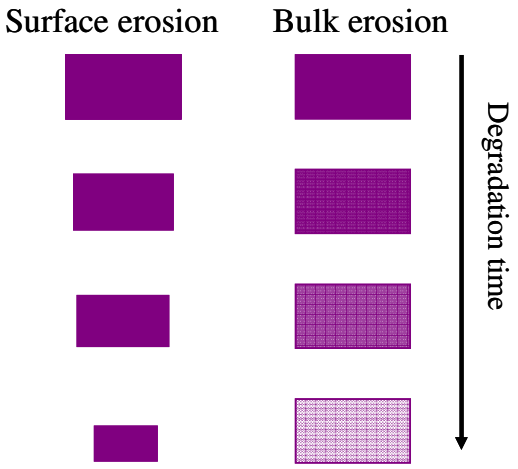

Figure 1.2 Schematic illustration of surface erosion and bulk erosion.[2]

The first pathway is observed in polymer networks with water soluble main-chains, whereby the cleavage of degradable crosslinks between the polymer chains leads to slow material dissolution. The second pathway refers to water insoluble polymers in

which the cleavage of hydrophobic side chains results in solubilization of the polymer. In the third pathway, the polymer main chain itself is degraded into water soluble monomers. Often, combination of two or more of the described mechanism occurs simultaneously during polymer degradation.[7] There are several factors that can influence the degradation process such as the chemical stability of the hydrolytically cleavable bonds in the polymer backbone, the hydrophylicity or hydrophobicity, the morphology of the polymer, the molecular weight and water diffusivity in the polymer matrix.[8] One of the most important factors is the susceptibility of the polymer backbone toward hydrolysis. For example, anhydrides can be hydrolyzed faster than ester bonds, which will hydrolyze faster than amide bonds. However, the degradation rate is also strongly dependent on the ability of water to penetrate into the polymeric matrix. Therefore the hydrophylicity/hydrophobicity will have a strong impact on the degradation rate.

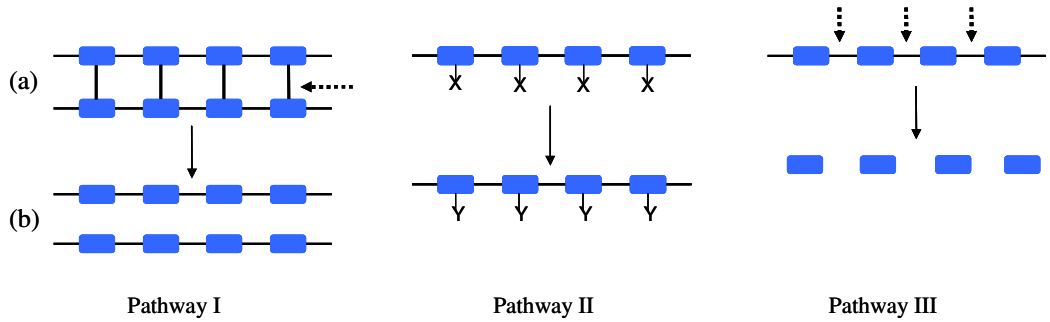

Figure 1.3 Pathways of chemical degradation. Pathway I involves the cleavage of crosslinks between the polymer chains, which will subsequently dissolve. In Pathway II hydrophobic chains are cleaved or transformed in polar groups, enabling the solubilization of the polymer. Pathway III involves the cleavage of bonds in the polymer backbone, leading to the formation of small soluble fragments.[7]

The degradation rate of linear polymers, such as poly(α-hydroxyacids) may be controlled by polymer composition, molecular weight and crystallinity. However, for linear polymers a heterogeneous degradation profile has been reported.[3] A better control of the degradation rate can be achieved by the synthesis of polymer networks. Here the degradation time can be varied by changing the monomer backbone chemistry, while the control of the final mechanical properties can be

obtained by changes in the network structure (e. g. crosslinking density) as shown in the case of polyanhydride[9] or polyurethane networks.[3]

1.1.1 Degradation of natural polymers

Besides synthetic polymers, naturally-derived polymers have been extensively investigated for biomedical applications and can be considered as the first biodegradable materials used clinically.[10] Many natural such as proteins and polysaccharides polymers can additionally to hydrolysis be easily degraded by naturally occurring enzymes, with a degradation rate depending on the implantation site and on the enzyme concentrations. Enzymes, in fact, contain molecular chain structures and develop conformation that allows “recognition” of chain sequences on biopolymers. Lacking biopolymer sequences recognition, most synthetic polymers are more resistant to enzymatic degradation. However, comparative studies have shown some increase of hydrolysis rates by enzymes, particularly with synthetic polyesters and polyamides.[7]

1.2 Polymer networks

For certain applications, e. g. in the biomedical field, several properties have to be adjusted simultaneously, e. g. mechanical strength, elasticity, and degradation rate. It has been shown that here polymer networks can be easily tailored to the demand of a specific application, by variation of crosslinking density or by altering the comonomer composition.[11,12]

Covalent polymer networks can be formed by reaction of polymers with several reactive groups and bifunctional crosslinkers (e. g. diepoxide, diisocianate). However, most of the synthetic routes used so far do not enable a thorough control of material properties. One main reason is related to the occurrence of side reactions during synthesis, ultimately resulting in the formation of dangling chains.[13] Mechanical properties of polymer networks are indeed directly related to both the chemical composition and the molecular structure of the system. Therefore a thorough investigation of the network architecture is highly needed, although extremely challenging to accomplish.

The most common parameters used to characterize the network structure include: (1) the molecular weight of the polymer chains between two neighboring crosslinks (M_c), (2) the mesh size (ξ) and (3) the effective network density (ν_e).[14] These parameters can be determined by using the equilibrium-swelling and the rubber-elasticity theories. However, both theories are based on ideal networks in which no defects, e.g. dangling chains or elastically inactive loops, are presents.[15] Other possibilities are restricted to the study of model reactions via low molecular weight compounds, followed by the characterization of resulting model products[16] or indirect investigation by FT-IR or NMR. However, a clear picture of the network architecture cannot be obtained, mainly because reacted groups are formed not only as a result of crosslinks, but also as a result of chain loop formation, which makes the all investigation highly challenging.

1.3 Hydrogels

Some of the biologically and medically highly relevant materials are polymer networks. A special class of polymers is represented by hydrogels, three-dimensional

networks formed from hydrophilic homopolymers, copolymers or macromers crosslinked (either physically or chemically) to form insoluble polymer matrices. Hydrogels are typically soft and elastic due to their thermodynamic compatibility with water and depending on their composition can be classified into synthetic, hybrid or biological hydrogels.[17,18] Commonly synthetic hydrogels are based on synthetic polymers, large molecule constisting of small repeating units (monomers) bonded together, e.g. poly(hydroxyethyl methacrylate) (PHEMA), poly(ethylene glycol) (PEG) or poly(vinyl alcohol) (PVA). In order to combine the properties of synthetic polymers (e. g. mechanical stability) with the biological activity of natural molecules, hybrid hydrogels have been developed. Hybrid hydrogels are usually referred to as hydrogel systems that possess components from at least two distinct classes of molecules, e. g. synthetic polymers and natural macromolecules, interconnected either covalently or non-covalently.[13,14] For instance, amino acid sequences have been incorporated into PEG hydrogels so that the degradation behavior of the final material was altered.[19,20] In contrast to hybrid hydrogels, biological hydrogels are composed of biopolymers or biopolymer-based materials only, offering the advantage of being biocompatible, biodegradable, by either enzymatic or hydrolytic mechanism, and be recognized by the biological enviroment.[21,7] Biopolymers are a class of polymers derived from animal or plant sources (e. g. collagen, hyaluronic acid), whereas macromolecules derived from biopolymers are referred to as biopolymer-based materials (e. g. gelatin). Most of the natural polymers used as biomaterials are constituents of the extracellular matrix (ECM), which is a complex three-dimensional structure that allows cell to grow, proliferate and differentiate within it (Figure 1.4). This gel-like matrix is composed mainly of water and two classes of macromolecules: 1) polysaccharides chains of the class of glycosaminoglycans, such as hyaluronic acid, chondroitin sulfate, dermatan sulfate, heparin sulfate and keratin sulfate and 2)

fibrous proteins like collagen, elastin, fibronectin and laminin, which have both structural and adhesive functions. The collagen fibers both strengthen and provide unique structural organization, the rubberlike elastin fibers give it resilience and various matrix proteins help cells attach in the appropriate locations. Gycosaminoglycans are negatively charged and can take up large amounts of water. This results in a swelling pressure, or turgor, which enables the ECM to withstand compressive forces.[22] Besides those, another important feature of the ECM is the susceptibility to cell-triggered proteolysis, which enables cell invasion and subsequent remodelling of the matrix, leading to regeneration.[23] Of the various ECM components of ECM-derived materials, gelatin and hyaluronic acid are the most frequently used as biomaterials. Both natural polymers will be presented in details in the section 1.4 and 1.5.

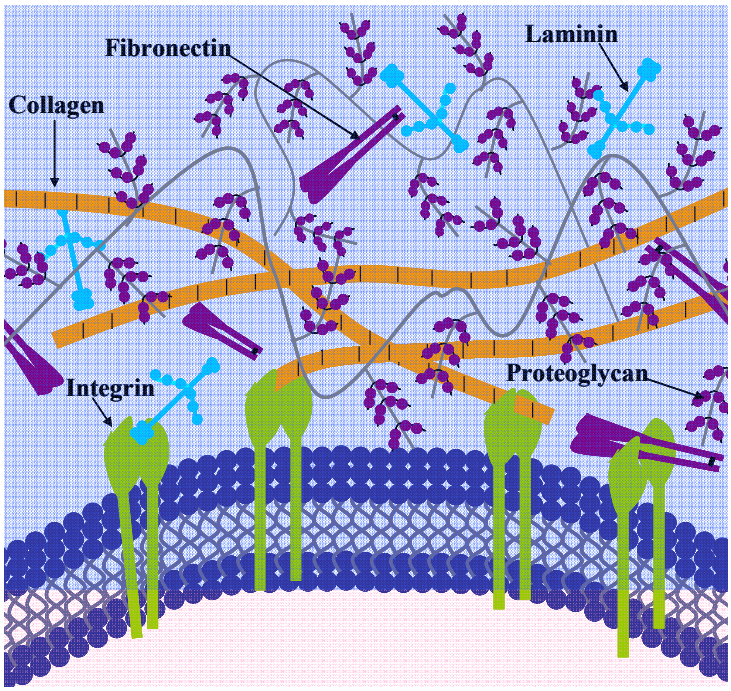

Figure 1.4 Scheme of the Extracellular matrix.

1.4 Gelatin-based hydrogels

Gelatin is a protein-based material obtained by hydrolytic degradation of naturally occurring collagens. Collagen is the major structural protein of most connective tissues, such as skin, bone and tendons, where it provides structural integrity to the tissues. The collagen chain consists of repetitive Gly-X-Y tripeptide units with proline and hydroxyproline most frequently found in the X and Y positions, respectively. Hydroxyproline is derived from proline by hydroxylation mediated by prolylhydroxylase.[24] The Gly-X-Y sequence allows for the formation of a highly regular triple helix, which consists of three molecular strands (α chains) that, due to the high proline content, are arranged into a left-handed helix. These three left-handed helix coils around each other to form a right-handed superhelix, stabilized by interchain hydrogen bonds.[25] Additional stability derives from intra- and intermolecular crosslinks, by the formation of aldol condensation- and aldimine type crosslinks, respectively.[26] Collagen can be converted into soluble gelatin by two processes (Figure 1.5): 1) acid pretreatment leading to type A gelatin, which have the same isoeletric point of collagen; 2) alkaline or basic pretreatment leading to type B gelatin, which has a greater proportion of carboxyl groups due to the conversion of many of the asparagine and glutamine residues into aspartate and glutamate residues and a lower isoeletric point compared to type A gelatine.[27] The conversion of collagen to gelatin involves the initial loss of the hydrogen bond and hydrophobic bonds, which helps to stabilize the helix, followed by the random breaking of covalent bonds between the chains, explaining the molecular heterogeneity of gelatin.[28] The use of gelatin, instead of collagen, may be advantageous for different reasons. First of all, the functionalization of collagen can be challenging due to the difficulties in solubilizing collagen under mild conditions and the resulting materials can be affected

by poor mechanical properties. Moreover, the potential potential antigenicity of collagen[29,30,31] can be minimized in gelatin as a result of heat denaturation and breakdown of the triple helix structure.[32,33]

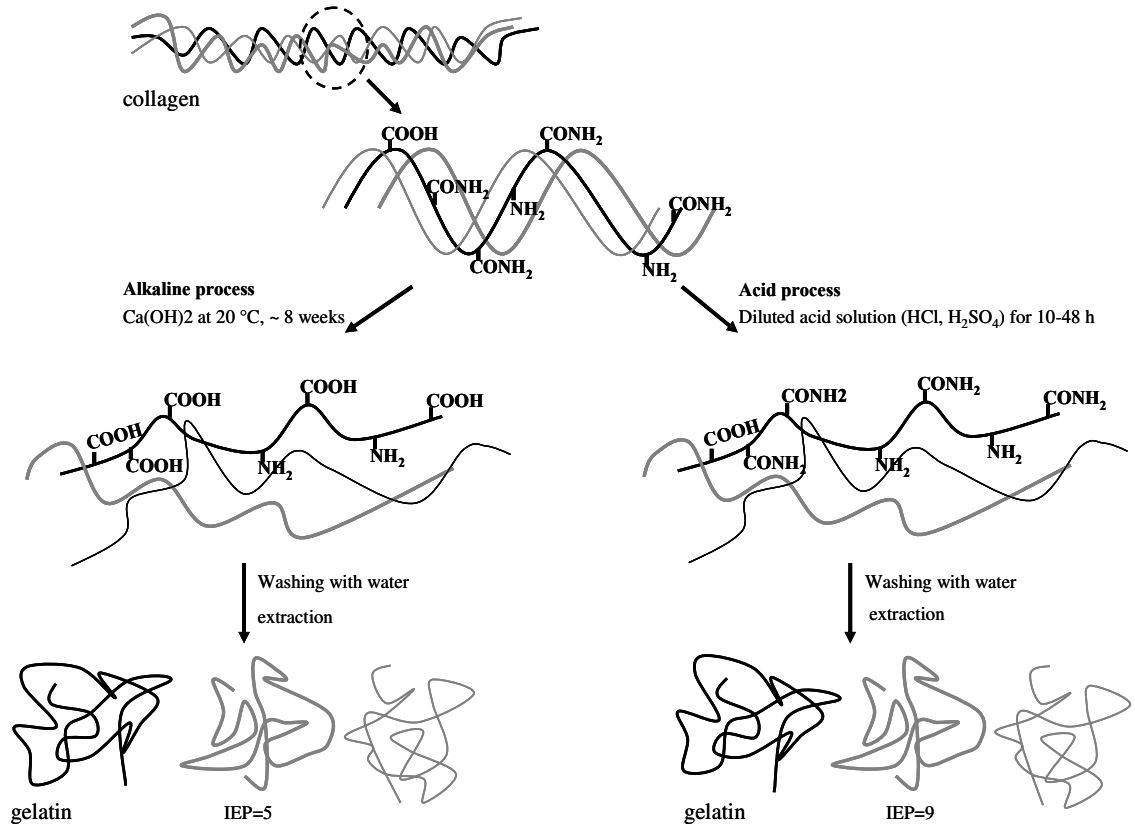

Figure 1.5 Conversion of collagen to gelatin by alkaline and acid process.[34]

Indeed, some epitopes responsible for collagen antigenicity are conformation dependent, so that they are active only when the molecule is in its native folded conformation.[35] Additionally, gelatin is soluble, biodegradable and has FDA approval as clotting agent.[36]

Gelatin has been widely used in food, pharmaceuticals, photographic industry and in many biomedical applications including hard and soft capsules, microspheres, sealant for vascular prostheses, wound dressing and adsorbent pad for surgical use, as well as three-dimensional tissue regeneration.[37,38] The extensive use of gelatin in different fields is directly related to its coil to helix transition. Gelatin, as denaturated collagen, dissolves in water above its melting temperature and exists in a flexible

random coil. By lowering the temperature below 35 °C gelatin forms physical thermoreversible gels as the chains undergo a conformational coil to helix transition during which they tend to recover the collagen triple helix structure.[39] The coil to helix transition has been investigated by X-Ray diffraction,[40] light scattering,[41] transmission electron microscopy,[42] DSC[43] and optical rotation measurement methods.[44] Since gelatin is an ECM-derived material, possible batch to batch variation may affect material reproducibility and needs to be carefully considered. Moreover, gelatin is only soluble in water and DMSO, limiting the range of synthetic procedures suitable for the formation of gelatin-based materials.

1.5 Hyaluronic acid hydrogels

Hyaluronic acid is a linear high molecular weight polysaccharide composed of alternating units of D-glucuronic acid and D-*N*-acetylglucosamine, linked together via alternating ß-1,4 and ß-1,3 glycosidic bonds (Figure 1.6).[45] HA is the only nonsulphated glycosaminoglycan and is found throughout the body, from the vitreous of the eye to the extracellular matrix of cartilage tissues. It is the most abundant gycosaminoglycan of the ECM, in which its structural and biological properties mediate its activity in cellular signaling, wound repair, morphogenesis and matrix organization.[46] Commercially available HA is obtained from different sources, mainly by extraction from umbilical cord, rooster comb, synovial fluid, vitreous humour or from certain strains of streptococcus bacteria.[47] In aqueous solution, HA is stiffened by inter-residue hydrogen bonds. As a consequence HA tends to adopt a highly extended conformation occupying a large hydrodynamic volume and forms gels even at low concentrations. The rheological properties of HA have been extensively studied. The viscoelastic properties have been examined as a function of

temperature, concentration and pH.[48] Hyaluronic acid behaved as a viscoelastic polymer with a crossover frequency of the elastic and viscous modulus dependent on the pH. At pH 2.5, HA showed a characteristic “paste-like” behavior, and the transition from the viscous to elastic region occurred at low frequencies. This behavior was explained with noncovalent interactions between polymer chains such as electrostatic or hydrogen bonds.[49]

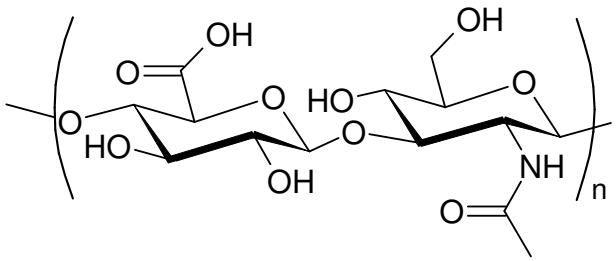

Figure 1.6 Structure of Hyaluronic acid.

Due to its viscoelastic properties, HA, even at concentrations of 0.1%, can impart over 80% of the total viscosity of some biological fluid. For instance, in the case of synovial joint fluid, under normal physiological conditions, HA behaves as a lubrificant at low shear rates (resting or walking) and prevents mechanical damage acting as a shock absorber and reducing the friction of the moving bones at high shear rates (running).[47]

Depending on the molecular weight, HA shows wide-ranging and often opposite biological functions. High-molecular-weight polymers ($4 \cdot 10^2$ to $2 \cdot 10^4$ kDa) are space filling, antiangiogenic, immunosuppressive, whereas low molecular weight polymers are involved in ovulation, embryogenesis, and protection of epithelial integrity and wound healing. Small hyaluronic acid fragments are inflammatory, immunostimulatory and angiogenic. HA is degraded by hyaluronidase. Several clinical applications of hyaluronic acid have been described. HA can be used to protect damaged tissues and provide space during ophtalmological surgeries. Its

major use is as substitute or replacement of the vitreous fluid lost during procedures such as cataract surgery or lens implantation.[50]

1.6 Crosslinking of Gelatin and Hyaluronic acid

Either gelatin or HA can be chemically modified or crosslinked to improve the mechanical properties and to control the degradation rate. Different strategies have been proposed for the chemical modification of gelatin. Chemical crosslinking typical utilizes bifunctional reagents such as glutharaldehyde,[51,52,53] cardodiimide,[54] diisocyanate,[16,55] acyl azides,[56,57] bis(vinylsulfonylmethane),[58] or less toxic crosslinkers such as genipin,[59,60] transglutaminase[61,62,63] and ethyl lysine diisocyanate (LDI) (Figure 1.7).[16] Gelatin has also been incorporated into synthetic polymer composites, including e. g. poly (L-lactic acid), polyurethanes, and PCL.

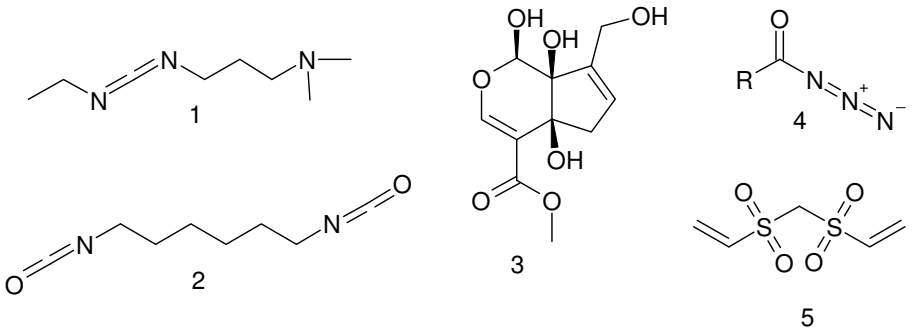

Figure 1.7 Chemical structures of typical bifunctional crosslinker used for synthesizing gelatin-based hydrogels. 1: 1-Ethyl-3-3(3-dimethylaminopropyl) carbodiimide; 2: 1,6-diisocyanatehexane; 3: genipin; 4: acyl azide; 5: bis(vinylsulfonyl)methane.

HA-based hydrogels have been obtained by using diepoxy compounds,[64] aldehyde crosslinking,[65] photocrosslinking,[66] divinyl-sulfone[67] (Figure 1.8), Diels-Alder chemistry.[68]

Although gelatin-based systems have been widely investigated, a method enabling the efficient control of mechanical properties and thorough understanding of

the network architecture is still missing. In order to establish defined structure-properties relationships the knowledge of the network structure is of paramount importance.

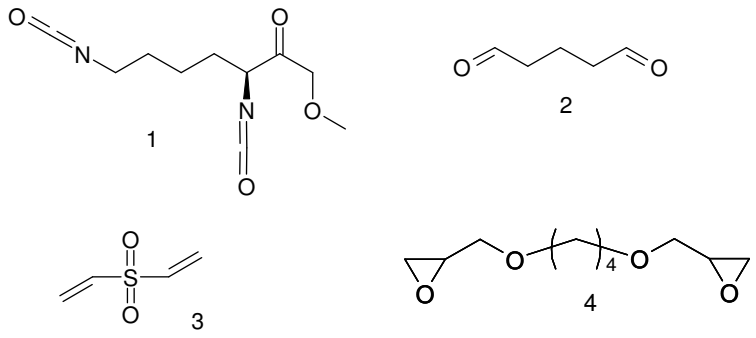

Figure 1.8 1: Chemical structure of some bifunctional crosslinker used for the synthesis of gelatin-based hydrogels and hyaluronic based hydrogels. 1: Ethyl ester L-lysine diisocyanate; 2: glutharaldehyde; 3: divinylsulfone; 4: 1,4-butanediol diglycidyl ether (BDDE).

1.7 Click Chemistry

In 2001 Sharpless and coworkers introduced the concept of "Click Chemistry", which refers to a class of reactions characterized by high selectivity, facile experimental setup, tolerance to a variety of solvents and functional groups, quantitative yields, and minimal synthetic work-up.[69] Although several chemical reactions including the Cu(I)-catalyzed azide-alkyne cycloaddition,[70] Diels-Alder cycloaddition[71], the thiol-ene reaction,[72] and the azide-nitrile cycloaddition[73] exhibit these features, the Copper(I)-catalyzed azide-alkyne cycloaddition is considered the most typical example of Click Chemistry. Therefore, the term Click Chemistry has often been used synonymously to denote the copper-catalyzed 1,3 dipolar cycloaddition. The 1,3-dipolar cycloaddition of azides and alkynes was discovered by Arthur Michael at the end of the 19th century and significantly developed by Rolf Huisgen in the early 1960s.[74] In the absence of the metal catalyst, this reaction is not

regioselective yielding a mixture of 1,4 and 1,5-regioisomers, is relatively slow and requires high temperatures to reach acceptable yields.[75] Furthermore, the two regioisomers are difficult to separate using the classical chromatographic procedures.[76]

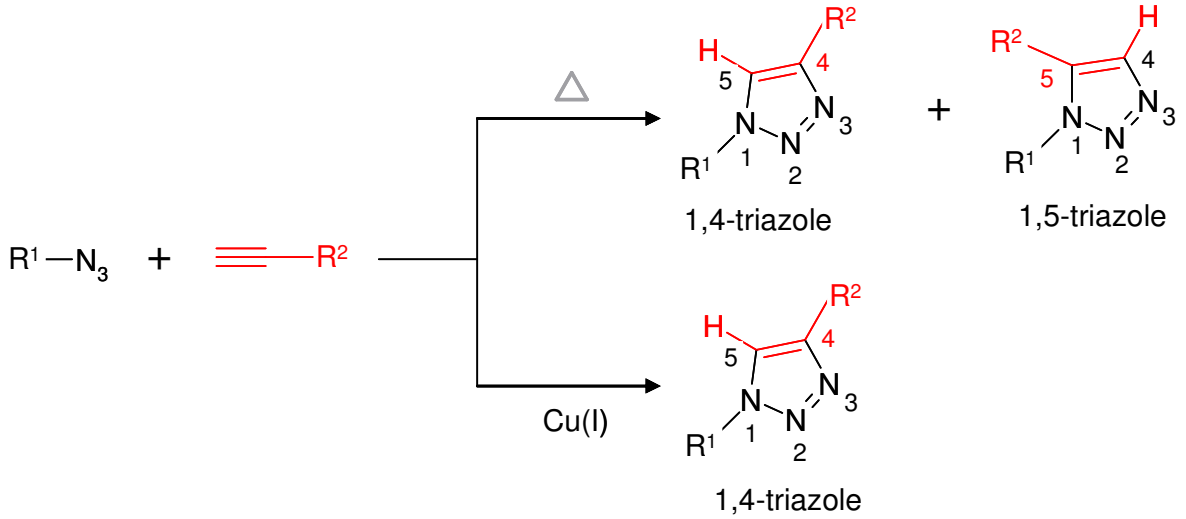

Figure 1.9 Products of the thermal 1,3-dipolar cycloaddition and copper-catalyzed cycloaddition between azide and alkyne.

The discovery that the use of catalytic amount of Cu(I) increases the reaction rate and the regioselectivity to give the 1,4-disubstitutes triazole (Figure 1.9), eliminating the need for elevated temperature, was reported independently by the Sharpless and Meldal groups. The great success of this reaction is in part due to the ease with which azides and alkynes can be introduced into a molecule and their stability under a variety of conditions. Both functional groups are basically inert toward biological molecules, they are small and unable to form hydrogen bonds. Although the thermal dipolar cycloaddition of azides and alkynes occurs through a concerted mechanism, a stepwise mechanism for the copper-catalyzed cycloaddition has been postulated on the basis of calculation and kinetic studies (Figure 1.10).

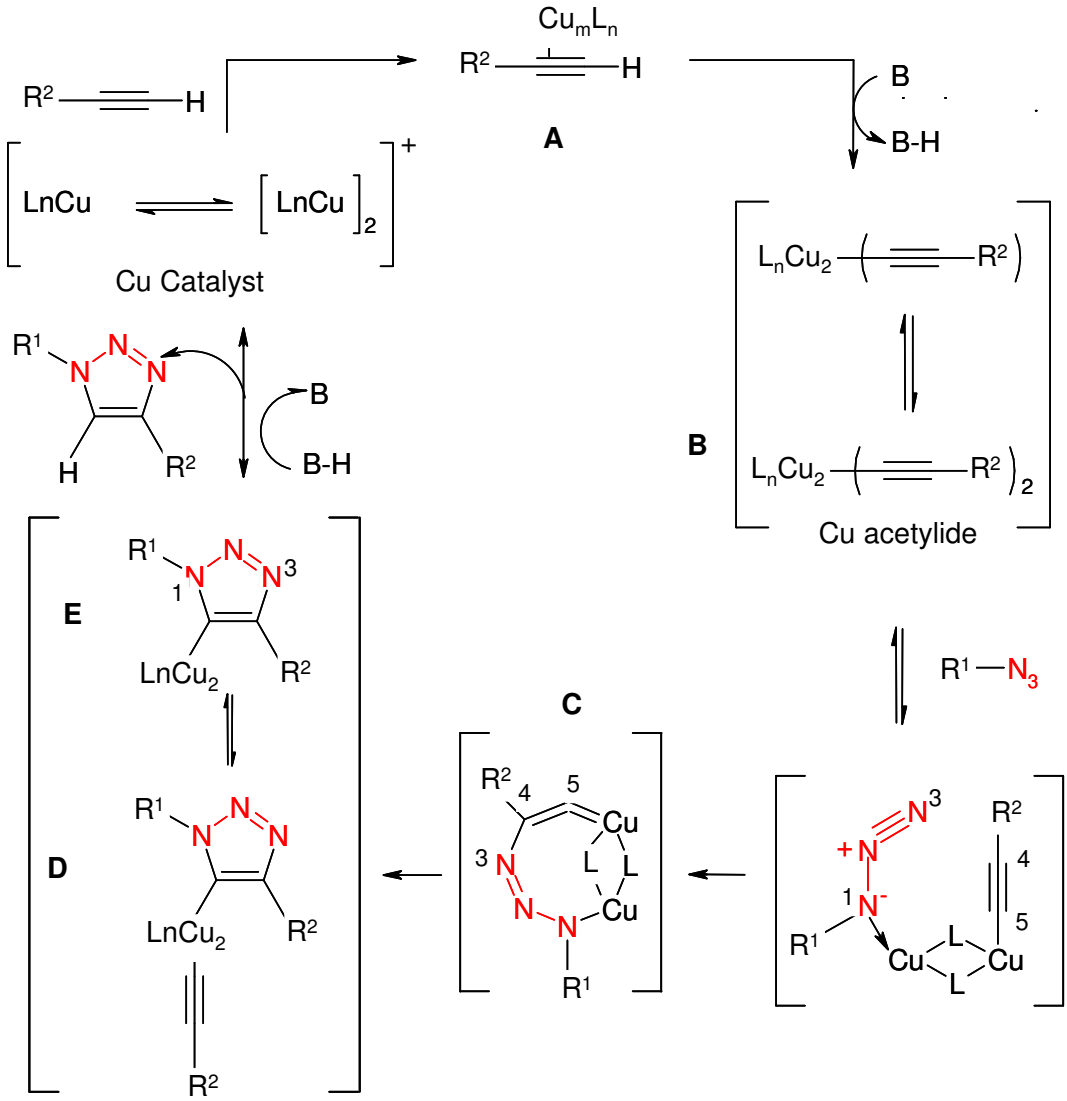

Figure 1.10 Proposed stepwise mechanism for the copper-catalyzed alkyne-azide cycloaddition.[77]

The proposed mechanism begins with the coordination of the alkyne to the Cu(I) species leading to the formation of the Cu(I)-acetylide complex (A); in the next step the alkyne replaces one of the ligands and binds to the copper atom via the terminal carbon (B). Complexation with azide activates it towards nucleophilic attack at N3 with the acetylide carbon C4, forming a metallocycle (C). The metallocycle generated in the last step undergoes ring contraction by a transannular association of the N(1) lone pair of electrons with the C(5)-Cu π* orbital, leading to the formation of the triazole-copper derivative (D). The protonation and the subsequent dissociation of the products terminate the reaction and regenerate the catalyst (E).[77,78,79]

The copper-catalyzed azide-alkyne cycloaddition is a particularly attractive reaction since it can proceed well in aqueous medium and is extremely chemoselective, enabling the modification of highly functional biomacromolecules such as polypeptides, nucleic acids, polysaccharides.

1.7.1 Applications of Click Chemistry

Since its discovery, click chemistry has also been applied in polymer chemistry for the synthesis of a variety of star polymers, brush, and graft copolymers, hyperbranched materials, dendritic structure[80,81,82] and hydrogels. The use of the click reaction allows the synthesis of highly complex structure with well defined architectures as described in the recent literature.[83,84,85,86,87] For instance, three and four-arm PS stars have been prepared by synthesis of azido-terminated PS via click chemistry and subsequent click coupling onto tri- and tetraalkyne coupling agents. The reaction was completed in three hours with a final yield of three- and four-arm stars of 90% and 83%, respectively.

Despite the many publications about click chemistry, what is still missing is the use of the specificity offered by this reaction to simultaneously address the formation of biopolymer networks with tailored properties and the elucidation of network architecture.

2. Aim of the Ph. D. thesis

The aim of this work was to develop biopolymer-based networks with defined molecular architecture. Biopolymer-based materials are of interest as they are renewable resources, and in view of biomedical applications offer sites for cell adhesion, susceptibility to hydrolytic and to cell-proteolytic degradation, they are non toxic and many of them non-immunogenic. However concerns exist about the low mechanical properties and batch-to-batch variations. In order to tailor and control the mechanical properties (e. g. Young's modulus, shear modulus and elongation at break), the swelling and degradation behavior, biopolymers need to be chemically modified or crosslinked, forming hydrogels. Different strategies have been proposed for their chemical modification. However, due to the presence of a large number of functional groups, many of these reactions are challenging to control, leading to incomplete conversion or side products formation. The understanding of the network architecture is crucial, in order to establish structure-property relationships.

From a synthetic point of view, the characterization of the network topology is extremely challenging, since the network may not be regular (e.g. heterogeneous crosslink density), may contain dangling chains and is not soluble, which restricts the range of applicable analytical methods.

Therefore the aim of this work will be the development of a method enabling:

- Wide tailoring of mechanical properties and degradation rate;
- Thorough characterization and understanding of the network architecture, including the quantification of grafting and crosslinking.

3. Strategies and concept

In order to synthesize materials with defined molecular architecture, a synthetic strategy that results in stable linkage, giving high yields without byproduct formation and which proceeds under benign conditions should be used. A chemical reaction that could satisfy all these requirements is the copper(I)-catalyzed azide-alkyne cycloaddition (or Click Chemistry). The copper-catalyzed azide-alkyne cycloaddition will be used as a simple but highly efficient method for the synthesis of well-defined gelatin-based networks. The first step in the synthesis of the hydrogels will be the incorporation of alkyne pendant groups into the gelatin backbone. Subsequently, the alkyne-functionalized gelatin will be dissolved at 45 °C, above the sol-gel transition, followed by addition of the crosslinker and the copper catalyst. The reaction will be performed above its sol-gel transition making sure that the crosslinking will take place in solution between the coiled chains, suppressing the renaturation of the triple helix structure. Crosslinkers with a different structure will be used to vary both the length and the chemical nature of the covalent netpoints between the gelatin chains. Specifically, the variation of the crosslinker molecular flexibility and crosslinking density, should enable the tailoring of the mechanical properties. The incorporation of a crosslinker with a rigid structure between the gelatin chains should reduce the molecular movements yielding networks with low swelling degree and high stiffness.

On the other hand, the use of crosslinkers with a flexible structure, even at high crossliker density, will allow some movement of the chains giving networks with higher swelling and elongation than the nework containing a rigid crosslinker. 4,4'-diazido-2,2'-stilbenedisulfonic acid is a suitable crosslinker with rigid structure, whereas 1,8-diazidooctane, 1,12-diazidododecane, and PEG-diazide will be selected as flexible crosslinkers. The resulting network will be then characterized by swelling behavior, thermo-mechanical properties and gelatin molecular organization.

During the synthesis of gelatin hydrogels dangling chains formation could occur. The final physical and mechanical properties are strongly affected by the network composition, e. g. number and ratio of grafts and crosslinks. Therefore a thorough understanding of the molecular structure is needed to discuss changes in the macroscopic properties.

A strategy for the elucidation of the network structure could be the labeling of the free azide groups with fluorescent dyes by the use of the chemoselective copper(I)-catalyzed azide-alkyne cycloaddition. Recently, there has been increasing interest in the synthesis and functionalization of fluorescent dyes for utilization in click chemistry. The presence of the eventually dangling chains, corresponding to the free azide groups, will be detected and quantified by using a confocal laser microscope and fluorescence spectroscopy. Fluorescent dyes will also be used for the detection of functional groups into the gelatin backbone which could potentially serve for the attachment of bioactive molecules.

It would be quite interesting to investigate if the synthetic strategy applied to protein-based materials could also enable the formation of defined polysaccharide-based networks. The synthesis of networks based on polysaccharides is quite challenging due to the presence of several functional groups (e. g. -OH, -COOH) and the easy hydrolysis of the glycosidic bond connections between sugar molecules

under acidic conditions. One possibility could be to use hyaluronic acid as starting material. The tailoring of material properties might be achieved varying the crosslinker molecular flexibility and crosslinking density. The resulting networks will be characterized by their swelling and mechanical behaviour.

The variation of the crosslinking density and crosslinker molecular flexibility could be also used as a method to control the change of material properties during degradation, which would be highly beneficial in view of potential biomedical applications. Therefore the degradation behaviour of gelatin-based hydrogels, under hydrolytic and enzymatic conditions, will be investigated. The change of material properties during degradation will be monitored by water uptake, tensile and rheological measurements, thermal properties and chains organization. The partially degraded materials will be characterized by using different mechanical tests, e.g. tensile and rheological measurements, in order to check which kind of stress the materials can stand during the degradation time.

Above discussed methods give materials based on biopolymer and synthetic components. It would be interesting to have all components based on biopolymers. A possible method would be to use controlled degradation to form gelatin-based telechelics, which could be used as crosslinkers for the preparation of gelatin-based networks. The preparation of fragments of different range of molecular weight should enable the tailoring of the material properties.

Degradative methods have extensively been applied to polyhydroxyalkanoates such as poly(3-*R*-hydroxybutyrate) (P3HB) or copolyesters, whereby especially trans-esterification[88] or the controlled degradation of copolymers with weak links have been studied.[89] Low molecular weight P3HB can also be obtained by degradation of high molecular weight P3HB, via acid-catalyzed methanolysis,[90] acid/ base hydrolysis[91] or thermal degradation.[92]

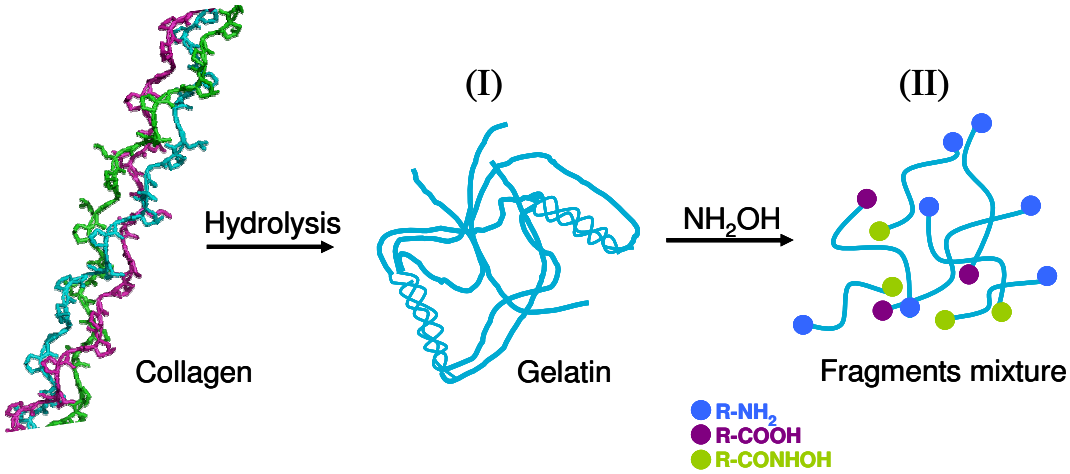

Figure 3.1 Gelatin is produced via the partial hydrolysis of collagen[93] (I); by the use of NH_2OH fragments with defined molecular weight and endgroups can be obtained (II).

The degradation mechanism (e.g. random chain scission or endgroup scission) has a strong influence on the structure of the obtained telechelics.[94] By monitoring the reaction by gel permeation chromatography and stopping the reaction at the right time point, fragments with the desired molecular weight are obtained.

However, to obtain defined and reproducible fragments, a method that allows the cleavage of only specific amide bonds should be used. One possibility could be the use of hydroxylamine, since Bornstein *et al.* reported the presence of hydroxylamine sensitive bonds in collagen.[95] Hydroxylamine specifically cleaves the bond between asparagin and glycine residues leading to the formation of aspartyl-hydroxamates and amino endgroups (Figure 3.2).

This method would be fast, likely easy to scale up, and inexpensive. The proposed mechanism of the hydroxylamine-mediated cleavage of gelatin is reported in figure 3.2. Gelatin fragments will be prepared by hydroxylamine mediated degradation and the resulting fragments mixture will be thoroughly investigated. The resulting fragments will be analyzed by SDS-PAGE and gel permeation chromatography. Additionally, the rheological properties of the resulting fragments and the molecular chain organization will be investigated.

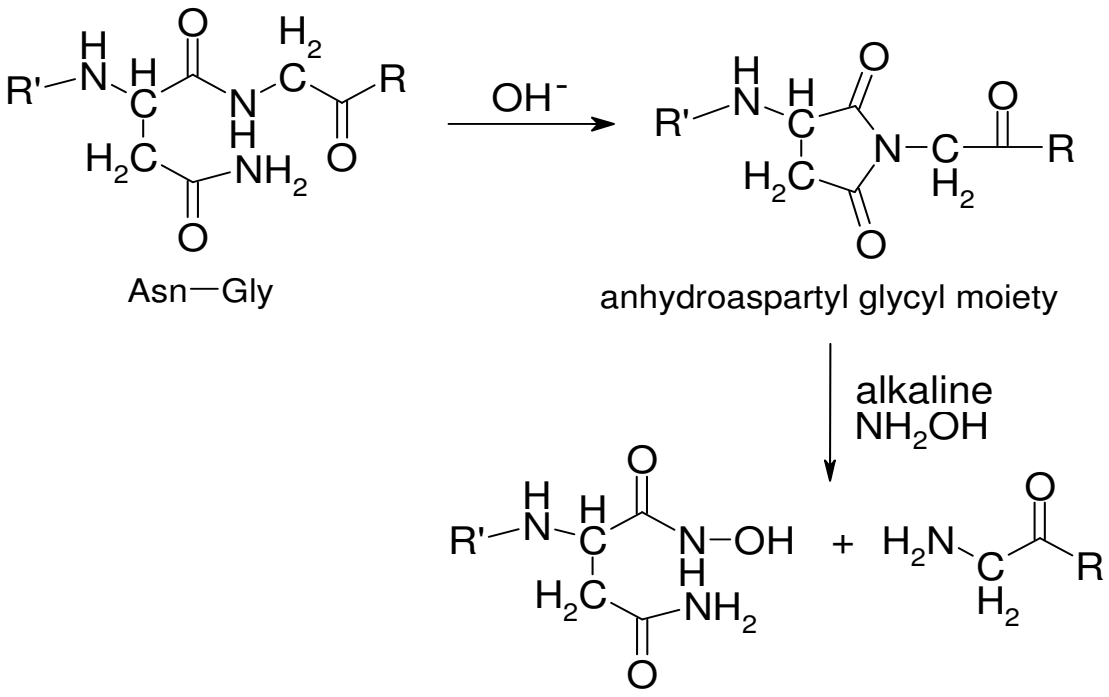

Figure 3.2 Proposed mechanism of NH_2OH-mediated cleavage of the Asn-Gly bond. The anhydroaspartyl mojety can be cleaved by hydroxylamine yielding fragments resulting in aspartyl hydroxamate C-terminus and an amino-terminal glycine.[96]

4. Synthesis of Gelatin-based Hydrogels with Tailorable Properties

In this chapter, the synthesis and characterization of gelatin-based hydrogels prepared by copper(I)-catalyzed azide-alkyne cycloaddition are described. First, the functionalization of gelatin is discussed, followed by the formation and characterization of the hydrogels.

4.1 Synthesis of alkyne-functionalized gelatin

Alkyne groups were introduced by coupling Ω-alkyne carboxylic acids to free amino groups of gelatin, i.e. propiolic acid and 4-pentynoic acid, predominantly via the amino groups of lysine and hydroxylysine.[97] In the literature molar contents of 2.9% for lysine and 0.8-1.5% for hydroxylysine are given.[98] The amount of free amino groups of the gelatin used in this study, determined by TNBS, was $27 \cdot 10^{-5}$ mol/g. Different strategies were used to introduce alkyne groups into the gelatin backbone. Gelatin was functionalized with propiolic acid or 4-pentynoic acid using a two steps procedure (Scheme 4.1). In the first step propiolic acid or 4-pentynoic acid was

activated by the use of diisopropylcarbodiimide (DIC). Subsequently, the activated Ω-alkyne carboxylic acid was reacted with the amino groups in gelatin to form stable amide bonds. The degree of modification determined by a spectrophotometric method (TNBS) was 88 mol-% and 65 mol-% for propiolic acid and 4-pentynoic acid, respectively. Due to the higher degree of functionalization, propiolic acid was used in the further experiments.

Trinitrobenzenesulfonic acid (TNBS) as a UV-chromophore reacts with primary amino groups of proteins at an alkaline pH to form a trinitrophenyl derivative and a sulfate ion.[99] By measurement of the yellow absorbance of the trinitrophenyl derivatve, the number of amino groups in proteins can be calculated, using equation 4.1:

$$\frac{moles\,lys}{g\,gelatin} = \frac{2(absorbance)(0.020\,liters)}{(1.4\times10^{4}\,liters/mole\cdot cm)(b)(x)} \qquad (4.1)$$

where $1.4*10^4$ is the absorption coefficient for 2,4,6-trinitrophenyl derivatised (hydroxyl)lysine residues, *b* is the cell path length in cm, and *x* is the sample weight in g. FT-IR spectroscopy confirmed the grafting of propiolic acid on gelatin, with the appearance of a new peak at 2115 cm^{-1}. The incorporation of the alkyne groups into the gelatin backbone led to changes in the physical and mechanical properties compared to pure gelatin.

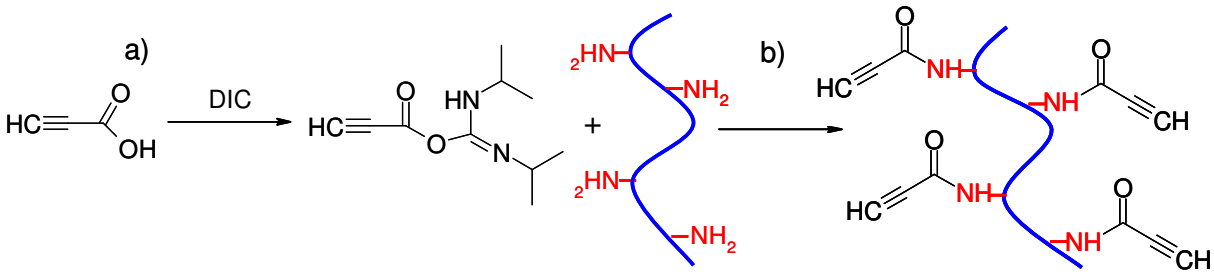

Scheme 4.1 (a) activation of propiolic acid by DIC, for 30 min at 0 °C; (b) functionalization of gelatin amino groups by reaction with activated propiolic acid at room temperature.

4.1.1 Rheological investigation of alkyne-functionalized gelatin

Dynamic shear oscillation measurements were used to characterize the viscoelastic properties of gelatin before and after derivatization. The thermal scanning rheological observation for both the elastic (G') and viscous modulus (G') of pure gelatin and alkyne-functionalized gelatin solution (5 wt. %) prepared at 40 ℃ is shown in Figure 4.1. The solutions were placed between the rheometer plates and heated at a rate of 3 ℃/ min from 0 ℃ to 50 ℃. Before the heating run, both solutions were equilibrated at the temperature of the rheometer forming a physical gel. The obtained gels showed a high G' value at low temperature, but on heating both moduli decreased and a crossover between G' and G'' occured. The crossover temperature is attributed to the sol-gel transition temperature and it indicates the transition from an elastic network to a solution. Interestingly, the sol-gel transition in alkyne-functionalized gelatin occurred at a higher temperature than in pure gelatin and the G', at low temperature, was higher for functionalized than for pure gelatin. Specifically, the alkyne-functionalized gelatin had a G' of 10 kPa, whereas for pure gelatin it was 3 kPa. The same solutions were cooled down at the rate of 3° C/min from 50 to 0 ℃ and the gelling temperature was determined from where the two moduli intersect during the cooling period. The evolution of the elastic modulus and loss modulus during the cooling run are shown in Figure 4.1(b). The gelling temperature of alkyne-functionalized gelatin was observed at higher temperature compared to pure gelatin solution. The physical gel formed by gelatin upon cooling can be described as an entangled network of triple helix connected via flexible

links.[53] The derivatization of gelatin in some cases hinders the renaturation of triple helices, leading to the formation of physical gels with low mechanical strength. Here, the presence of alkyne moieties in the gelatin backbone gave hydrogels with higher strength and gelation occurred at a temperature where pure gelatin solution has a low elastic modulus. This rheological observation could be partially explained by the formation of π-hydrogen bonds between terminal alkynes and hydrogen donor groups (OH, NH_2).[100,101]

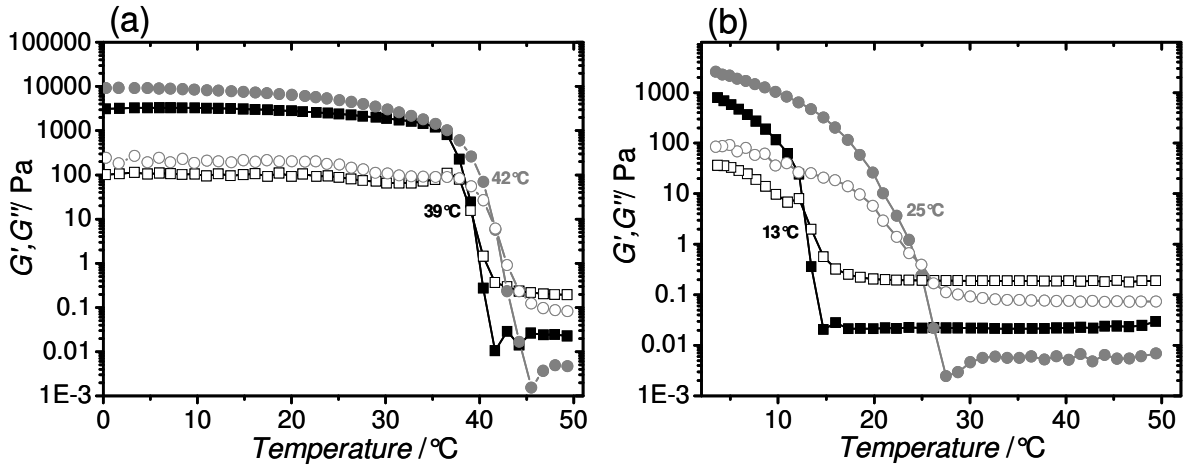

Figure 4.1 Evolution of the elastic (G') and viscous (G'') modulus as a function of temperature during the heating ramp (a) and cooling ramp (b) for gelatin (G' ■ and G''□) and alkyne-functionalized gelatin solutions (G'● and G'' ○).

4.1.2 Investigation of molecular organization of alkyne-functionalized gelatin

In order to evaluate the influence of propiolic acid on the molecular organization of the gelatin chains, WAXS measurements were performed (Figure 4.2). The WAXS spectra of gelatin shows three peaks at 2θ = 8°, 20° and 31°, which correspond to the diameter of the triple helix, the amorphous halo, and the amino

acids contact along the axis of single helices, respectively.[102,103] The same molecular organization was observed in the alkyne-functionalized gelatin, with only a slight decrease of the peak intensity at 8° and 31°. Therefore, the incorporation of the acetylenic function did not have a major effect on the molecular organization of the gelatin backbone.

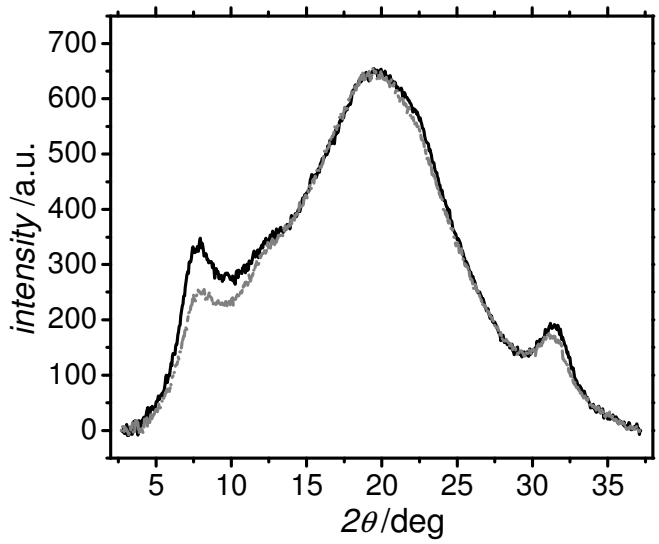

Figure 4.2 WAXS spectra of a dried gelatin film (—) and an alkyne-functionalized gelatin film (—).

4.2 Synthesis of azide building blocks

Different azide building blocks were selected to vary both the length and the chemical nature of the linkage between the gelatin chains. The compounds 1 and 3 are commercial available, whereas 2 and 4 have been synthesized (Figure 4.3).

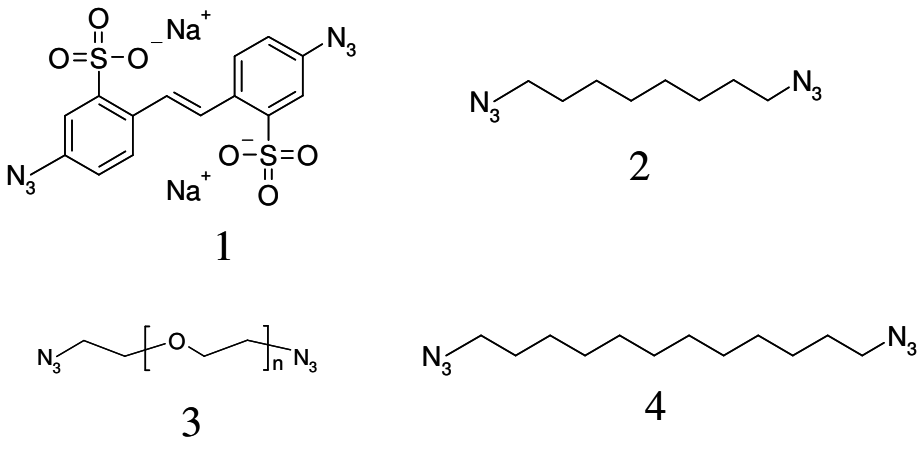

Figure 4.3 Structure of the azide bulding blocks used in the synthesis of gelatin-based hydrogels. (1) 4,4-diazido-2,2'-stilbenedisulfonic acid; (2) 1,8-diazidooctane; (3) PEG-diazide; (4) 1,12-diazidododecane.

Even though organic azides are generally safe compounds and the danger of their explosive decomposition decreases with increasing molecular weight,[104,105] the isolation or purification of lower organic azides can be challenging.[106] One of the most common methods for the synthesis of alkyl azides is the nucleophilic substitution of alkyl bromides with sodium azide (NaN_3)[107,108] from the corresponding alkyl bromide in various solvents. Here, the synthesis of 1,8-diazidooctane or 1,12-diazidododecane was accomplished by reacting 1,8-dibromooctane or 1,12-dibromododecane respectively with sodium azide (DMSO, 25 °C, 24 hours) (Scheme 4.2). The successful introduction of the azido groups was confirmed by NMR, in which the complete conversion of the bromo group to an azide group was given by a resonance shift (3.4→3.3) of the terminal methylene group (Figure 4.4).

$$\text{Br-(CH}_2\text{)}_n\text{-Br} \xrightarrow[\text{DMSO}]{\text{NaN}_3} \text{N}_3\text{-(CH}_2\text{)}_n\text{-N}_3$$

Scheme 4.2 General scheme for the synthesis of 1,8-diazidooctane and 1,12-diazidododecane starting from the corresponding dibromides.

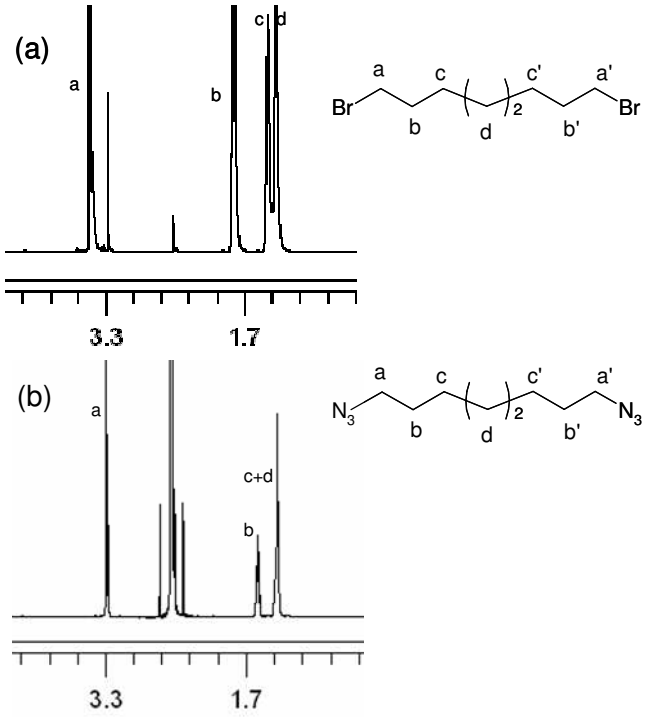

Figure 4.4 ^{1}HNMR spectra of (a) 1,8-dibromooctane and (b) 1,8-diazidooctane in dmso-d6. The diazide formation is confirmed by the shift of the methylene group when is bound to the azide.

4.2.1 Synthesis of gelatin-based hydrogels

Gelatin based hydrogels were successfully synthesized by the use of the copper(I)-catalyzed azide-alkyne cycloaddition (here also referred to as Click Chemistry). Click chemistry was used as a simple but highly efficient method for the synthesis of well defined gelatin networks with controlled architecture and varied mechanical properties.

The alkyne-functionalized gelatin was dissolved at 45 ℃ in a mixture 1:1 water/ ethanol, above the sol-gel transition temperature, so that the gelatin chains were in a random coiled state. Therefore, the crosslinking took place in solution where the crosslinker molecules are free to diffuse forming crosslinks between the coiled chains.

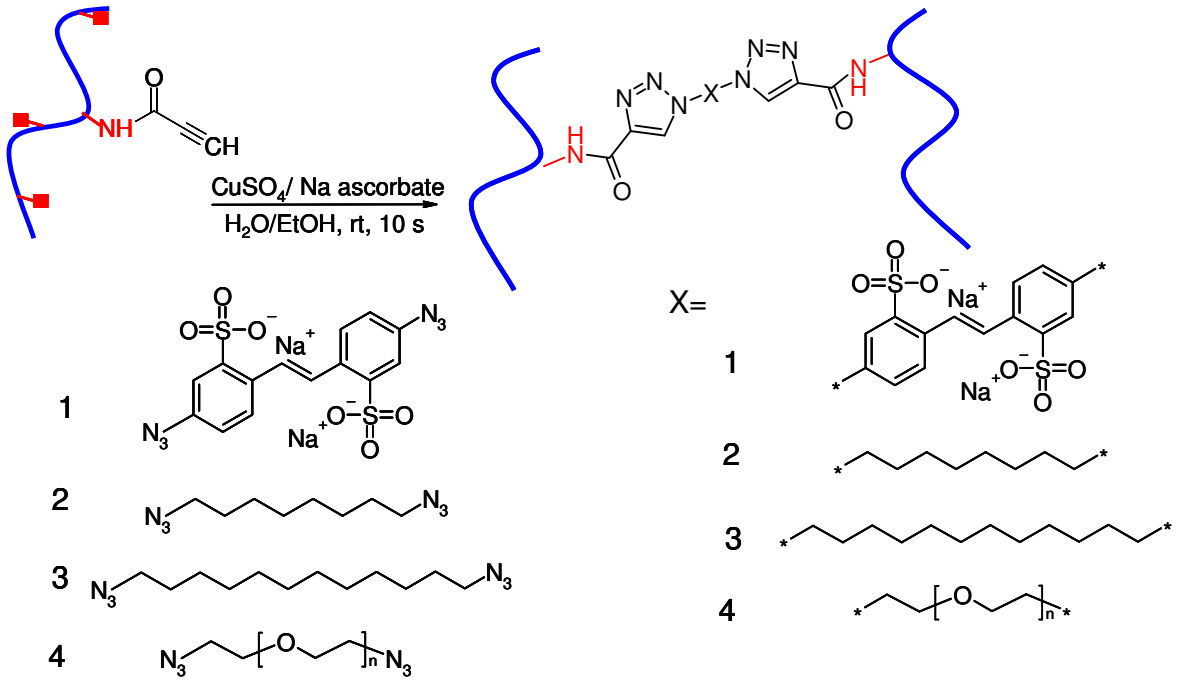

Scheme 4.3 Synthesis of gelatin-based networks using as crosslinker (1) 4,4'-diazido-2,2'-stilbenedisulfonic acid, (2) 1,8-diazidooctane, (3) 1,12-diazidododecane and (4) PEG-diazide.

When the gelatin solution is cooled down below the sol-gel transition temperature, the renaturation of the triple-helices will be hindered due to the presence of covalent netpoints. Some helicity may occur where no crosslinks have been formed,[109] resulting in e. g. structural defects in the chemical network.

Once gelatin was completely dissolved, a diazide, specifically 4,4'-diazido-2,2'-stilbenedisulfonic acid, 1,8-diazidooctane, 1,12-diazidododecane and PEG-diazide (Mw =1108 g/mol, PDI 1.2) was added, followed by the copper catalyst. These crosslinkers were selected on the base of their molecular flexibility, to tailor the resulting material properties. Four different alkyne:azide ratios were used: 0.5:1, 1:1, 5:1 and 10:1. The hydrogels were extensively washed with EDTA for copper removal. The hydrogels are referred to as NGs_x (network of gelatin with 4,4'-diazido-2,2'-stilbenedisulfonic acid as crosslinker), NGo_x (1,8-diazidooctane as crosslinker), NGd_x (1,12-diazidododecane as crosslinker) and NGp_x (PEG as crosslinker). The x stands for the alkyne:azide ratio (Scheme 4.3). Different stoichiometric ratios of

alkyne:azide, as well as different crosslinker types, were used to obtain hydrogels with tunable mechanical properties.

4.2.2 Investigation of molecular organization in gelatin-based networks

The incorporation of crosslinks between gelatin chains can reduce or suppress the renaturation of the triple helix structure.[110,111,112] In order to investigate the effect of different crosslinker types and the alkyne: azide ratio on the gelatin chain helicity, WAXS measurements of NGs and NGo networks were performed (Figure 4.5). The NGs and NGo systems were chosen as an example of networks containing a rigid crosslinker and a flexible crosslinker, respectively. The WAXS spectra of non-crosslinked gelatin, as described before, display three peaks at 8°, 20° and 31°. The WAXS spectra of the NGs and NGo films, showed peaks at 20° indicating the presence of amorphous regions, whereas no peak was detected at 31°. NGs hydrogels synthesized with increasing crosslinker molar ratio displayed a decreasing 8° peak intensity, correlating to a decreasing renaturation of triple-helical collagen-like structures.[113] A minimal signal intensity was observed in that region for NGo samples synthesized with an alkyne:azide ratio 1:1, in contrast to NGs hydrogels. These observations can be explained with the flexible structure of the crosslinker in NGo, which cannot suppress completely the renaturation of the triple helix. On the other hand, NGs bulky aromatic systems are likely to permanently inhibit helix formation due to the steric hindrance between 4,4'-diazido-2,2'-stilbenedisulfonic acid crosslinked chains.[114] Hence, the molecular structure of the crosslinker is responsible

for the different structural organization in both chemical systems and together with the crosslinking density can be used to control the helicity of gelatin-based networks.

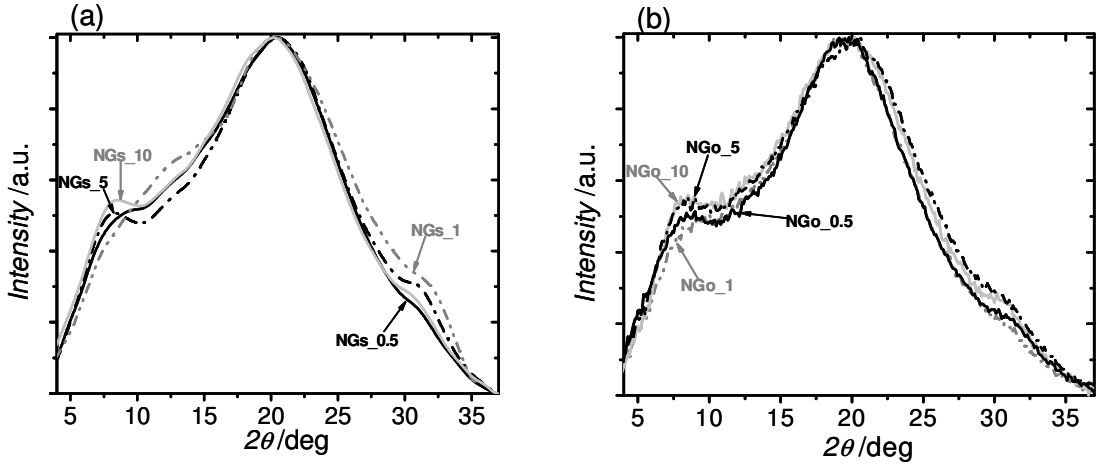

Figure 4.5 WAXS spectra of dry gelatin networks. (a) NGs networks: (—) NGs_0.5, (---) NGs_1, (-·--·) NGs_5, (—) NGs_10. (b) NGo networks: (—) NGo_0.5, (---·) NGo_1, (-·--·) NGo_5, (—) NGo_10. An increase in crosslinker amount resulted in a suppression of the peak at 8° and 31°, which correspond to the triple helix and the single helix, respectively.

4.2.3 Investigation of swelling behavior of gelatin networks

The swelling ratio is one of the most important structural parameters for evaluating hydrogel properties and it is correlated to the network structure. The pore size of a polymer network and the interaction between the polymer and the solvent will determine the degree of swelling.[115] The mechanism of hydration of gelatin has been described as a capillary phenomenon of water molecules penetrating the tiny interstices of triple-helical fibrils in the gelatin matrix.[116] Herein, the water absorption capability of gelatin-based hydrogels was determined gravimetrically and volumetrically and the following equations for the determination of the water uptake (*H*, eq. 4.2) and the swelling ratio (*Q*, eq. 4.3) were used:

$$H = \frac{W_s - W_d}{W_d} \tag{4.2}$$

$$Q = 1 + \frac{\rho_2}{\rho_1}\frac{W_s - W_d}{W_d} \tag{4.3}$$

where ρ_2 is the density of the dry gelatin networks, obtained by calculation based on the weight/volume ratio of dry samples, ρ_1 is the density of the swelling medium (buffer solution, 1.09 g/mL), and W_s and W_d are the sample weights in the dry and swollen state, respectively. Regardless of the composition, hydrogels crosslinked with decreasing crosslinker amount displayed an increase of *H* and *Q*. This finding indicates that the extent of crosslinking had a strong influence on the water absorption capability of gelatin hydrogels. At the same time, the swellability was also significantly affected by the crosslinker structure, as shown in Figure 4.5 and 4.7. The hydrogels containing a crosslinker with a rigid backbone resulted in the lowest swelling ratio (150-250 vol.-%), whereas those containing PEG-based crosslinker gave the highest degree of swelling (300-420 vol.-%) as resulting from the long and flexible aliphatic chain. The hydrogels containing 1,8-diazidooctane and 1,12-diazidododecane as crosslinkers showed no significant differences in the degree of swelling at an alkyne to azide ratio of 0.5:1 and 1:1, while decreasing the amount of azide functional groups large differences between the two crosslinker type were observed. The order of increasing swelling ratio for the gelatin hydrogels was NGp >NGd >NGo >NGs. The variation of the crosslinker density and the crosslinker type allowed the tuning of the hydrogels swelling (*Q:* 150-470 vol.-%; *H*: 350-1900 wt.-%) properties.

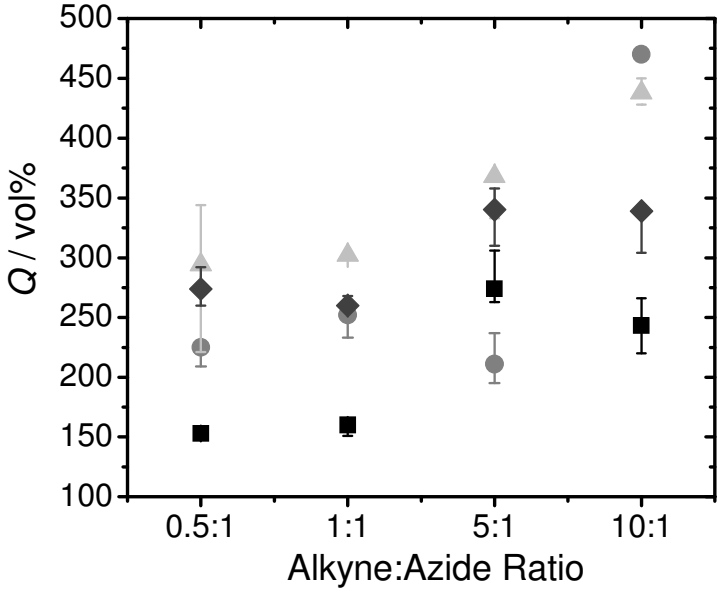

Figure 4.6 Degree of swelling of NGs (■), NGo (●), NGd (♦) and NGp (▲) networks, in PBS buffer, at 37 °C.

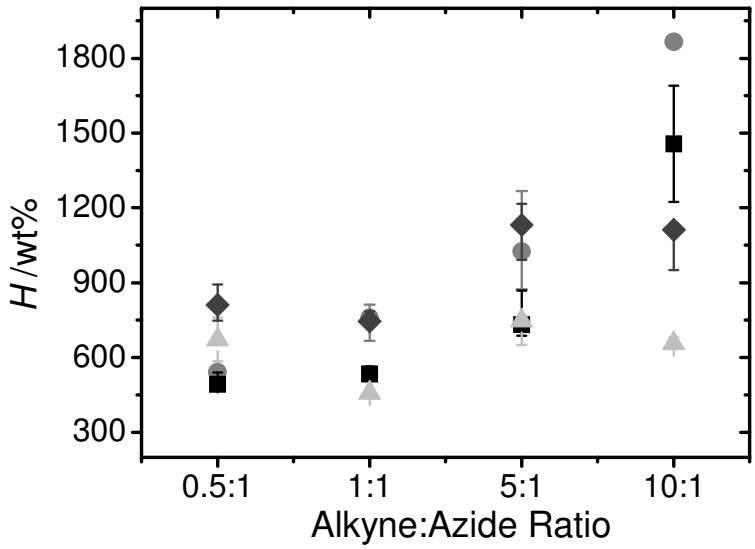

Figure 4.7 Water uptake of NGs (■), NGo (●), NGd (♦) and NGp (▲) networks, in PBS buffer, at 37°C.

4.2.4 Investigation of mechanical properties of gelatin-based hydrogels

Hydrogels prepared with different crosslinker types and different alkyne:azide ratios were characterized by rheological measurements. Dynamic mechanical spectra of NGs and NGo swollen hydrogels at 37 °C are shown in Figure 4.8. For reason of clarity only the elastic modulus is reported. In the whole range of frequency investigated, the elastic modulus (G') was always higher than the viscous modulus (G'') and independent from the frequency. This behaviour is typical for elastic hydrogels.[117] The increase of the elastic modulus was accompanied to a decrease in the degree of swelling. Hydrogels NGs showed a higher G' and lower swelling degree when compared to those of NGo at all alkyne:azide ratios, indicating that the crosslinker structure had an influence on the gel properties. Specifically, the G' of NGs hydrogels increased from 1 kPa to 16 kPa, whereas within the NGo series increased from 0.1 kPa to 10 kPa. By variation of the alkyne:azide ratio, hydrogels with different mechanical strength were successfully obtained. By increasing the crosslinker amount, increased values of G' were observed. Moreover, hydrogels prepared with low crosslinker content showed a G'-frequency independence in the low frequency range only.

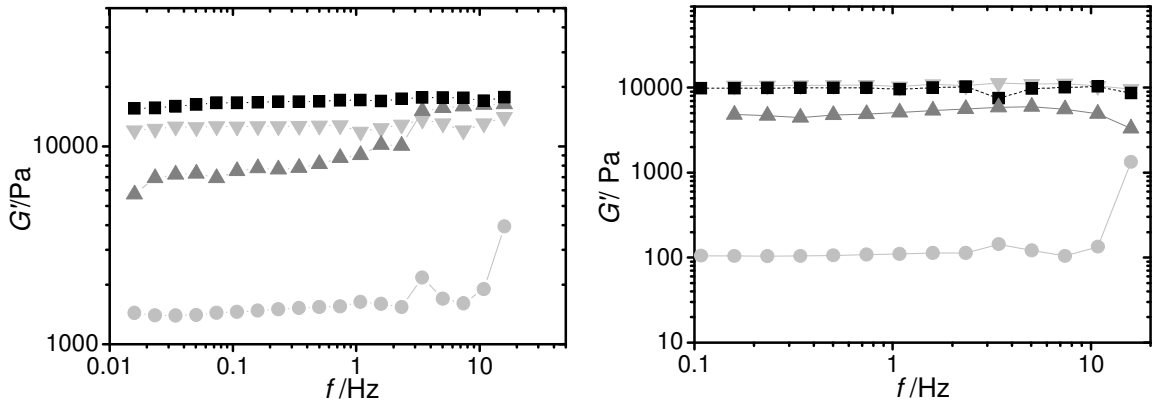

Figure 4.8 Rheological spectra of (left) NGs hydrogels at 37°C: NGs_0.5 (■), NGs_1 (▼), NGs_5 (▲) and NGs_10 (●). On the right NGo_0.5 (■), NGo_1 (▼), NGo_5 (▲) and NGo_10 (●).

To determine the effect of the crosslinker structure and crosslinker density on the hydrogel elasticity, further mechanical tests were performed. Herein, the mechanical properties of swollen hydrogels investigated by tensile tests at 25 °C are reported. The overall network stiffness increased by increasing the crosslinker content (50→635 kPa). The use of crosslinkers with different structures resulted in large variation in mechanical properties at an alkyne:azide ratio of 0.5:1 (130→ 389 kPa) and 1:1 (90→ 635 kPa), whereas no significative differences were observed at the 5:1 and 10:1 ratios (Figure 4.9). The elongation at break ε_b and the σ_{max} increased with decreasing the crosslinker amount, from the ratio 0.5:1 until 5:1, due to the major extensibility of the network chains (Figure 4.10). At the ratio 10:1, a decrease of elongation at break and maximum tensile strength was observed and the same trend was found in all hydrogel compositions. A summary of the mechanical properties is reported in table 4.1. Interestingly, the *E* modulus of NGo_10 was significantly higher compared to NGs_10. Because of the rigid structure of the crosslinker contained in the NGs system, one would expect a high modulus for the sample NGs_10. However, in this particular case has to be considered that the low amount of crosslinker and its flexible structure could enable the physical

reorganization of some gelatin chains (as described in section 4.2.2). Therefore, the Young's modulus determined for NGo_10 was higher than NGs_10, due to the contribution of physical and chemical crosslinking. This finding is also confirmed by the rheological measurements. Since the measurements were performed at 37 °C, where the defolding of the triple helix occurs, the G' of NGs_10 was at least one order of magnitude higher than those of NGo_10. In this case, only the contribution of the chemical crosslinking was measured. Another interesting aspect was observed at the ratio 5:1, where the highest value of tensile strength was measured. This behavior could be also explained with the renaturation of some triple helix.

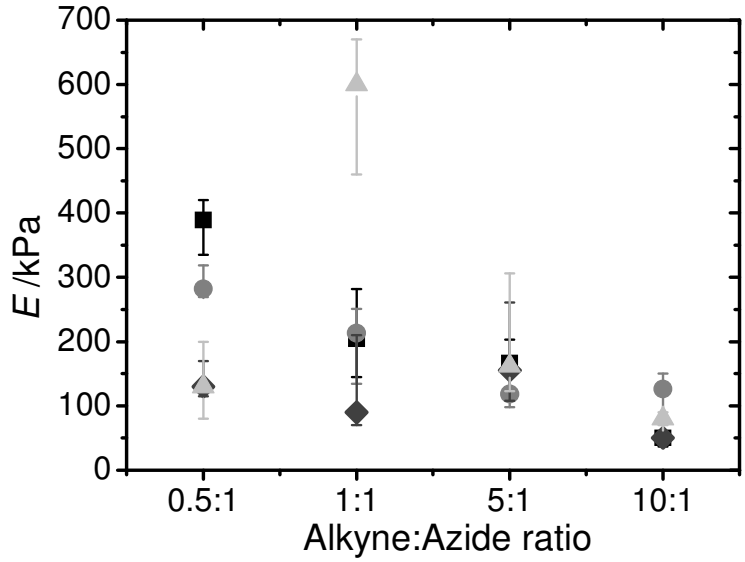

Figure 4.9 Young's modulus (E) of swollen gelatin-based hydrogels as a function of the crosslinker type and crosslinker amount. NGS (■), NGo (●), NGd (♦) and NGp (▲).

Although some physical reorganization of gelatin chains at low amount of crosslinker was observed, the elastic properties of the resulting hydrogels showed that the mechanical properties were successfully tailored by the variation of crosslinker content and type. However, a careful investigation of the network topology needs to be performed in order to thoroughly define the structure-property relationships of gelatin-based hydrogels. Results are shown in section 4.3.

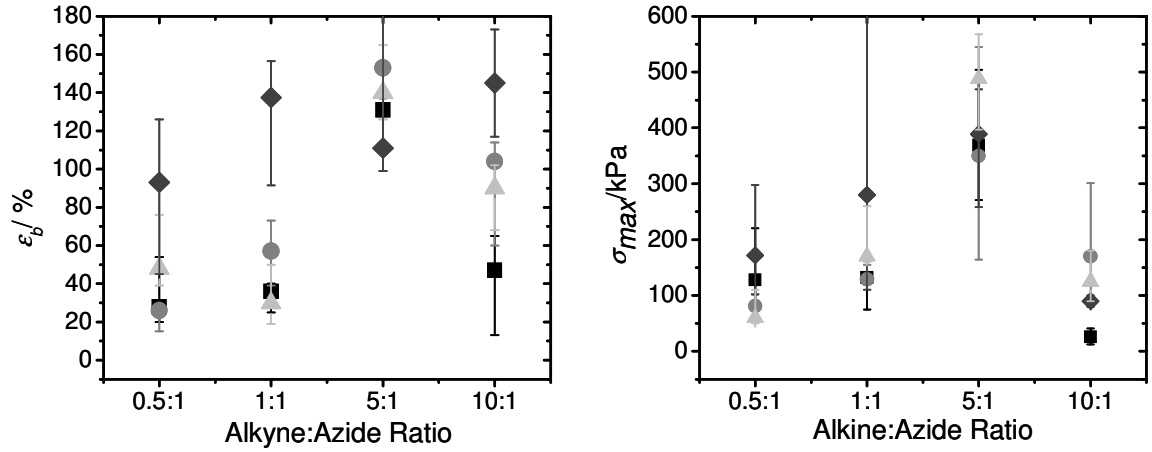

Figure 4.10 Elongation at break (ε_b) and maximum tensile strength (σ_{max}) of swollen gelatin-based hydrogels as a function of the crosslinker amount and crosslinker type. NGS (■), NGo (●), NGd (♦) and NGp (▲).

Table 4.1 Summary of mechanical properties of gelatin hydrogels determined by tensile tests: the median value and the lowest and highest values are given. E = Young's modulus, ε_b = elongation at break, σ_{max} = tensile strength.

Sample ID	E kPa (range)	ε_b % (range)	σ_{max} kPa (range)
NGs_0.5	389 (335-420)	28 (20-54)	128 (90-220)
NGs_1	204 (145-505)	36 (25-40)	132 (75-142)
NGs_5	166 (153-203)	131 (111-137)	369 (271-504)
NGs_10	50 (37-60)	47 (13-65)	26 (12-41)
NGo_0.5	282 (269- 319)	26 (15-27)	81 (58-103)
NGo_1	213 (134-251)	57 (39-73)	129 (108-155)
NGo_5	118 (98-146)	153 (108-205)	350 (154-545)
NGo_10	126 (75-150)	104 (60-114)	170 (80-211)
NGd_0.5	130 (115-170)	93 (45-126)	172 (102-298)
NGd_1	90 (70-210)	138 (92-156)	280 (110-650)
NGd_5	155 (115-261)	111 (99-205)	389 (258-464)
NGd_10	50 (40-60)	145 (117-173)	90 (80-100)
NGp_0.5	130 (80-200)	48 (39-76)	60 (50-110)
NGp_1	635 (460-970)	30 (19-50)	170 (160-260)
NGp_5	162 (123-306)	140 (126-165)	488 (397-696)
NGp_10	80 (80-90)	90 (68-102)	125 (90-180)

4.2.5 Thermal transitions of gelatin-based hydrogels

Besides the changes in mechanical properties, as a result of the crosslinking density and crosslinker type, the thermal properties need also to be investigated. By the use of Temperature Modulated DSC (TMDSC), the glass transitions of dry gelatin networks were successfully determined. As observed in table 4.2, T_g is decreased in networks with decreased crosslinker content, likely explained by the corresponding increased chain mobility.

Table 4.2 Glass transition temperature of gelatin hydrogels in the dry state.

Sample ID	Alkyne: Azide molar ratio	T_g(℃)
NGs_0.5	0.5:1	73
NGs_1	1:1	60
NGs_5	5:1	57
NGs_10	10:1	47
NGo_0.5	0.5:1	90
NGo_1	1:1	64
NGo_5	5:1	72
NGo_10	10:1	n.d.

Moreover, the glass transition temperature observed for NGs was lower than for NGo systems. In the literature, it has been reported that a correlation between the lenght of the crosslinker and the glass transition temperature exists.[118,119] In particular, long and flexible crosslinkers, should decrease the T_g compared to crosslinkers with a rigid structure, since the newly formed bonds will give still some mobility to the chains. However, the T_g of NGo systems, which contain a flexible crosslinker was

higher then the system containing a rigid linker. A first explanation could be that long and flexible crosslinkers can give a denser network, resulting in an increase of T_g. Another explanation could be that the flexible crosslinkers may not inhibit completely the renaturation of the collagen-like triple helix, as discussed in section 4.2.2. Therefore, if a low triple helical content is present, this will contribute to the crosslinking density and an increase of T_g will be determined.

By the use of TMDSC, the glass transition was determined for dry samples only. Since the synthesized materials are hydrogels, it would be desirable to know the thermal transition in aqueous environment. One method for the determination of the glass transition in water is the DMTA, which however requires samples with defined geometry and suitable mechanical properties. Since the hydrogels synthesized in this work were too soft (G':0.1-12 kPa; E: 50-635 kPa) for DMTA measurements, an alternative method was successfully developed for the determination of T_g. Sample NGs_10 (thickness: 2.5 x 1.5 cm) was compressed and the variation of the compression stress was measured as a function of the temperature. The measurements were performed in a static and cyclic mode. As shown in Figure 4.11, the sample started to became softer at approximately 12 °C and a reduction of the stress was observed until 30 °C (static mode). After that point a constant value of stress was measured. In the second case, compression cycles were performed and a stress reduction was again observed between 12 and 30 °C, indicating a thermal transition from a glassy to a rubbery state. By determination of the first derivative of the obtained curve, a T_g value of 22 °C was successfully obtained, which is in agreement with other covalently-crosslinked, gelatin-based hydrogel systems.[16]

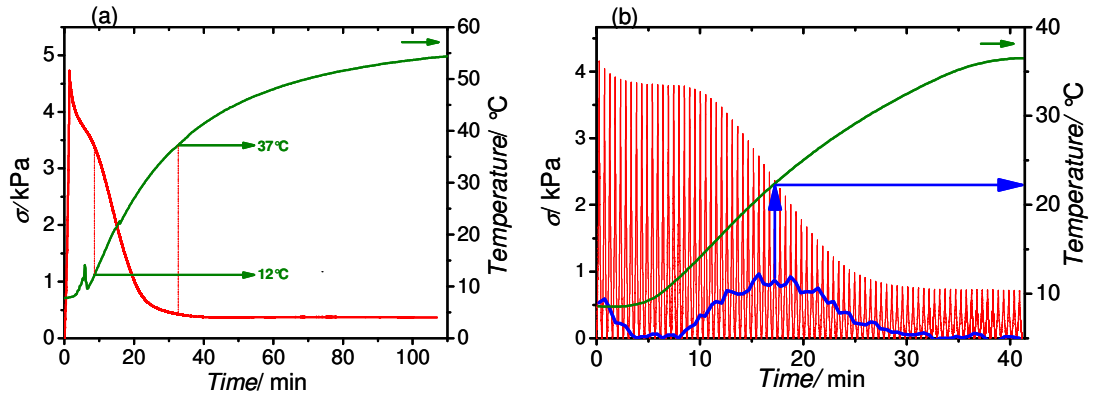

Figure 4.11 Compression measurements of gelatin_based hydrogels in a static mode (a) and cyclic mode (b). Stress: (—) red line; temperature: (—) green line; first derivative: (—) blue line.

4.3 Gelatin networks architecture

During the network formation, different structures can be formed so that structural imperfections might be present in the resulting network. These imperfections include dangling chains, i.e. chains attached to the network at only one side, elastically inactive loops, as a result of intramolecular reactions, physical chain entanglements and spatial heterogeneity. A possible reason for these defects could be related to the conditions in which the network has been synthesized, such as stoichiometric imbalances or incomplete conversion.[105] The final physical and mechanical properties of the network will be affected by the chemical composition and the crosslink density of the network. Even though the crosslinking density has a great influence on the network properties, the presence of dangling chains will definitely affect material (e.g. thermal, mechanical) properties and functions.[120] For these reasons, investigation of the network architecture is extremely important in order to establish defined structure-property-functions relationships.

During the formation of gelatin-based hydrogels, by a reaction between the alkyne-functionalized gelatin and a diazide crosslinker, three different events are likely to happen (scheme 4.4):

- if a low amount of crosslinker is used, it is very likely that the crosslinker will react on both sides. As a consequence, no dangling chains should be present, whereas free alkyne groups will be observed;
- using an amount of crosslinker corresponding exactly to the alkyne moieties, ideally all the azide groups should react with the alkyne functionalities forming a “perfect” network;
- using an excess of crosslinker, it is likely that grafting will occur reducing the number of covalent crosslinks.

In order to verify the postulated hypothesis the structure of the synthesized network was investigated by using a method based on the fluorescent labeling of the free azide and alkyne functional groups.

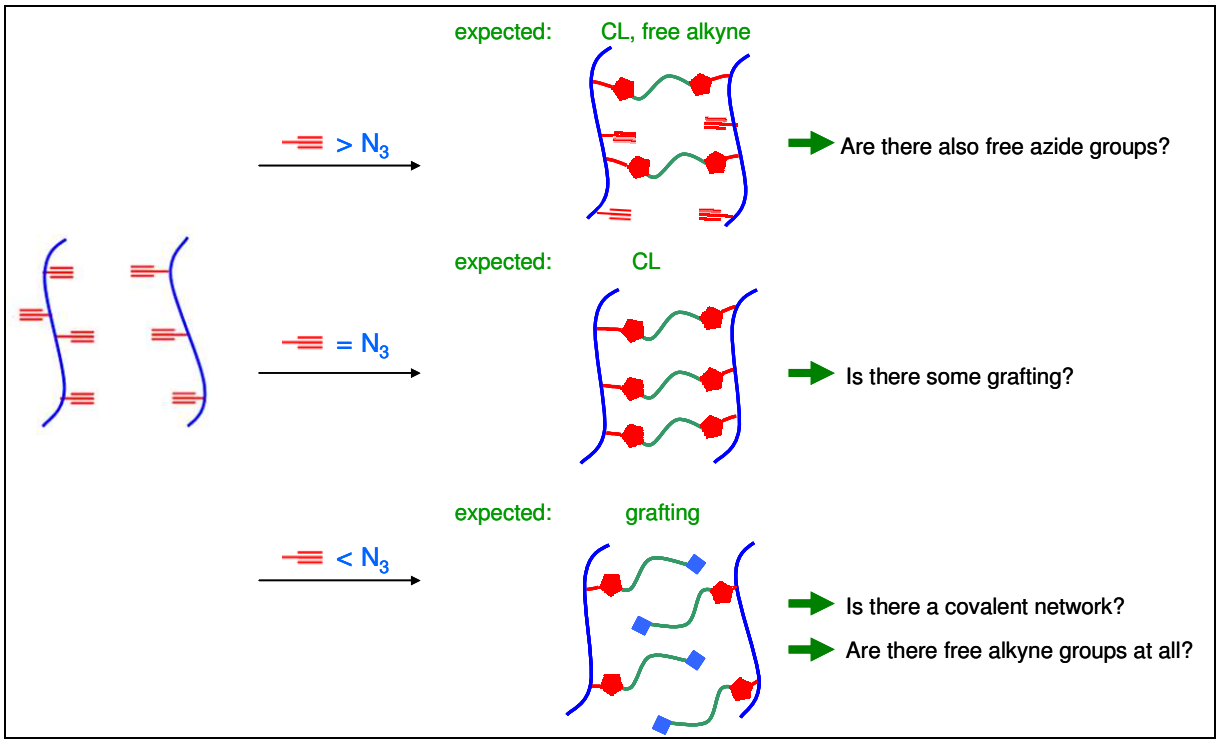

Scheme 4.4 Investigation of gelatin-based networks structure.

4.3.1 Synthesis of alkyne and azide functionalized fluorescent dyes

Fluorescein and its derivatives are the most popular reagents for covalently labeling of proteins due to their relatively high absorptivities and excellent fluorescence quantum yields.[121] The alkyne- and azido-dye used here were synthesized adopting a procedure from the literature.[122] Specifically, the alkyne- or azide-functionalized fluorescein was obtained by the EDC mediated coupling of 4-azido-pentanoic acid and 4-pentynoic acid, respectively, with fluoresceinamine (Figure 4.12). The resulting products, 2-(3-hydroxy-6-oxo-6*H*-xanthen-9-yl)-5-pent-4-ynamidobenzoic acid (**1**) and 5-(5-azidopentanamido)-2-(3-hydroxy-6-oxo-6*H*-xanthen-9-yl)benzoic acid (**2**), were characterized by NMR and the formation of the new compounds was furthermore confirmed by their fluorescence. Fluoresceinamine did not show any fluorescence; however the conversion of its amine to an amide restores the fluorescent properties, by changing the electronic influence of the nitrogen electron ione pair.[123] The products **1** and **2** will be referred to as alkyne- and azido-functionalized fluorescein dyes.

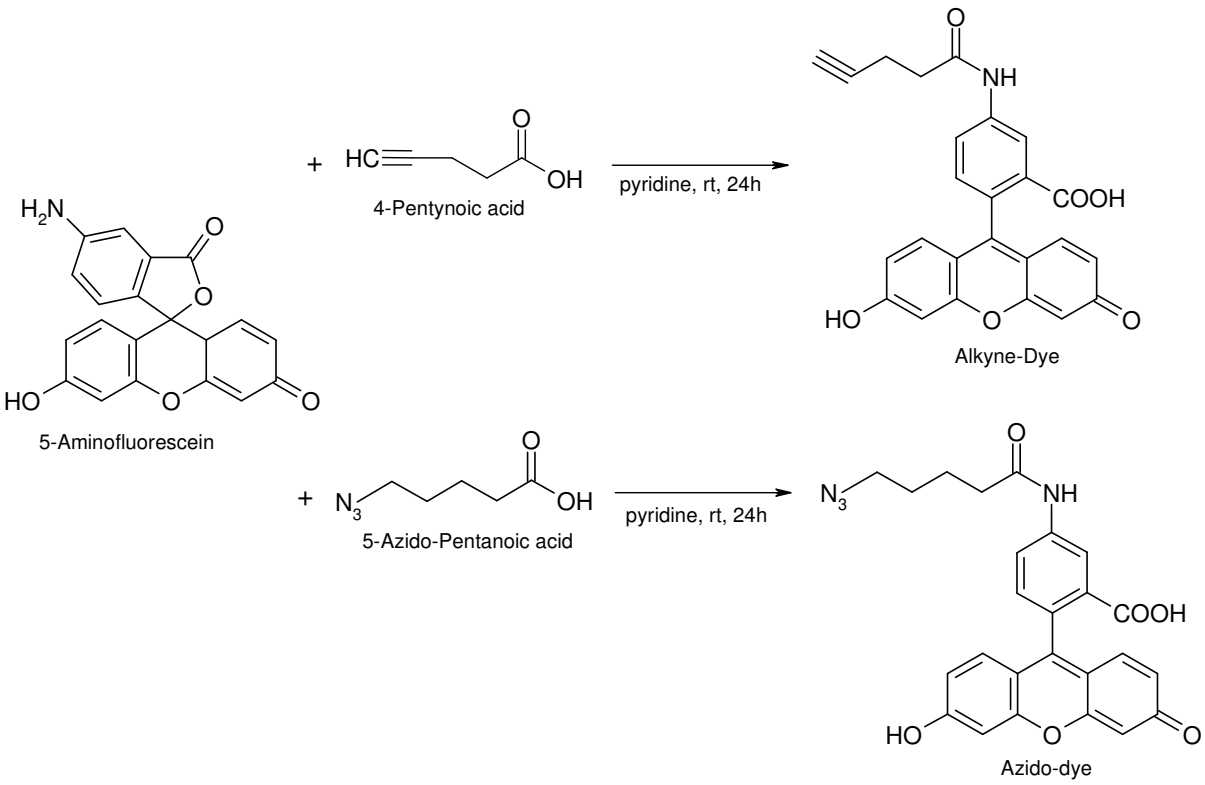

Figure 4.12 Synthesis of alkyne-functionalized fluorescein and azido-fluorescein by reaction of 5-Aminofluorescein with 4-pentynoic acid and 5-azido-pentanoic acid, repespectively.

4.3.2 Labelling of Gelatin networks with alkyne- and azido-functionalized fluorescein dye

In order to elucidate the network structure gelatin-based hydrogels were, firstly, labeled with an alkynyl-functionalized fluorescent dye. Here, NGs networks at different alkyne to azide ratio were allowed to react with an alkyne-functionalized fluorescent dye using $CuSO_4 \cdot 5H_2O$ and sodium ascorbate as catalyst, to check the presence of dangling chains. The hydrogels were incubated with the fluorescent dye for three days at room temperature. After three days, the hydrogels were extensively washed with PBS buffer, 1:1 methanol/ H_2O solution, and water to remove copper and the eventual non-covalently attached fluorescent dye.

As a control, gelatin hydrogels were incubated with the fluorescent dye without the copper catalyst, to exclude the possible physical absorption of the dye onto the hydrogel surface. The successful functionalization of the free azide groups was confirmed by using confocal laser scanning microscopy (CLSM).

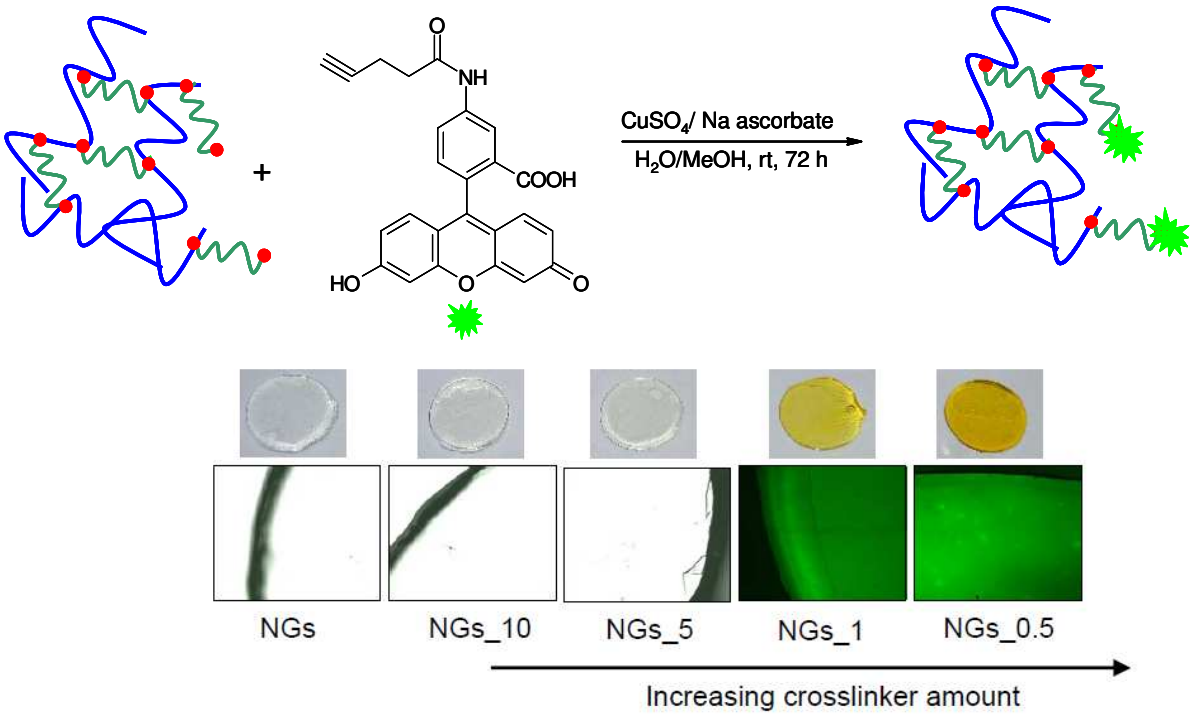

Scheme 4.5 Labelling of gelatin hydrogels by reaction of the free azido groups with alkyne-functionalized fluorescein. The hydrogels were imaged by using CLSM. The resulting images show the presence of dangling chains in sample with a high crosslinking density.

As shown in scheme 4.5 gelatin networks with an alkyne:azide ratio 5:1 and 10:1 did not show any fluorescence, whereas a moderate and strong fluorescent labeling was observed at a ratio 1:1 and 0.5:1, respectively. The absence of fluorescence at the lower crosslinker amount shows that the bifunctional crosslinker reacted on both sides with the gelatin-alkyne groups. The fluorescence observed using an equimolar ratio between alkyne and azide or a crosslinker amount higher than the alkyne groups could be explained with the presence of dangling chains in the network structure. The amount of fluorescent dye attached to the free azido groups within the

network was determined by fluorescence measurement. For this purpose, the hydrogels were degraded in an alkaline solution (pH 14) at 50 °C. Subsequently, the obtained solutions were adjusted to pH 10 and the fluorescence was measured. Because of the pH sensitivity of fluorescein, all measurements were performed at the same pH value. The amount of attached dye was quantified by the use of a calibration curve determined for the fluorescein dye. The values are reported in the Table 4.3.

The amount of dye reported as µmol of dye/g of hydrogel was 0.21 µmol/g for NGs at an alkyne:azide ratio 0.5:1, and 0.036 µmol/g for NGs at the ratio 1:1. This result suggests that the number of dangling chains was higher at the alkyne:azide ratio 0.5:1 than at 1:1 ratio, as expected. Since the largest variation in mechanical properties between hydrogels containing different types of crosslinkers were observed at the ratio 1:1, the structure of the other networks at this particular ratio was investigated. NGo_1, NGd_1 and NGp_1 were reacted with an alkyne-fluorescent dye, as described before, and the fluorescent labeling, was observed and quantified by confocal laser scanning microscopy and fluorescence spectroscopy, respectively. Moderate fluorescence intensity was observed in NGo_1 and NGd_1, while a really weak fluorescence was detected in NGp_1. Interestingly, the presence of localized fluorescence spots was observd in NGd_1 (Figure 4.13). The amount of dye bound to the free functional azide groups was 0.015 µmol/g in NGo_1, 0.018 µmol/g in NGd_1 and 0.0063 µmol/g in NGp_1. Here the difference in fluorescent properties could be explained with the structure and the length of the crosslinker.

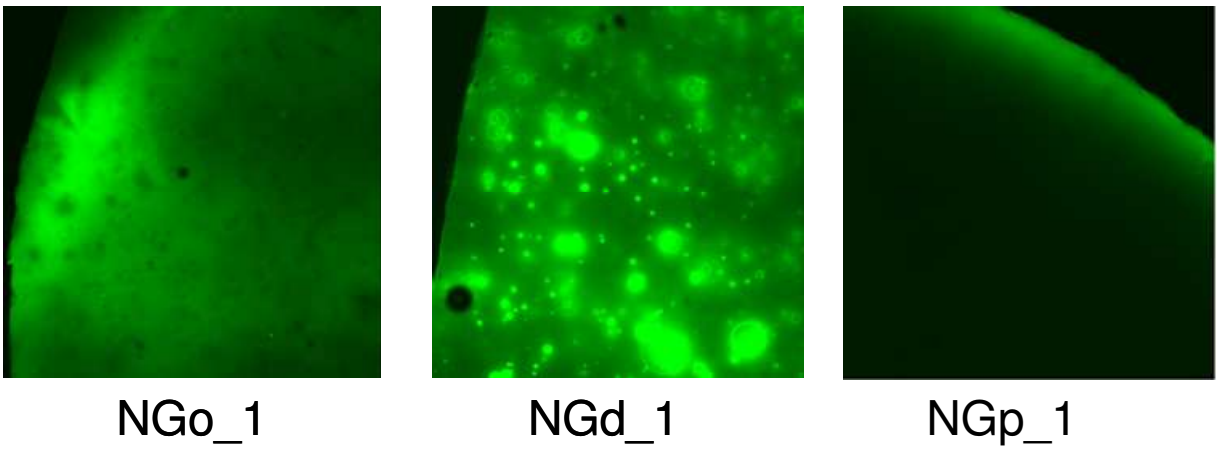

Figure 4.13 Confocal laser scanning microscopy images of NGo_1, NGd_1 and NGp_1 after incubation with alkyne-fluorescein dye. As shown in these pictures NGp_1 contains the lowest amount of dangling chains.

Long and flexible linkers like 1,12-diazidododecane or PEG-diazide can easily reach the alkyne groups on the gelatin backbone, resulting in a low number of dangling chains. Crosslinkers with a rigid structure like 4,4-diazidostilbenedisulfonic acid do not allow a further crosslinking when the network is starting to form. For this crosslinker type, a high fluorescence was observed and the highest amount of dye attached to the hydrogel was found. At the alkyne:azide ratio 5:1 and 10:1 the networks consist only of crosslinking and almost no difference in the mechanical properties were observed. At the ratio 0.5:1 and 1:1 the neworks consist of crosslinking and dangling chains, which seems to have an effect on the elastic properties of the networks. For instance, at the ratio 1:1 the E modulus varied from 90 kPa to 635 kPa.

The investigation of the structure of gelatin based hydrogels to check the presence of dangling chains that could have an influence on the mechanical properties of the resulting material is of fundamental importance. However, the presence of other free functional groups within the hydrogels which could be used as drug linking point would be also important. For this purpose, gelatin based hydrogels crosslinked with 4,4'-diazido-2,2'-stilbenedisulfonic acid, at different alkyne: azide

ratios were reacted with an azido-functionalized dye, using the same procedure as described above. The labeling of the free functional groups within the hydrogel was detected by confocal laser scanning microscopy (CLSM) and fluorescence spectroscopy as well.

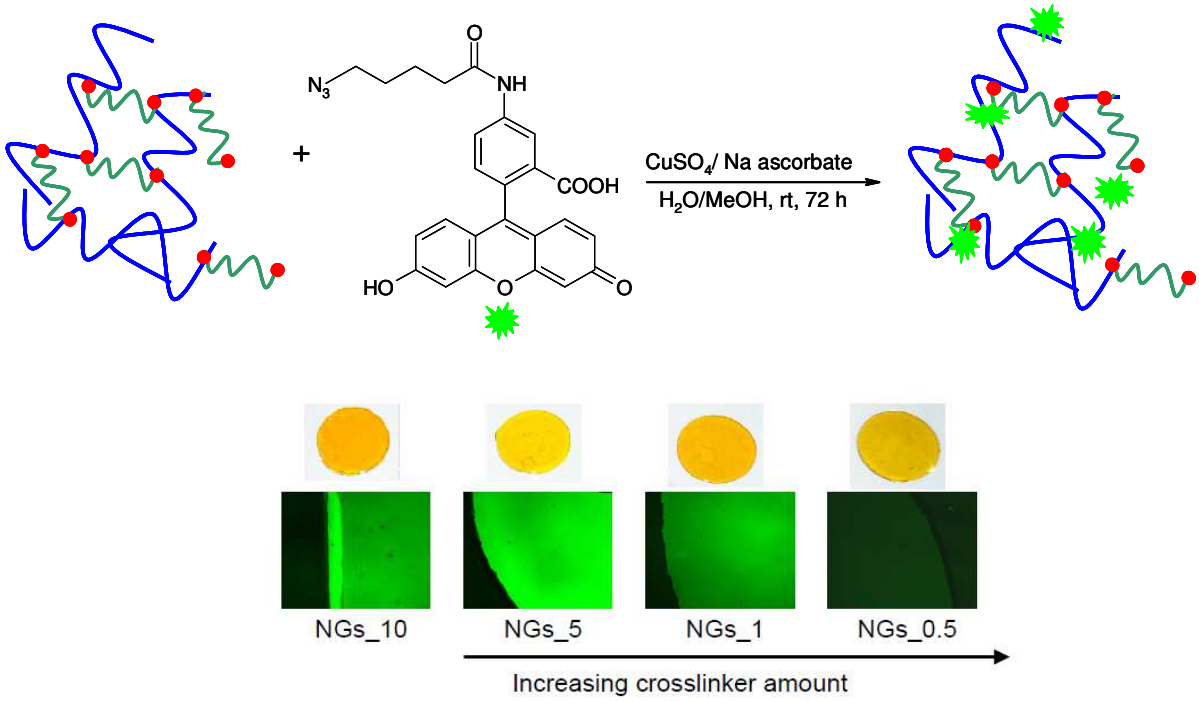

Scheme 4.6 Labelling of gelatin hydrogels by reaction of the free alkyne groups with azido-functionalized fluorescein. The confocal laser scanning microscopy images show the presence of fluorescence in all the hydrogels composition.

Increased fluorescence intensity by decreasing the amount of crosslinker was observed. Free alkyne groups were found at all alkyne:azide ratio as shown in Scheme 4.6. The presence of free alkyne groups was evaluated also in the systems NGo_1, NGd_1 and NGp_1. As shown by confocal microscopy images, free functional groups were found in all the hydrogel compositions (Figure 4.14). The amount of dye bound to the free alkyne groups was determined as well, and is reported in Table 4.3. The amount of free alkyne groups detected in NGs_5 and NGs_10 was lower than the expected value. The amount of crosslinker used for the synthesis of these hydrogels is significantly lower compared to the alkyne groups, therefore a high content of alkyne functionalities should be detected. On the other

hand, in samples containing a lower amount of crosslinker some helicalization took place, as described in section 4.2.2 and therefore some of the free alkyne groups may not be accessible for the labeling with fluorescein dye.

Another possible explanation for the determination of a low amount of alkyne groups, could be the alkyne homocoupling, a process which is also catalyzed by copper.[78]

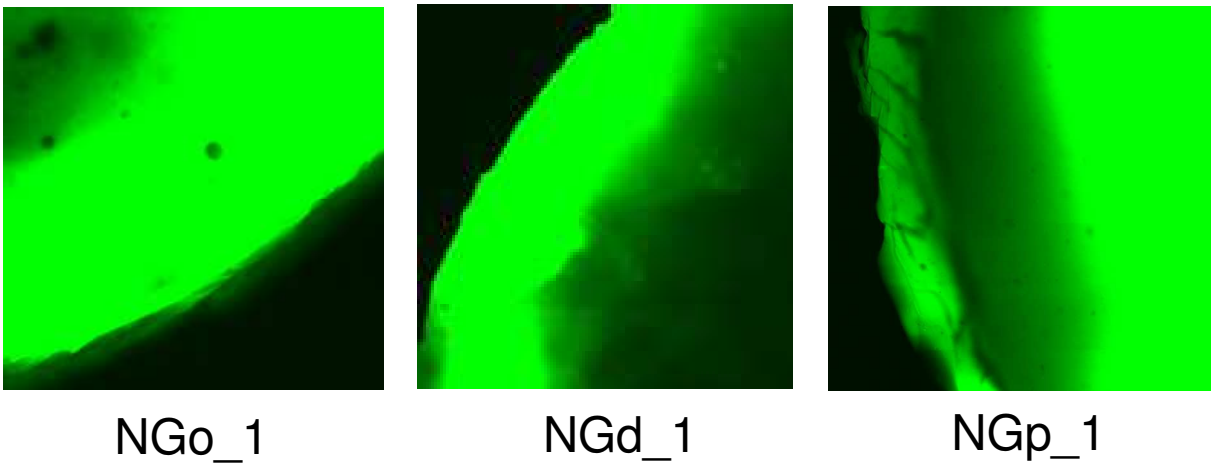

Figure 4.14 Confocal laser scanning microscopy images of NGo_1, NGd_1 and NGp_1 after incubation with azido-fluorescein dye.

Table 4.3 Amount of fluorescent dye bound to the free alkyne and azido groups within the gelatin hydrogel. The values are reported as µmol of fluorescent dye/gram of hydrogel. F-alk: alkyne-functionalized fluorescein; F-N_3: azido-functionalized fluorescein.

Sample	µmolF[a]/ g Hydrogel
NGs_0.5 + F-alk	$2.08 \cdot 10^{-1}$
NGs_1 + F-alk	$3.62 \cdot 10^{-2}$
NGo_1 + F-alk	$1.50 \cdot 10^{-2}$
NGd_1 + F-alk	$1.80 \cdot 10^{-2}$
NGp_1 + F-alk	$6.30 \cdot 10^{-3}$
NGs_0.5 + F-N_3	$4.14 \cdot 10^{-2}$
NGs_1 + F- N_3	$4.30 \cdot 10^{-1}$
NGs_5 + F- N_3	$1.67 \cdot 10^{-2}$
NGs_10 + F- N_3	$2.00 \cdot 10^{-1}$
NGo_1 + F- N_3	$2.45 \cdot 10^{-1}$
NGd_1 + F- N_3	$3.98 \cdot 10^{-1}$
NGp_1 + F- N_3	$3.24 \cdot 10^{-1}$

a: µmol of Fluoresceint dye

However, in this case higher values of elastic moduli would have been observed. The alkyne groups could be potentially used as drug linking point choosing the system with the mechanical and physical properties appropriate for the required applications.

The use of fluorescent dyes enabled the understanding of the network structure and the postulated hypothesis could be verified. As shown in scheme 4.7, when an amount of alkyne higher than the azido functional groups is used the resulting network will consist of crosslinks and free alkyne groups, as expected. When an equal ratio between the two functional groups is used, a covalent network containing also dangling chains and free alkyne groups is formed. In the last case, if an excess of crosslinker is used, a covalent network with a higher number of dangling chains compared to the previous one is obtained, as confirmed by fluorescence measurements.

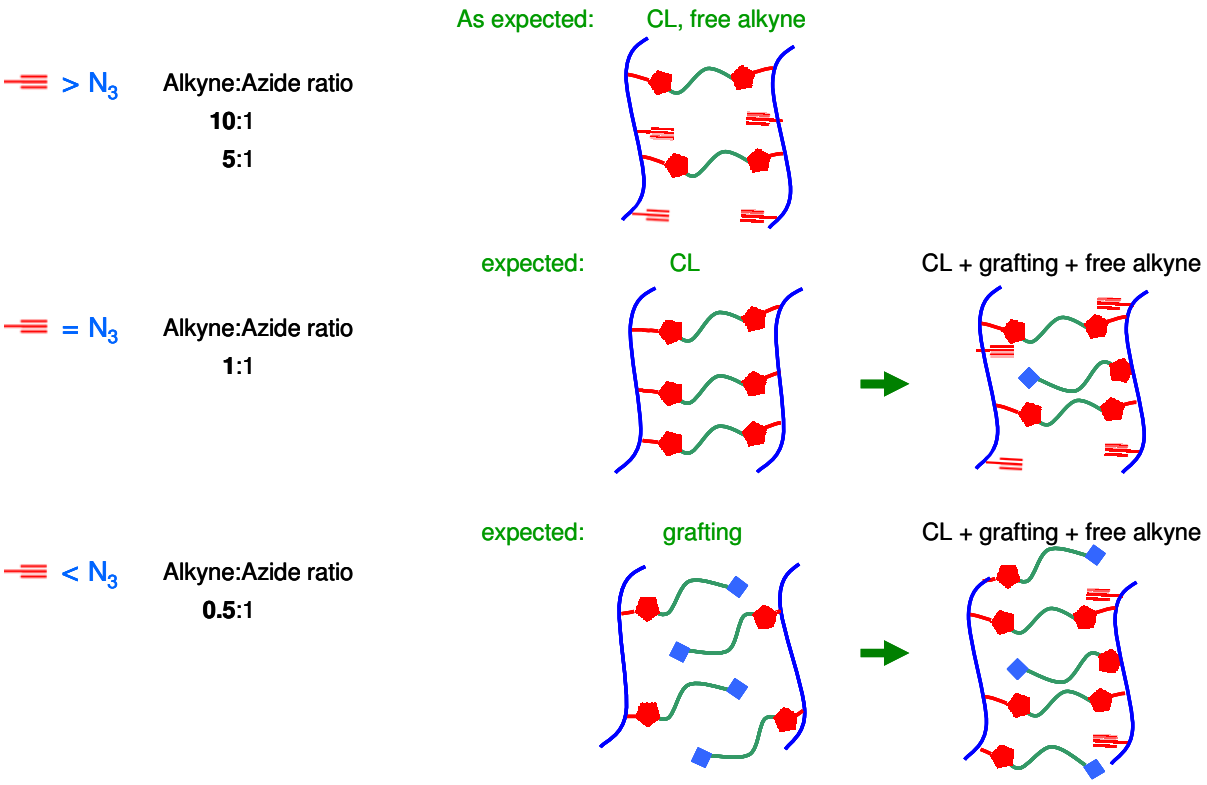

Scheme 4.7 Elucidation of the structure of gelatin based hydrogels.

By using the resulting amount of dye reacted with the free azide and alkyne groups, a quantification of the crosslinliking and grafting was possible. The amino content of the gelatin used in this study was 270 µmol/g. After the functionalization of the amino groups with propiolic acid, an alkyne content of 194.4 µmol/g was measured.

After the network formation, considering the grafting and free alkynes groups, the crosslinking (*c*) amount will be:

$$c = 194.4\,\mu mol - x - y \qquad \text{(eq. 4.4)}$$

where 194.4 µmol are the alkyne groups available for the cosslinking, x is the detected amount of dangling chains and y is the amount of free alkyne functionalities detected after the network formation. The values x and y are determined, here, considering the dry mass of the hydrogels, since the alkyne content of gelatin after functionalization was determined on the dry material. By determing the ratio between the values obtained from eq. 4.4 and the number of alkyne groups, the amount of crosslinking and grafting were determined for all the hydrogel compositions investigated. The values are reported in the table 4.4. The crosslinking (%) in the table 4.4 is referred to the percentage of alkyne groups involved in the formation of covalent netpoints.

Table 4.4 determination of the amount of graft and crosslinking in gelatin-based hydrogels.

Sample ID	Crosslinking (%)[a]	Graft (%)	Azide groups (µmol)	Alkyne groups (µmol)	(%)
NGs_0.5	98.5	0.57%	1.14	0.27	0.13
NGs_1	97	0.1	0.20	2.45	1.2
NGo_1	96	0.06	0.12	4	2
NGd_1	96	0.05	0.11	4.2	2.1
NGp_1	97	0.022	0.044	2.58	1.3

a: The percentage is related to the amount of alkyne groups available on the gelatin chains

The determination of the grafing and crosslinking content enabled the correlation of the mechanical properties to the nework structure. As reported in table 4.3 the highest amount of dangling chains was observed in sample NGs_0.5, in which an excess of crosslinker was used. At this ratio, one would expect a high degree of grafting accompanied by a low number of direct crosslinks, due to the large excess of crosslinker used. However, the percentage of alkyne groups which forms the crosslinking is similar to NGs_1. This means that the predominat reaction is the crosslinking. At the alkyne:azide ratio 1:1, by variation of the crosslinker type, different contents of dangling chains were found. The largest variations in mechanical properties (e.g. Young's modulus) were observed at this particular ratio, whereas at the ratios 5:1 and 10:1 almost no differences were observed. Even though, the content of dangling chains is low compared to the amount of crosslinking, it affected the final properties of the gelatin-based hydrogels. A crosslinking amount of 100% was not reached in any composition because it is likely that not all the crosslinker will react.

4.4 Summary

The Copper catalyzed azide-alkyne cycloaddition was used to prepare a series of well-defined gelatin-based hydrogels with controlled architecture and varied mechanical properties. Gelatin-based hydrogels were synthesized via a two steps procedure. In the first step, alkyne pendant groups were introduced in the gelatin backbone, while in the second step the gelatin hydrogel were synthesized by the use of different azide crosslinkers. Different types of crosslinker were used to vary both the length and the molecular flexibility of the linkage between the gelatin chains, in order to tailor the material properties. By variation of the alkyne:azide ratio and of the

crosslinker type the elastic modulus (*E*: 50 kPa→ 635 kPa, *G'*: 0.1 kPa→16 kPa), elongation at break (26%→153%) and the swelling degree (150→470 vol.-%) could be tailored. At the same alkyne:azide ratio, hydrogels containing a crosslinker with a rigid structure (NGs) showed a lower swellability of those containing longer and flexible crosslinker. However, the highest amount of dangling chains was found in the NGs hydrogels and a high water uptake should be observed. The triazole units formed during the click chemistry reaction have a pseudoaromatic nature that allows π-stacking.[124] In NGs hydrogels the aromatic rings of the crosslinker and the additional triazoles could contribute to strong noncovalent interactions, which could result in a decreased swellability.

The use of different crosslinker types and crosslinker amount affected also the renaturation of the gelatin triple helix. To correlate the final properties of the crosslinked network to their chemistry, a method that allows a detailed understanding at the molecular level was developed. The method developed is based on the labeling of free functional groups within the hydrogel with fluorescent dyes. In order to check the presence of eventual dangling chains, the hydrogels were reacted with an alkyne-functionalized dye and subsequently characterized by confocal laser scanning microscopy and fluorescence spectroscopy. The presence of dangling chains was observed in hydrogels synthesized using an alkyne:azide ratio of 0.5:1, due to the excess of crosslinker compared to the available alkyne groups. Interestingly, dangling chains were also observed using an equal molar ratio between alkyne and azide groups. A possible explanation could be found in the mechanism of the network formation. It might be that after the formation of a certain number of covalent netpoints, the movements of gelatin chains are reduced. Therefore, additional crosslinking will be possible only if the crosslinker is flexible and long

enough to reach another free alkyne group. Indeed, the highest amount of dangling chains was observed for NGs (0.20 μmol), whereas a low amount was detected for NGo (0.12 μmol), NGd (0.11 μmol) and NGp (0.044 μmol).

The gelatin hydrogels were reacted also with an azido-functionalized fluorescent dye, to check the presence of free alkyne functional groups, which could be used for the attachment of drugs and bioactive compounds. Free alkyne groups were observed in all the networks investigated. Surprisingly, the amount of free alkyne groups detected in the networks NGs5 and NGs10 was lower than expected. A possible explaination could be that the low amount of crosslinker used for the synthesis of both networks, could not hinder the physical reorganization of the gelatin chains, as observed in the WAXS measurements. Due to the conformation of some chains, the azido-functionalized fluorescent dye could not react with all the free alkyne groups and a low amount was detected.

5. Synthesis and Characterization of Hyaluronic acid-based Hydrogels

The data presented in this chapter have been published as: S. Piluso, B. Hiebl, S. N. Gorb, A. Kovalev, A. Lendelin, A. T. Neffe, Hyaluronic Acid-Based Hydrogels Crosslinked by Copper Catalyzed Azide-Alkyne Cycloaddition with Tailorable Mechanical Properties, *Int. J. Artif. Organs*, **2011**, *34*, 192-197.

In this chapter, hyaluronic acid-based hydrogels with defined properties were synthesized transferring the method applied to gelatin to a polysaccharide. The resulting material properties were characterized by water uptake, rheological measurements and microindentation.

5.1 Synthesis and characterization of alkyne-functionalized hyaluronic acid

Alkyne-functionalized hyaluronic acid was obtained by EDC/NHS mediated coupling of propargylamine to the carboxylic groups (Scheme 5.1) resulting in

functionalization of about 20 mol % of the carboxylic acid groups (determined by integration of the ^{1}H NMR).

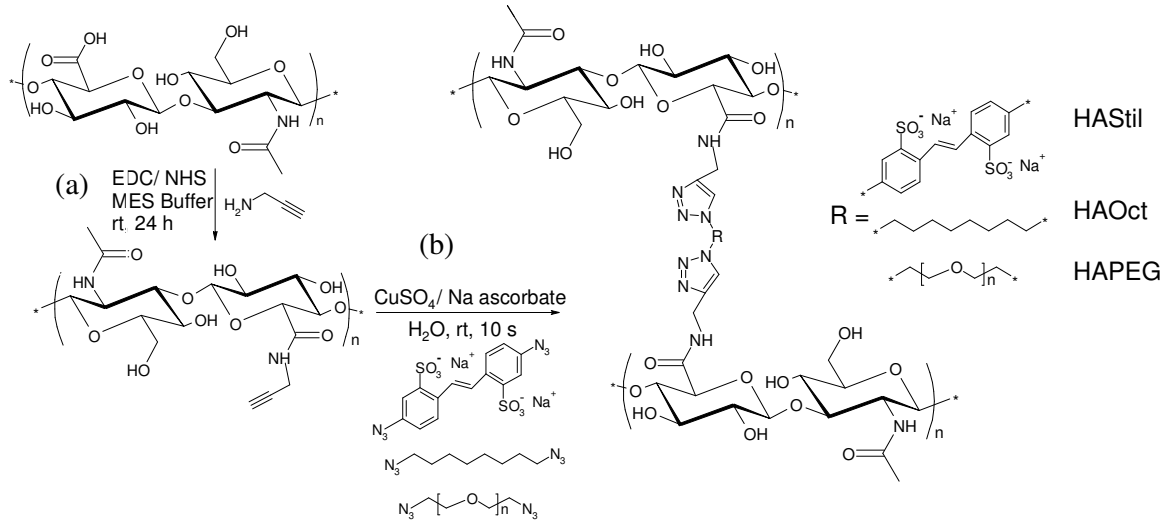

Scheme 5.1 a) Functionalization of hyaluronic acid; b) formation of hydrogels by the use of click chemistry.

The viscoelastic behaviour of hyaluronic acid (HA) before and after functionalization was investigated (Figure 5.1). "Both HA and alkyne-functionalized HA (HAPA) behaved in rheological measurements of their 1.5 wt.-% solutions in water as non-Newtonian fluids and showed shear thinning with frequency increase and low viscosity at higher shear rates. HAPA behaved as a viscous fluid in the frequency range investigated and showed a lower viscosity than HA. The different behavior of HA and HAPA gels can be explained with a change in polymer chain interactions due to the presence of the alkyne groups, whereby the amide groups in HAPA have a lower tendency to form hydrogen bonds than the free carboxylic acids in HA".[45]

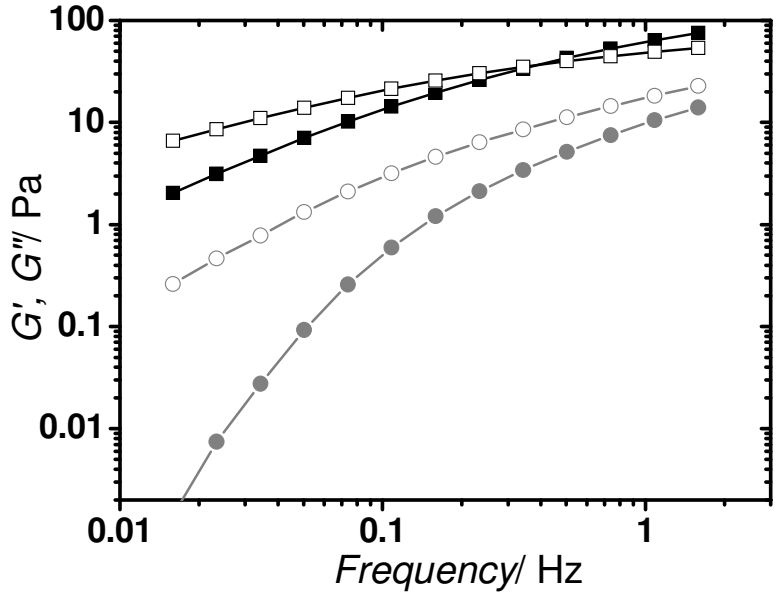

Figure 5.1 Rheological characterization of hyaluronic acid (G': -■-, G'': -□-) before and after functionalization with propargylamine (G': -●-, G'': -○-).

5.2 Synthesis of hyaluronic acid-based hydrogels

Hyaluronic acid-based hydrogels were synthesized by the use of the copper(I)-catalyzed alkyne-azide cycloaddition reaction (Scheme 5.1). Alkyne-functionalized hyaluronic acid was dissolved in a mixture H_2O/EtOH (2:1), and then a diazide, followed by the catalyst was added. As for gelatin-based hydrogels, crosslinkers with different molecular flexibility were chosen in order to tailor the mechanical properties of the resulting networks. Specifically, 4,4'-diazido-2,2'-stilbenedisulfonic acid, 1,8-diazidooctane and PEGdiazide (M_W = 1108 g·mol^{-1}, PDI<1.2,) were used as crosslinkers. 1,8-diazidooctane was synthesized as described in Chapter 4. Three different alkyne:azide ratios were used: 1: 0.5, 1:1 and 1:1.1. The hydrogels formed in less then 10 s at room temperature. The gels were repeatedly washed in 0.05 M

EDTA solution for copper removal and then equilibrated in distilled water. The hydrogels are referred to as HAStil (4,4'-diazido-stilbenedisulfonic acid as crosslinker), HAOct (1,8-diazidooctane crosslinker), and HAPEG (PEGdiazide crosslinker). Figure 5.2 shows a picture of the different hydrogel compositions. The resulting hydrogels were characterized by FT-IR, water uptake, rheology and indentation tests. Finally, cytotoxicity tests of hydrogel eluates with L929 mouse fibroblasts were performed.

HAStil HAOct HAPEG

Figure 5.2 Picture of Hyaluronic acid-based hydrogels synthesized by the use of three different type of crosslinkers.

5.3 Characterization of hyaluronic acid-based hydrogels

The copper catalyzed cycloaddition of the three different diazides linkers to the alkyne-functionalized hyaluronic acid gave the polymer networks depicted in Scheme 5.1. "The conversion at the alkyne:azide ratio 1:1 for the stilbene and octane crosslinkers was nearly complete, since no free azide could be observed in the IR. In the case of the PEGdiazide crosslinker, in the IR the azide stretching peak at 2110 cm^{-1} can be clearly observed, which is likely due to a grafting reaction".[45] In order to determine the water uptake, hyaluronic acid hydrogels were incubated at 37 °C in

PBS buffer at pH 7.4. The water uptake was determined as the ratio between the weight of the swollen hydrogels, and the weight of the dry networks. The uptake of water into the hydrogels (4590-6480 vol.-%, see Table 5.1) was composition dependent, whereby the more rigid stilbene crosslinker resulted in lower water uptake than the more flexible octane linker. A possible explanation could be that crosslinkers with flexible structure do not hinder completely the movements of the biopolymer chains, enabling the uptake of more water compared to rigid structures.

"The rheologically determined bulk properties of all investigated hydrogels are typical for covalently crosslinked hydrogels. Specifically, higher elastic moduli (G') than viscous moduli (G'') as a function of frequency were observed for all investigated hydrogels, while both moduli were frequency independent (Figure 5.3). G' could be tailored in the range of 0.55 to 3.7 kPa. By variation of the crosslinking density and crosslinker type, the hydrogel properties, e.g. water uptake and elastic moduli, could be tailored. Comparing the hydrogels with the two shorter crosslinkers, HAOct and HAStil, the more flexible linker 1,8-diazidooctane gave higher elastic moduli than the more rigid stilbene. On the other hand, the water uptake was also higher for the HAOct gels than for the HAStil gels. This behaviour could be due to the coexistence of grafting and crosslinking together".[45] The grafted chains can interact with each other, forming entanglements or physical interactions, giving higher stiffness to the resulting network, but allowing at the same time the uptake of more water. This means that the number of direct crosslinks might be higher for the HAStil hydrogels, than for HAOct. By variation of the alkyne/azide ratio, keeping constant all the other parameters, for some hydrogels composition an increased elastic modulus was not accompanied by a decreased water uptake.

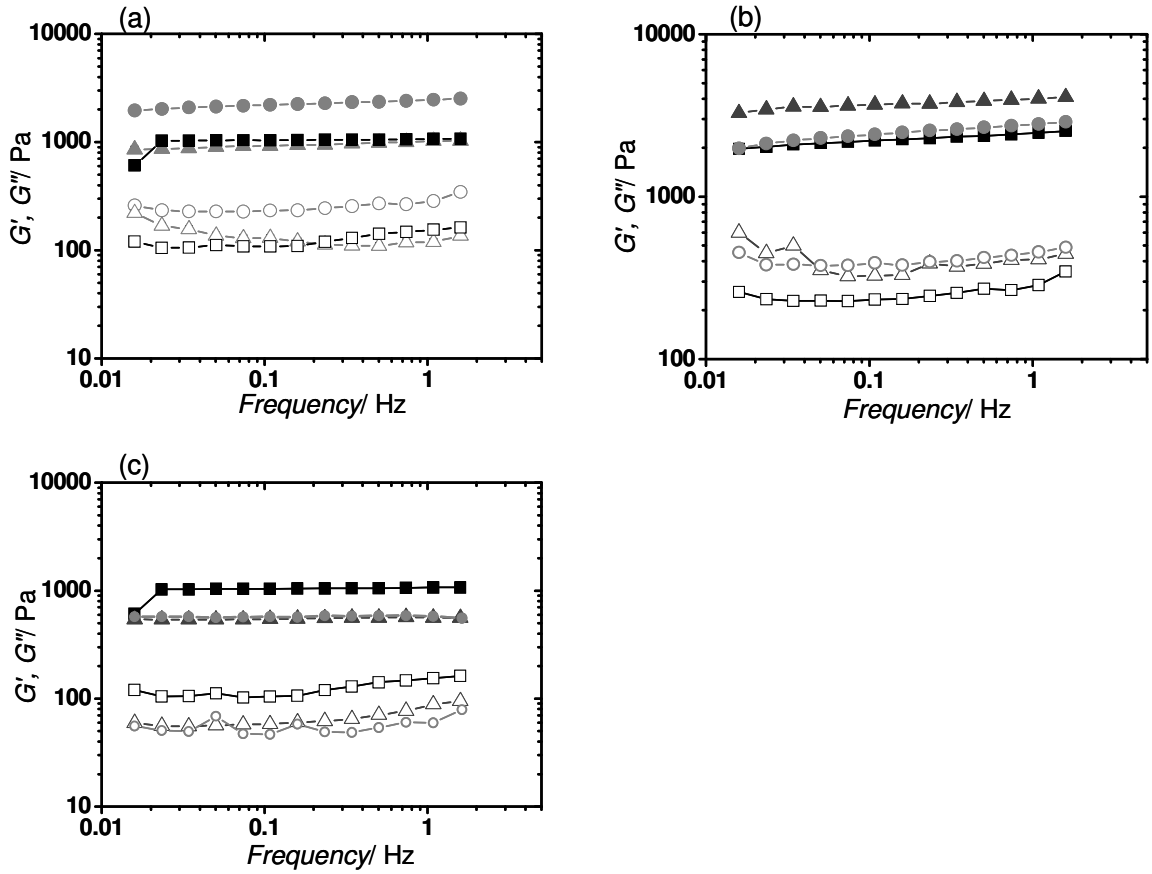

Figure 5.3 (a) Rheological characterization of hyaluronic acid-based hydrogels by variation of crosslinker type (●) HAOct, (▲) HAPEG and (■) HAStil. (b) Rheological investigation of HAOct as a function of the alkyne:azide ratio: 1:0.5 (▲), 1:1 (■),1:1.1 (●). (c) Rheological investigation of HAStil as a function of alkyne: azide ratio: 1:0.5 (▲), 1:1 (■),1:1.1 (●).

Hydrogel mechanical properties were determined also by microindentation. In microindentation, the recorded force-distance curves were used to calculate the elasticity modulus of the hydrogels[125] and to estimate the adhesion force (retracting process) by using the Johnson-Kendall-Roberts (JKR) model, which considers the surface attraction between two solids.[126] This model is suitable for the determination of the elastic modulus of soft materials since the effects of intermolecular forces between the microindenter tip and the sample can influence microindentation testing. "For all hydrogels, elastic moduli were determined from the unloading part of the curve to consider only the elastic behavior and not the plastic deformation of the

sample".[45] The retraction profile (Figure. 5.4) shows the presence of a negative peak corresponding to the adhesive force between the sphere and the hydrogel.

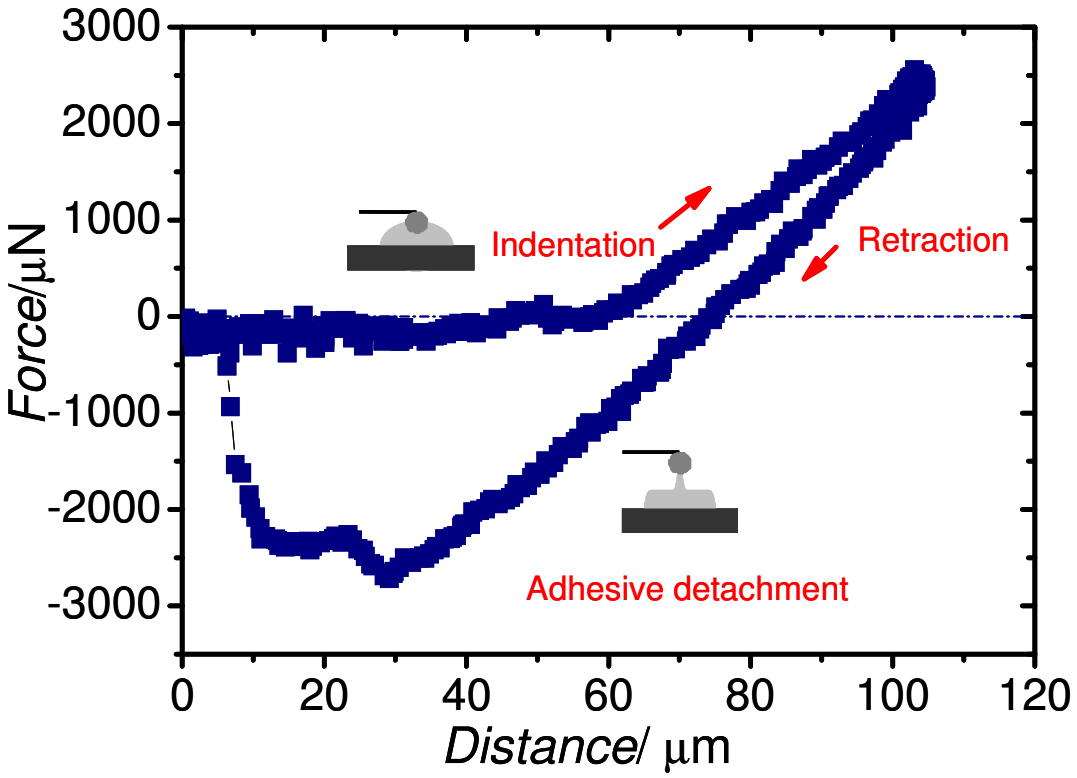

Figure 5.4 Force-distance curve used for evaluation of the elasticity and adhesive properties of the hydrogel determined by microindentation.

"The investigation of local mechanical properties by microindentation gave higher elastic moduli than the corresponding rheologically determined moduli. Microindentation can measure local elastic properties of the surface. The latter is important, because the hydrogel properties can be different at the surface from the bulk, therefore the response of the surface layer to the applied stress can also be different. Measured elastic moduli were comparable with other biological hydrogels, such as sea anemone mesogloea (1 kPa),[126] NIH 3T3 fibroblasts (5-17 kPa),[127] and attachment pads of grasshoppers (21.9-64.1 kPa).[125] Moreover, HAStil and HAOct showed stronger adhesive properties than HAPEG. Therefore, the crosslinker type affected the adhesion".[45] Interestingly, the crosslinking density had no influence on

measured adhesion. The observed difference in adhesion does not correlate with elasticity modulus. This means that the material chemistry and not material mechanics is mainly contributing to adhesive properties. The mechanical data determined by rheology and microindentation are summarized in Table 5.1.

Table 5.1 Influence of crosslinker type and alkyne:azide ratio on mechanical properties and swelling degree of hydrogels.

Sample ID	G' [kPa]	E [kPa]	W_a [J/m^2]	H [wt.-%]
HAPEG 1:1	0.9	0.8	0.03	4882 (±15)
HAStil 1:0.5	0.55	26 (± 8)	0.09 (± 0.01)	4880 (±340)
HAStil 1:1	1	19 (± 3)	0.11 (± 0.03)	4590 (±290)
HAStil 1:1.1	0.6	21 (± 9)	0.1 (± 0.01)	5120 (±500)
HAOct 1:0.5	3.7			5920 (±800)
HAOct 1:1	2.2			6480 (±70)
HAOct 1:1.1	2.5	21 (± 9)	0.11 (± 0.01)	4710(±1180)

G': shear modulus, E: Young's modulus, W_a : Work of adhesion, H: water uptake.

"In order to determine the amount of copper after washing, copper levels in the gels were determined by ICP-MS and gave for the dried materials copper contents of 6.8 mg/kg (HAStil), 280 µg/kg (HAOct), and 3.7 mg/kg (HAPEG), respectively. Cytotoxicity tests were performed to verify the possibility of using these hydrogels for biomedical applications such as soft tissue regeneration (Figure 5.5). Therefore, L929 cells were exposed to eluates of the three different hydrogel types. No cytotoxic effect was detected for the HAStil gel (1:1 ratio). Cell incubation with eluates from HAOct and HAPEG gave cytotoxic effects. The evaluation of toxicity is preliminary only. The copper level determined were low (the given values were determined on dry samples, i.e., the wt.-% copper content in swollen hydrogels is about 50 times

lower than the given numbers) and did not correspond to the measured toxicity level of the eluates".[45] Therefore, the copper- catalyzed alkyne-azide cycloaddition can be used to synthesize biocompatible polymer networks, if copper is removed by washing with EDTA. The determination of free azide groups, especially for the aliphatic crosslinkers, remains to be performed.

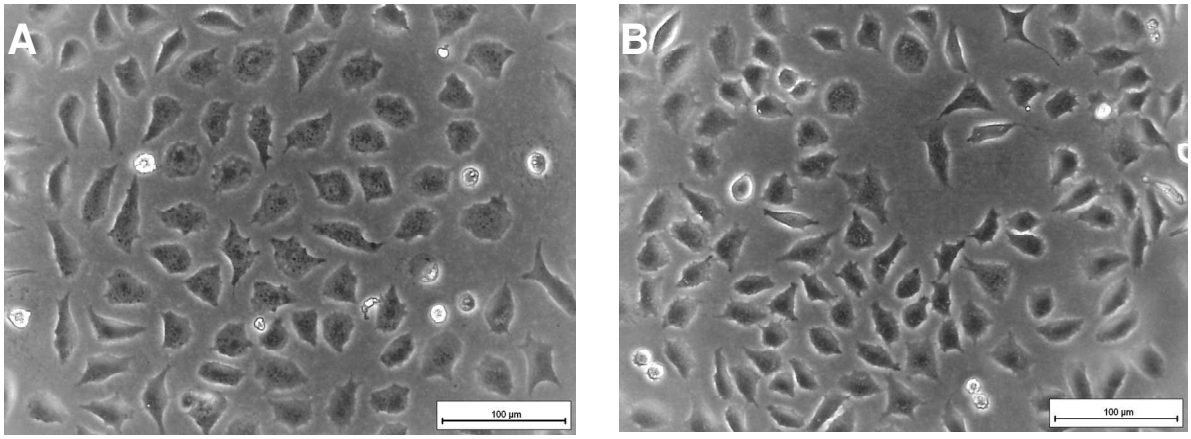

Figure 5.5 (A) L929 cells on polystyrene and (B) after exposition to eluates of HAStil (ratio 1:1). No morphological changes or cell lysis were observed.

5.4 Summary

By the use of the copper(I)-catalyzed alkyne-azide cycloaddition, hyaluronic acid-based hydrogels with tailorable properties could be prepared. Hydrogels were prepared by using a two-step synthetic route. In the first step of the synthesis alkyne groups were incorporated into the polysaccharide backbone. The functionalization with propargylamine affected the viscoelastic properties of hyaluronic acid. Hyaluronic acid behaved as a viscous fluid (G''>G') in the low frequency range, whereas an elastic behaviour (G'>G'') was observed with the increase of frequency due to interaction between the polymer chains. After the functionalization, hyaluronic

acid behaved predominantly as a viscous fluid, due to the lower tendency of the amide groups in HAPA to form hydrogen bonds compared to the free carboxylic acids in HA. In protein-based biopolymers, as described in chapter 4, an increase of the thermal stability and the mechanical strength was observed after the functionalization of gelatin amino groups with propiolic acid.

In the second step, alkyne-functionalized hyaluronic acid was crosslinked with three different crosslinker types. By variation of molecular parameters, like crosslinker type and crosslinking density, the local and bulk mechanical properties (G': 0.55 kPa→ 3.7 kPa; E: 0.8 kPa→ 26 kPa) of the hydrogels could be tuned in the kPa range. The elastic moduli of the hydrogels were comparable to soft tissues such as brain tissue. The washed materials contained at most 6.8 mg copper per kg dry weight and the eluate of the gel crosslinked with diazidostilbene did not show toxic effects on L929 cells. The method used for synthesizing gelatin-based hydrogels enabled the formation of hyaluronic acid-based hydrogels with defined properties. However, the mechanical properties (e.g. shear modulus) of gelatin-based materials, were significantly higher (at least one order of magnitude) compared to hyaluronic acid-based hydrogels. The different behaviour of the resulting networks could be due to the inherent properties and structure of the biopolymers used as starting materials. The protein-based biopolymer enabled the formation of hydrogels with higher mechanical stiffness compared to those obtained from the polysaccharide-base biopolymer, which formed soft networks able to take up great amount of water.

6. Influence of Hydrolytic and Enzymatic Degradation on the Material Properties of Gelatin-based Hydrogels

In this chapter, investigations of the hydrolytic and enzymatic degradation of gelatin-based hydrogels are discussed. The partially-degraded materials were characterized by water uptake, mass loss, tensile tests, thermal properties and WAXS.

6.1 Hydrolytic degradation of gelatin-based hydrogels

Here the hydrolytic and enzymatic degradation of gelatin-based hydrogels with different crosslinking density and crosslinker types was investigated. Although the chemical reactions responsible for hydrogel degradation are known, the change of material properties during degradation is not and has to be investigated. Moreover,

the influence of the network structure is expected to play a major role. Physical and mechanical properties of hydrogels are highly dependent on the polymer backbone chemistry and crosslinking density. Therefore, the degradation behavior will also be a function of the network topology.[128]

6.1.1 Change of physical properties during degradation

To study the degradation of hydrogel networks, NGs and NGo sample compositions were investigated, whose synthesis and network structure are reported in section 4.2.1. Dried networks were incubated with 5 mL PBS in a 37 °C water bath for 6 weeks time. At selected time points, the samples were removed from the degradation medium and weighed. The water uptake (*H*) was then determined using the equation 4.2, where the wet and dry masses of the partially-degraded network are referred to the selected degradation time points. At the same time, the mass loss (μ) of retrieved samples was determined as follow:

$$\mu = \frac{m_0 - m_d}{m_0} \qquad \text{(eq. 6.2)}$$

where m_0 is the initial dry mass of freshly-synthesized samples. Figure 6.1 shows water uptake and mass loss profiles of NGs networks (synthesized at different alkyne:azide ratios) during the course of hydrolytic degradation.

Variations of water uptake during degradation are ruled by the change of crosslinking density and are in good agreement with the mechanical behavior of partially-degraded hydrogels. As expected, an increase of water uptake at the

macroscopic level was dictated by a decrease of crosslinking density on the molecular scale. For example, the degradation profile of sample NGs_10, having the lowest crosslinking density of all studied samples, reveals an initial stage (ca. 3 weeks time) characterized by a constant increase in water uptake. The second stage had a drastic increase; finally, decrease of water uptake was observed again. The drastic increase observed in the second phase could be likely due to the auto-catalyzed hydrolysis[129] of amide bonds, resulting in increased network mesh size. In the final phase of degradation, the sample weight is decreased due to the cleavage of remaining amide bonds and consequent release of formed oligomers. Hydrogels NGs_5, showed 40 wt.-% increase of water uptake after six weeks of hydrolytic degradation, following a similar trend as samples NGs_0.5 (35 wt.-% increase), but in contrast to samples NGs_1 (nearly-constant *H*). Also in this case, the water uptake profiles can be explained by considering the change of network architecture during the course of hydrolysis. Even though hydrogels NGs_0.5 are highly crosslinked, the increase in water uptake is likely to be related to the higher content of dangling chains compared to hydrogels NGs_1 (section 4.3.3). The highest degradation rate was found for NGs_10, which underwent a mass loss of about 34 wt.% after 1 day and 65 wt.% after six weeks of hydrolytic degradation.

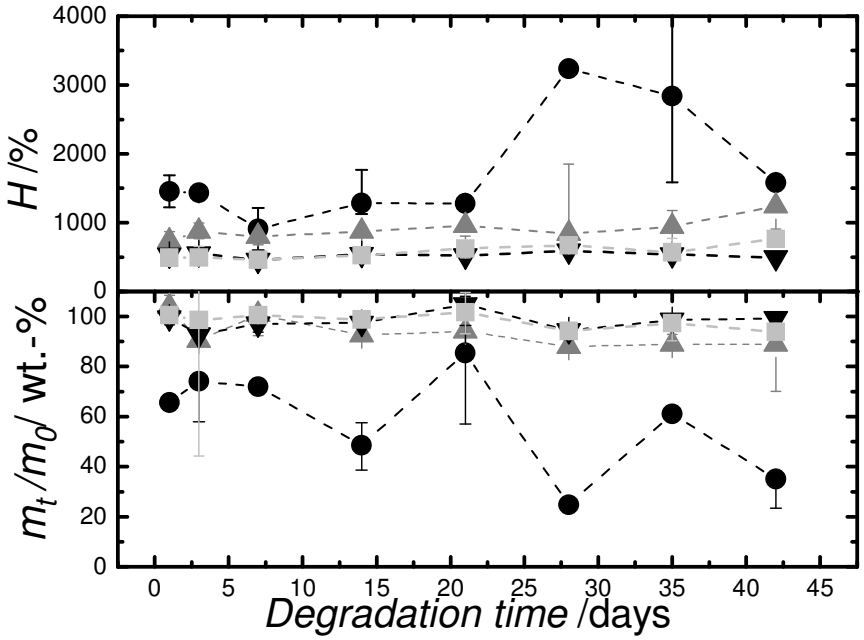

Figure 6.1 Water uptake (H) and remaining mass (m_t/m_0) of NGs hydrogels during hydrolytic degradation at 37 °C. (●) NGs_10, (▲) NGs_5, (▼) NGs_1 and (■) NGs_0.5.

On the other hand, networks with increased crosslinking density appeared to be less sensitive to degradation in the time frame investigated. Infact, the presence of more crosslinker units may cause an increasing of hydrophobicity compared to NGs_10 samples, where the hydrophilicity of gelatin has a predominant effect. Specifically, NGs_1 showed a mass loss of 0.8 wt.% after 6 weeks, while NGs_0.5 and NGs_5, showed a mass loss of 6 wt.% and 11 wt.%, respectively.

Figure 6.2 shows the water uptake and the mass loss of NGo hydrogels during the degradation time. As described for NGs networks, the increase of water uptake is directly related to the decrease of crosslinking density. NGs_0.5 and NGs_5, showed a mass loss of 6% and 11%, respectively.

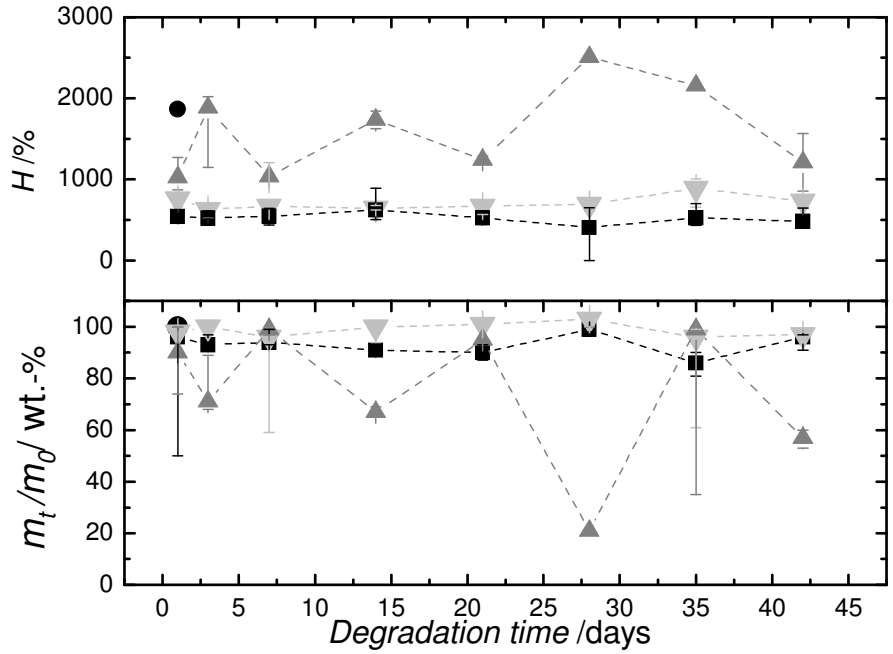

Figure 6.2 Water uptake (*H*) and remaining mass (m_t/m_0) of NGs hydrogels during hydrolytic degradation at 37 °C. (●) NGo_10, (▲) NGo_5, (▼) NGo_1 and (■) NGo_0.5.

The water uptake of NGs_0.5 and NGs_1 was almost constant, while NGo_5 showed an increase of 37 wt.-% in the last stage of degradation. Interestingly, the sample NGo_10 was degraded after 1 day of hydrolytic degradation. As described in chapter 4, NGo_10 is a very soft hydrogel with a G' of 0.1 kPa at 37 °C. Consequently, the low crosslinking density and the high diffusion of water, led to the fast degradation of this sample. The increase in water uptake of NGo_5 was associated with a decrease in mass loss of 43 wt.-% after six weeks of degradation.

The crosslinker type had almost no influence on the degradation behavior of samples with high crosslinking density, whereas it strongly affected the degradation profile of samples with lower crosslinking density. Samples NGs_5 showed a significantly slower decrease in water uptake and mass loss compared to samples NGo_5. This difference could be related to the more flexible structure of 1,8-diazidooctane compared to 4,4'-diazido-2,2'-stilbenedisulfonic acid, which allows for more water diffusion into the gel matrix.

6.1.2 Change of mechanical properties during degradation

The knowledge of the degradation time interval, especially the time frame in which the mechanical properties (like tensile strength and elasticity) are maintained, is extremely important for materials e. g. intended for biomedical applications. For these reasons, the change of mechanical properties was studied during hydrolytic degradation of the gelatin-based hydrogels. Figure 6.3 summarizes the change of rheological and tensile properties in partially-degraded NGs hydrogels.

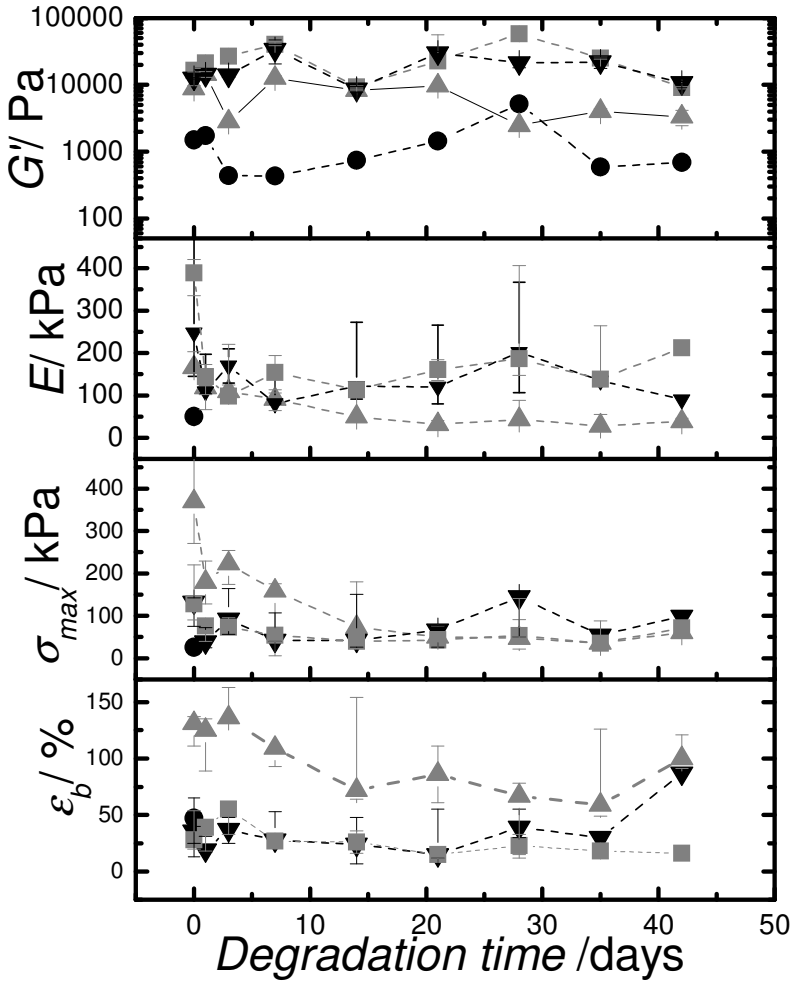

Figure 6.3 Change of material properties during hydrolytic degradation of NGs hydrogels at 37 °C from top to bottom: shear modulus, G'; Young's modulus, E; maximal tensile strength, σ_{max}; elongation at break, $\varepsilon_{b.}$ (●) NGo_10, (▲) NGo_5, (▼) NGo_1 and (■) NGo_0.5.

No significant changes were observed during rheological measurements (shear modulus (G')). G' of sample NGs_10 was not decreased during the course of degradation, even though a consistent mass loss was observed in the same degradation time frame. A possible explanation could be that changes in G' are only observed when elastic network chains are cleaved. Moreover, hydrolysis of elastic chains results in the formation of two non-elastic dangling ends, which leads to increased water uptake and mass loss, without a change in G'.

The change in mechanical properties was also monitored by tensile tests. Tensile tests could be performed for samples NGs_0.5, NGs_1 and NGs_5 for the time frame investigated, while these tests could not be performed for samples NGs_10, even after 1 day of degradation. Young's modulus (E) was decreased from 389 kPa (t= 0) to 212 kPa (t= 6 weeks) in samples NGs_0.5, while a decrease from 204 kPa to 90 kPa and from 166 kPa to 38 kPa was observed in samples NGs_1 and NGs_5, respectively. In contrast to samples NGs_5 (369 → 60 kPa), a slight decrease of maximum tensile strength (σ_{max}) was observed for samples NGs_0.5 and NGs_1. The tensile strength of NGs_5 decreased already after one day of degradation. A possible reason for that could be that at 37 °C the defolding of the triple helices occurred, leading to a decrease of the crosslinking density of the sample. The elongation at break (ε_b) was almost constant for the highly crosslinked networks, while an initial decrease and large variation between replicas was observed for NGs_5.

These mechanical investigations showed that the hydrolytic degradation affected the elasticity of the gelatin-based hydrogels, even if a decrease in mass loss or an increase in water uptake was not observed for all the samples. It is very likely that a certain number of amide bonds was hydrolyzed, leading to a decrease in the mechanical properties. However the fragments formed were not small enough to be

released from the matrix and no mass loss was observed. The same behavior has been reported for the hydrolytic degradation of polyester urethanes networks, in which the formation of non-linear fragments due to the cleavage of ester bonds led to a decrease of T_g and E modulus before a mass loss could be observed.[3]

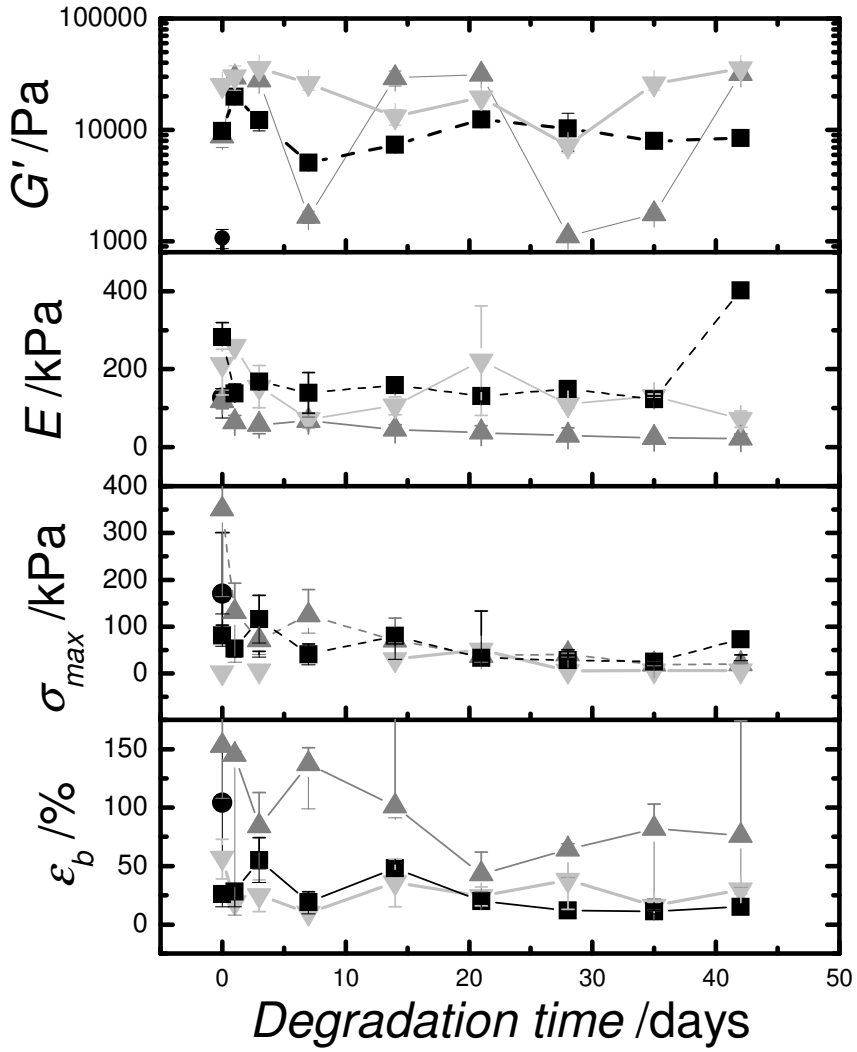

Figure 6.4 Change of material properties during hydrolytic degradation of NGo hydrogels at 37 °C. From top to bottom: shear modulus, G'; Young's modulus, E; maximal tensile strength, σ_{max}; elongation at break, $\varepsilon_{b.}$ (●) NGo_10, (▲) NGo_5, (▼) NGo_1 and (■) NGo_0.5.

Figure 6.4 shows the mechanical investigation of NGo hydrogels during degradation. The change of mechanical properties was monitored by rheology and tensile tests. The shear modulus (G') did not show a clear trend in the time frame investigated, whereas large variations between measurements were observed. The investigation

of mechanical properties by tensile tests could be performed for all samples, except for NGo_10. *E* was slightly decreased in highly crosslinked networks, whereas a strong decrease (118 kPa → 57 kPa) was observed in NGo_5 already after 3 days of hydrolytic degradation. This drastic decrease could be explained, like for NGs_5, with the disaggregation of the triple helices. This decrease corresponds to the observed increase in water uptake and mass loss. Ultimately, an *E* value of 22 kPa was observed after six weeks of hydrolytic degradation. Similarly, σ_{max} and ε_b were decreased in all hydrogels investigated during the course of degradation.

6.1.3 Investigation of molecular organization

In order to elucidate the change of molecular network structure, WAXS measurements were carried out on the partially degraded gelatin hydrogel samples. Figure 6.5 depicts the WAXS spectra of the NGs series before degradation, and after three and six weeks of degradation. The spectrum of NGs_0.5 shows a slight formation of single helix (as peak at 31°) after 6 weeks. This behavior is in agreement with the increase in water uptake due to the formation of more dangling chains. Almost no changes were observed in the molecular organization of NGs_1. The WAXS spectra of NGs_5 and NGs_10 (Figure 6.5 (c)- (d)) depicts before the starting of degradation a low intensity peaks at 8 °C and another small peak at 31 °C, corresponding to the triple and single helix, respevtively. Both signals disappeared completely after 3 and 6 weeks of degradation. In the NGo series a low intensity peak at 8° was observed at time zero for all the samples. After 3 weeks of degradation only the amorphous peak was visible. The sample NGo_10 was degraded after 1 day due to the defolding of the triple helices as showed in Figure 6.6-(d).

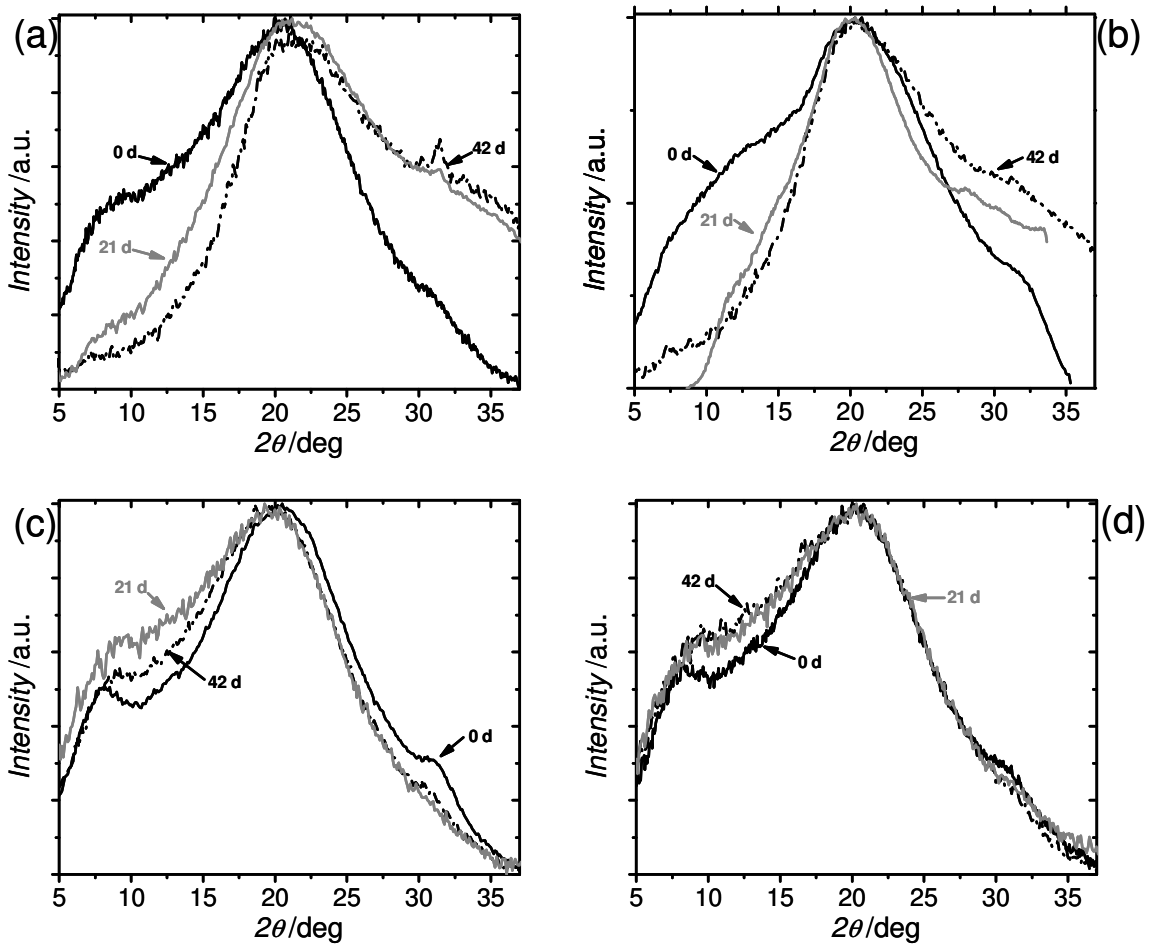

Figure 6.5 WAXS spectra of freeze-dried gelatin-based hydrogels: (a) NGs_0.5, (b) NGs_1, (c) NGs_5 and (d) NGs_10 at t=0d (——), t= 3days (—) and t=6 days (---).

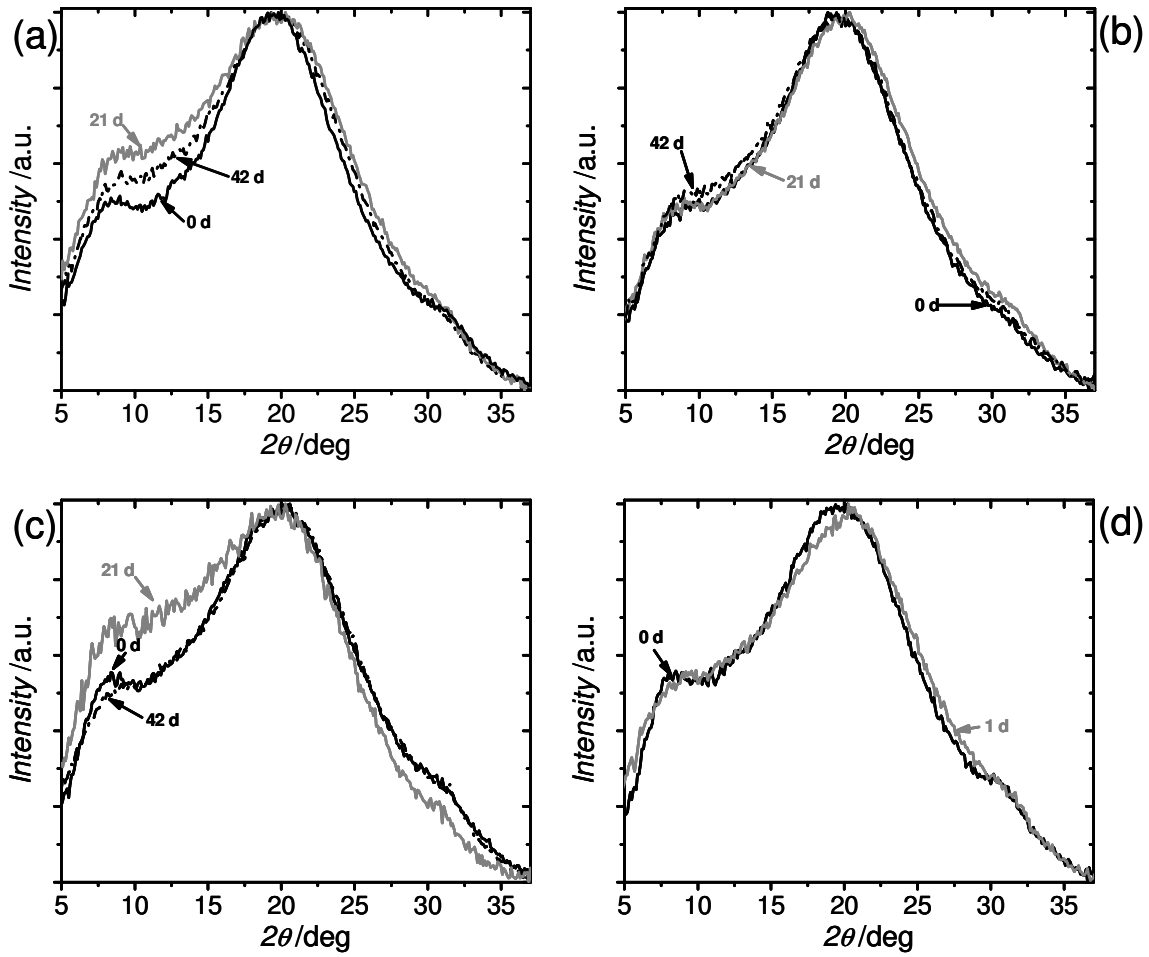

Figure 6.6 WAXS spectra of freeze-dried gelatin-based hydrogels: (a) NGo_0.5, (b) NGo_1, (c) NGo_5 and (d) NGo_10 at t=0d (—), t= 3days (—) and t=6 days (---).

6.1.4 Hydrolytic degradation of gelatin-based hydrogels at 70 °C

The hydrolytic degradation of the gelatin based hydrogels proceeded slowly at 37 °C. In order to study the relative differences in material properties over time, reducing the length of the experiment, a second degradation study was performed under accelerated conditions by increasing the temperature to 70 °C.[130] At this temperature, also the highly crosslinked networks are in the rubbery state. Therefore the diffusion of water into the network is higher than at 37 °C, leading to fast changes

in material properties (e. g. water uptake, mass loss, *E* modulus). To investigate the influence of the crosslinking density and crosslinker type on the degradation behavior, NGs1 and NGs_5, and NGo_1 and NGo_5 were studied. The hydrolytic degradation of the hydrogels at 70 °C was much faster compared to that at 37 °C. Changes in water uptake and mass loss taking place upon degradation as a function of incubation time are plotted in figure 6.7. Such data reveal that both sample compositions experienced a fast increase in the water uptake with degradation. An increase from 725 wt.-% to 1859 wt.-% was observed for NGs_1, while for NGs_5 it increased from 1137 wt.-% at day 1 to 2680 wt.-% after 10 days. A higher water uptake was observed for the sample with lower crosslinking density, while a similar degradation profile was observed for the mass loss.

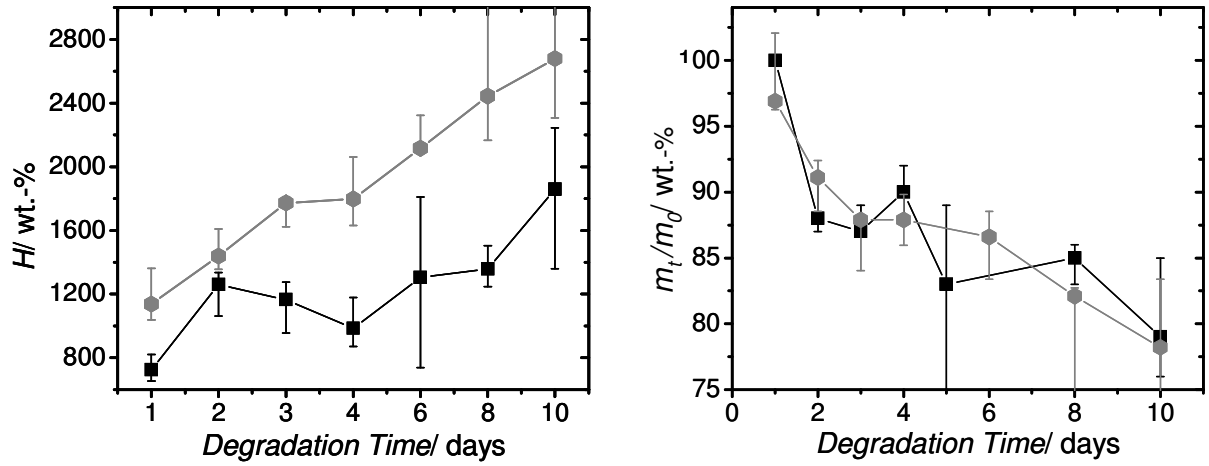

Figure 6. 7 Water uptake (*H*) and remaining mass (m_t/m_0) of NGs hydrogels during hydrolytic degradation at 70 °C. (●) NGs_5 and (■) NGs_1.

In addition to monitoring the water uptake and the mass loss of the gelatin-based hydrogels as function of time, the mechanical properties were also studied, in order to understand the changes occurring within the network during the degradation process. A decrease in the *E* modulus was observed, however the large variations between the measurements make difficult the interpretation of these data (Figure 6.8). The decreased hydrogel elasticity was associated with a continuous increase in

water uptake, whereas no mass loss was observed at day 1 and only 12 wt.-% after 2 days. These observations can be explained with the formation of fragments not small enough to be released from the matrix, and therefore no changes in the mass loss could be observed. The elongation at break and the maximum tensile strength decreased during the first two days of degradation and slightly increased till the last day of degradation. A similar trend was observed in the mechanical properties of NGs_5.

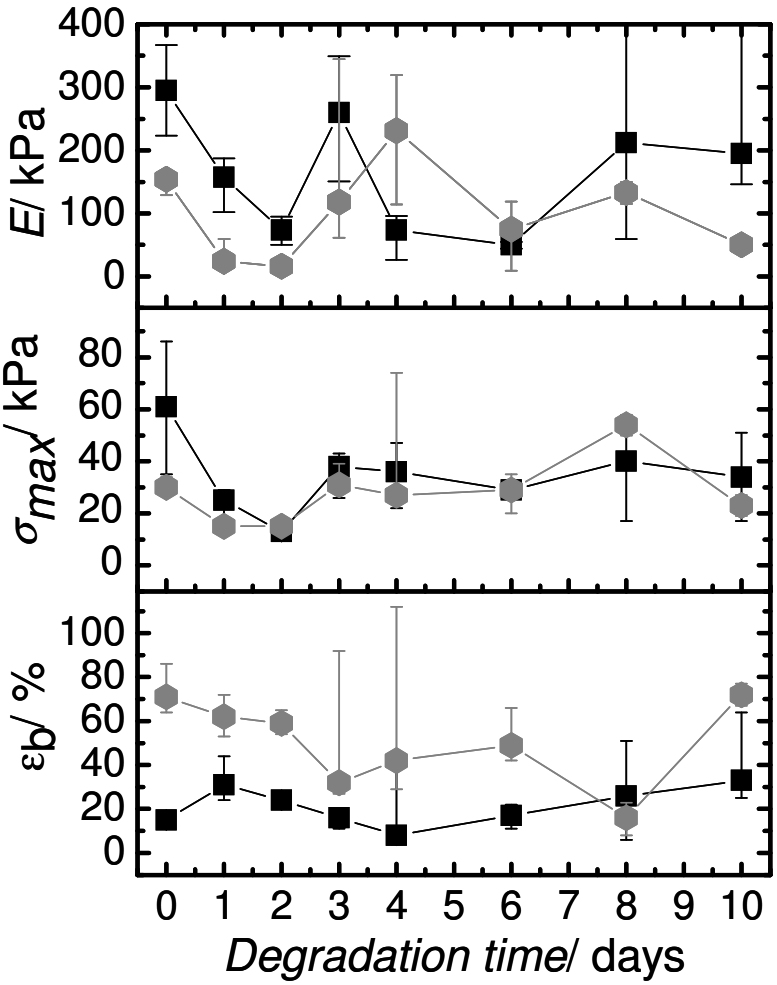

Figure 6.8 Change of material properties during hydrolytic degradation of NGs hydrogels at 70 °C. From top to bottom: Young's modulus, E; maximal tensile strength, σ_{max}; elongation at break, $\varepsilon_{b.}$ (●) NGs_5 and (■) NGs_1.

The hydrolytic degradation at 70 °C was investigated also for samples NGo_1 and NGo_5. The water uptake was increased at each time point investigated during hydrolytic degradation while no significant differences were observed between the two samples (Figure 6.9).

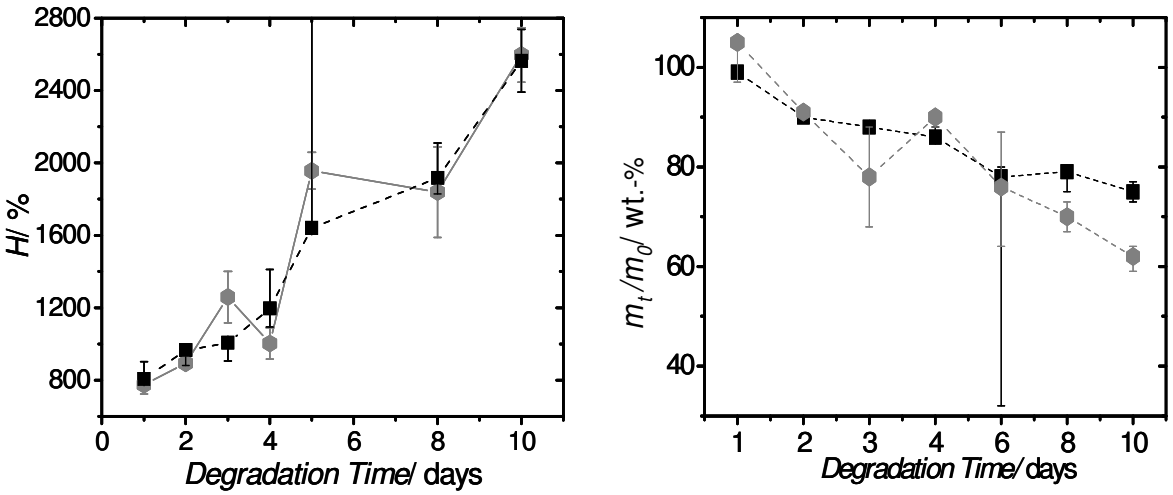

Figure 6.9 Water uptake (H) and remaining mass (m_t/m_0) of NGo hydrogels during hydrolytic degradation at 70 °C. (●) NGo_5 and (■) NGo_1.

The changes in mechanical properties were monitored. The E modulus decreased constantly during the degradation time and almost no differences between the two samples compositions could be detected (Figure 6.10). The maximum tensile strength was almost constant during the overall degradation time. The elongation at break did not show a clear trend and large variation from time point to time point was observed. In order to understand the degradation behavior of the NGs and NGo systems during the hydrolytic degradation, the thermal properties were investigated by TMDSC measurements in the dry state as showed in Figure 6.11. For NGs_1 and NGs_5, the T_g reached a final value of 31 °C and 22 °C, respectively. For NGo_1 the final observed value was 51 and 22 °C for NGo_5. For all investigated networks, the T_g decreased and then increased drastically after 3 days of degradation. This behaviour could be due to the initial formation of dangling chains (decrease of T_g) and the subsequent formation and release of small fragments, which resulted in an

increase of T_g. After the third day a continuous decrease of T_g was observed for all the networks investigated.

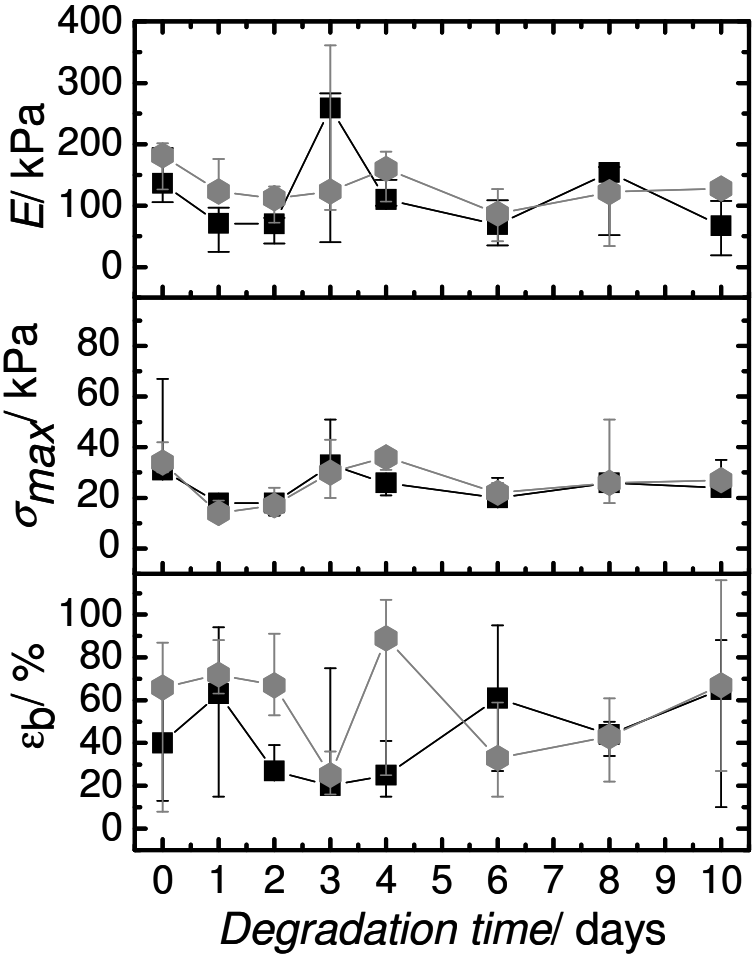

Figure 6.10 Change of material properties during hydrolytic degradation of NGo hydrogels at 70 °C. From top to bottom: Young's modulus, E; maximal tensile strength, σ_{max}; elongation at break, $\varepsilon_{b.}$ (●) NGo_5, and (■) NGo_1.

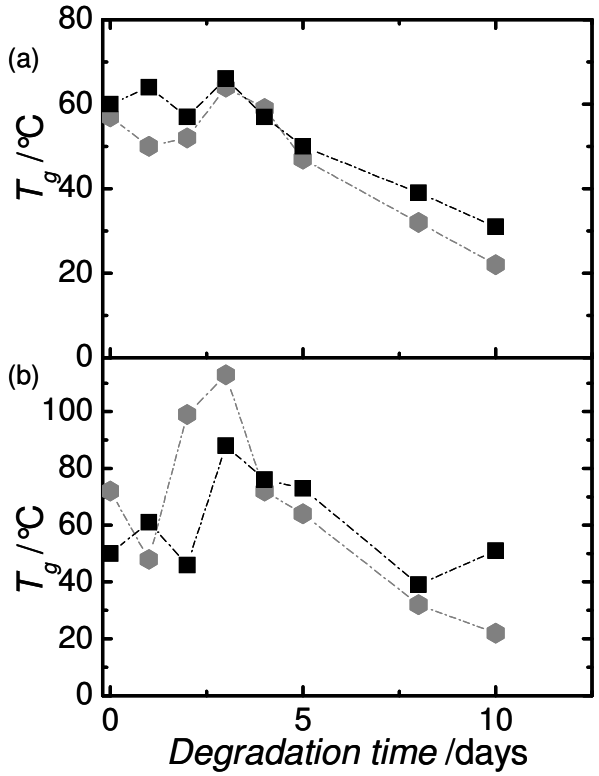

Figure 6.11 Change of thermal properties during hydrolytic degradation of NGs (top) and NGo (bottom) hydrogels at 70 °C. (●) NGs_5, (■) NGs_1, (●) NGo_5, and (■) NGo_1. The hydrogel were measured in the dry state.

6.1.5 Investigation of molecular organization hydrogels degraded at 70 °C

To gain a better understanding of the gelatin molecular organization, WAXS measurements were performed (Figure 6.12). Interestingly, after eight days of hydrolytic degradation at 70 °C some renaturation of the triple helix, described by a peak at 8°, was observed in all hydrogel compositions. This observation could explain the increase of E modulus observed in all gelatin systems after eight days. Samples NGs_5 and NGo_1 showed also a sharp diffraction peak at 31°, due to the

presence of salt derived from PBS buffer used during the synthesis of alkyne-functionalized gelatin.

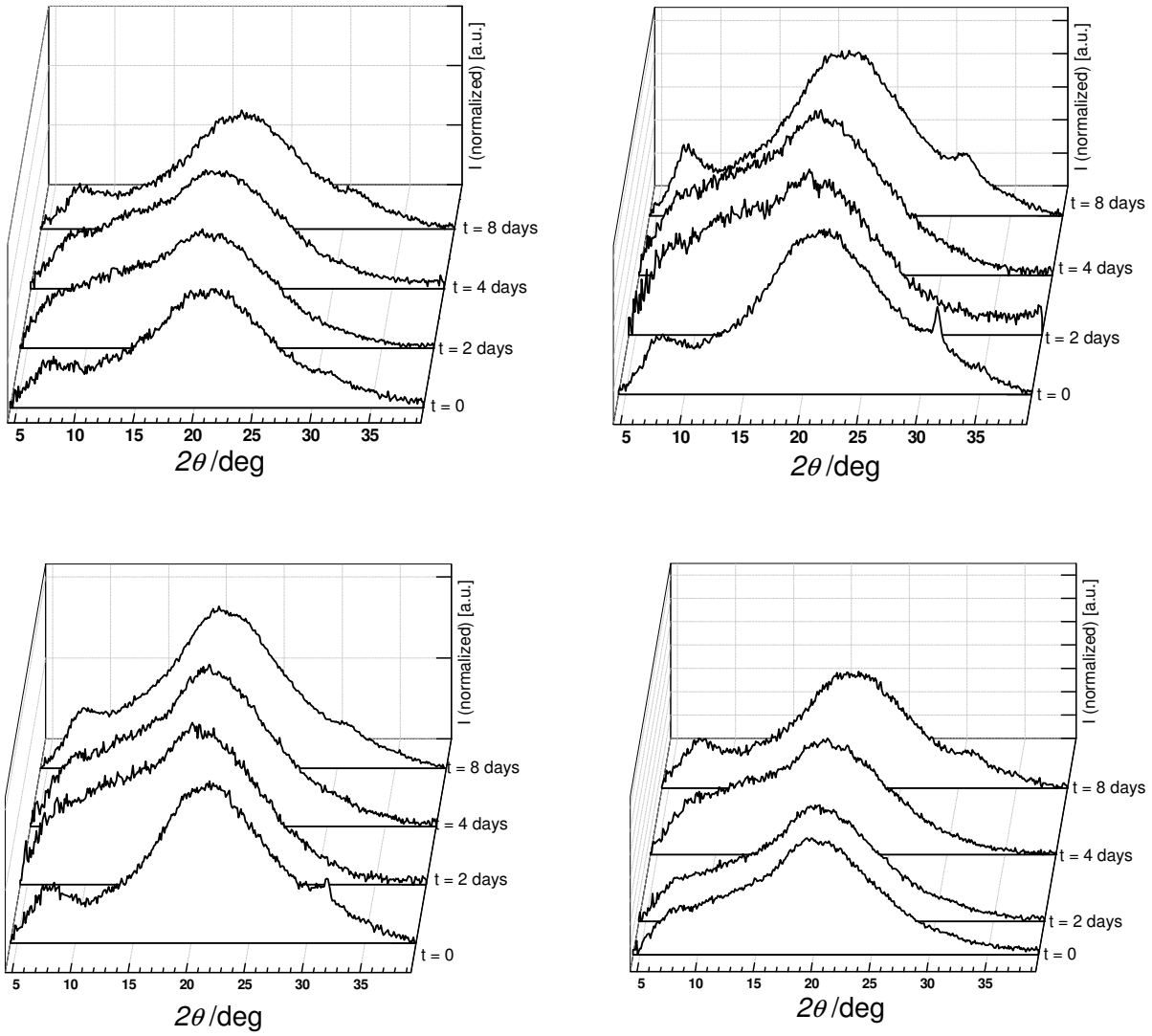

Figure 6.12 WAXS spectra of freeze-dried gelatin hydrogels after 10 days of hydrolytic degradation at 70°C: NGs_1 and NGs_5 (on the top) and NGo_1 and NGo_5 (bottom).

Scheme 6.2 depicts the proposed mechanism for the hydrolytic degradation of gelatin-based hydrogels. In the first stage of hydrolytic degradation, an increase in water uptake is observed. During the course of degradation the random scission of the gelatin amide bonds leads to the formation of an increasing number of dangling chains, detected as a decrease in the mechanical strength. However, at this stage no loss of mass from the hydrogel is observed. Subsequently, the microscopic breaking

of a higher number of amide bonds, leads to the formation of small fragments, which can be released from the hydrogel matrix, resulting in a mass loss. The last phase of the degradation process is the disintegration of the network. The different stages of degradation are observed at different time points depending on the composition and topology of the network investigated. During the hydrolytic degradation, the softness of the networks increased, however no decrease in the size was observed. This kind of behavior is consistent with a bulk degradation mechanism, and similar to a mechanism proposed for polyester urethane networks.[3]

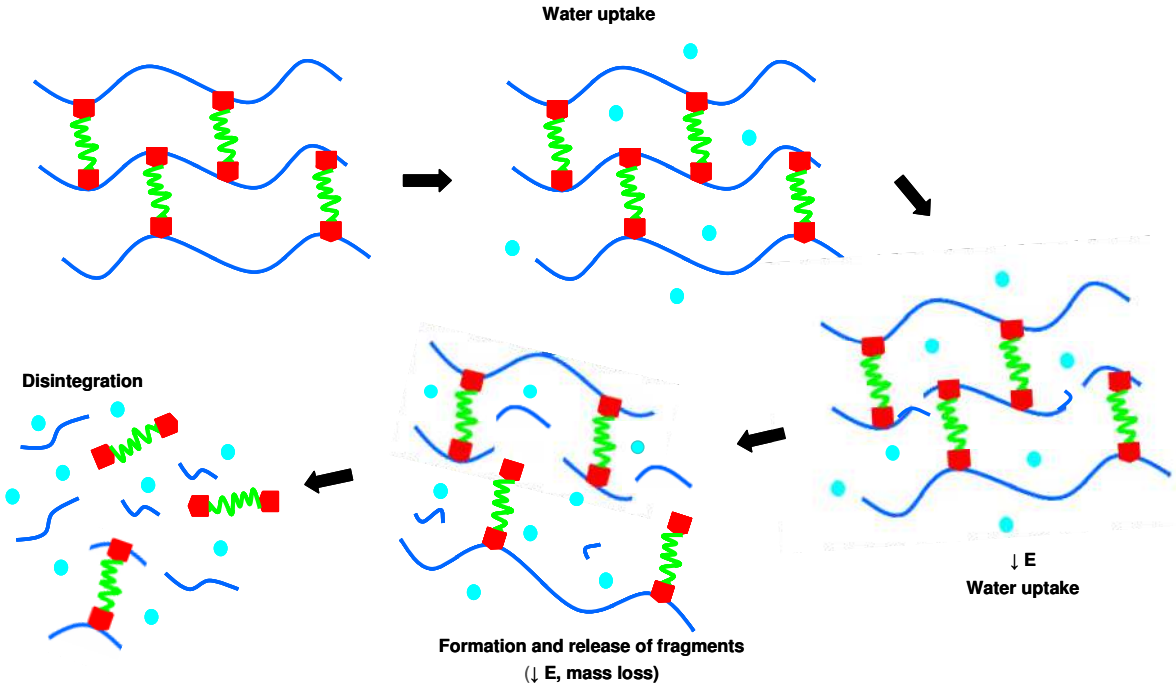

Scheme 6.2 Proposed mechanism for the hydrolytic degradation of gelatin-based hydrogels.

6.2 Enzymatic degradation

Materials intended for biomedical application require fundamental understanding concerning also their enzymatic degradation. Hydrogel degradation was performed in PBS buffer (pH 7.4, 0.5 mM $CaCl_2$) at 37 °C, using collagenase (30

µg/ mL). The networks investigated were NGs and NGo at all alkyne:azide ratios. At predetermined time points, hydrogel samples were removed from the medium and characterized by water uptake, mass loss, tensile tests, DSC and WAXS measurements. The rate of degradation of gelatin hydrogels was determined using collagenases such as clostridium histolyticum collagenase (CHC). This enzyme hydrolyses collagen at unique sites that are characterized by a covalent bond between a glycine residue and a leucine or isoleucine residue, followed by an alanine or leucine residue.[131] In contrast to tissue collagenases, CHC makes multiple scissions per chain.[132] CHC is commercially available in purified forms and has a broad spectrum of action cleaving all types of collagen.

Generally, for in vitro experiments CHC is often used, because this enzyme was the only one available in adequate purified quantities for long time[133] due to low cost in production compared to tissue collagenases.

6.2.1 Change of material properties

The enzymatic degradation of NGs and NGo hydrogels was monitored by changes in water uptake, mass loss and mechanical properties. The samples NGs_5 and NGs_10 degraded considerably faster than NGs_0.5 and NGs_1, indicating that the crosslinking density highly affected the degradation rate. The samples with a low crosslinking density experienced the fastest degradation dissolving completely in the degradation medium within 1 hour. On the other hand, the water uptake and mass loss of NGs_1 and NGs_0.5 could be measured for 24h and 8 hours, respectively.

The NGs hydrogels took 24 hours for complete degradation, whereas the degradation of NGo hydrogels was completed in 8 hours. The water uptake of NGs_1

was increasing during the degradation time and a mass loss of 40 wt.-% was observed at 3 h of degradation (Figure 6.13). However, no significant decrease in mechanical properties could be detected within the first three hours. The elongation at break and the maximum tensile strength were constant within the first three hours and decreased afterwards. NGs_0.5 showed an increase in water uptake associated with a decrease in mass loss.

Tensile tests could be performed only for three hours (Figure 6.14). An initial decrease followed by an increase in Young's modulus was observed, whereas the elongation at break and the maximum tensile strength after an initial decrease showed almost a constant value. Figure 6.13 shows the water uptake and mass loss of NGo hydrogels. Within this series only NGo_0.5 showed some resistance against enzymatic degradation, while the other samples degraded immediately. The water uptake was continuously increasing during the eight hours, while the mass decreased by 16 wt.-% after 1 h and of about 40 wt.-% in the next seven hours. Afterwards the sample dissolved completely.

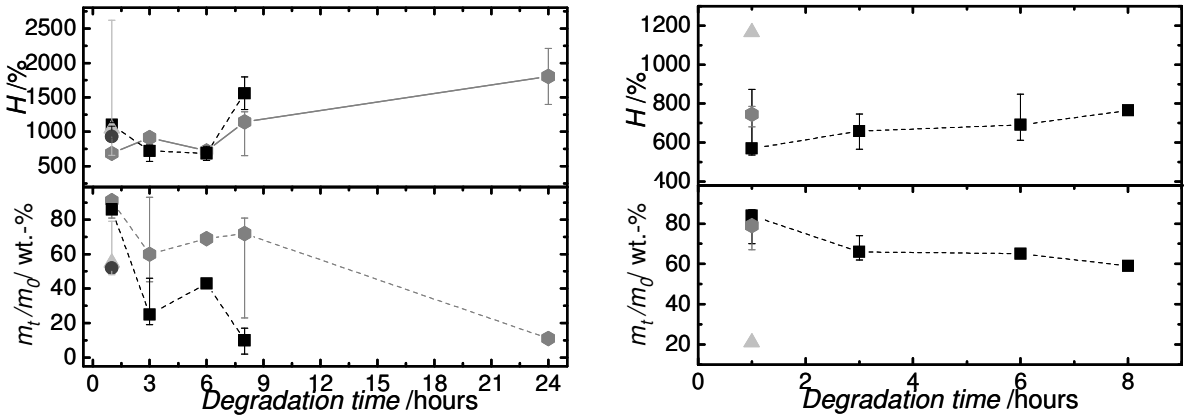

Figure 6.13 Water uptake (H) and remaining mass (m_t/m_0) of NGs (left) and NGo (right) hydrogels during enzymatic degradation. (●) NGs_10, (▲) NGs_5, (●) NGs_1, (■) NGs_0.5 and (●) NGo_10, (▲) NGo_5, (●) NGo_1, (■) NGo_0.5

The mechanical properties could be measured only at 1 h of degradation and a drastic decrease in E modulus from 282 kPa to 62 kPa was detected. The thermal properties were also investigated. The T_g for NGs_1 did not show a clear trend and in the end increased (Figure 6.15). This could be likely due to the reorganization of the gelatin chains into the triple helix structure. The T_g of NGo_0.5 was decreasing in agreement with the decrease of mechanical strength and the mass loss observed.

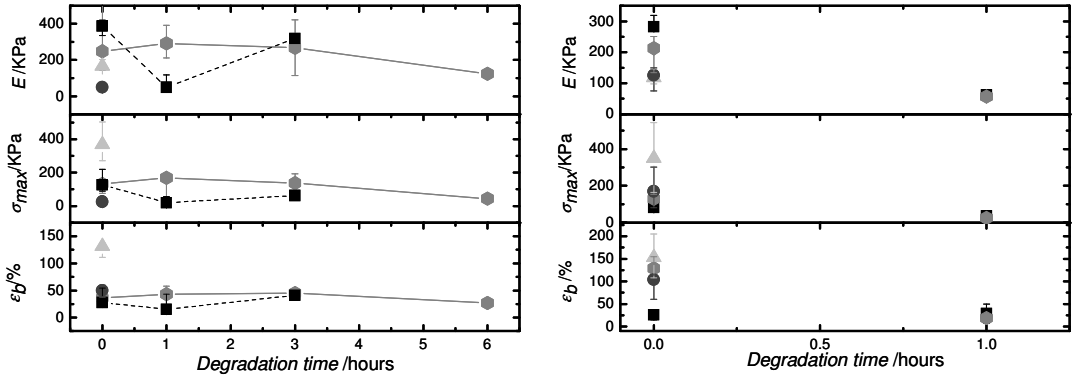

Figure 6.14 Change of material properties of NGs (left) and NGo (right) hydrogels during enzymatic degradation. From top to bottom: Young's modulus, E; maximal tensile strength, σ_{max}; elongation at break, ε_b. (●) NGs_10, (▲) NGs_5, (●) NGs_1, (■) NGs_0.5 and (●) NGo_10, (▲) NGo_5, (●) NGo_1, (■) NGo_0.5

During the time frame investigated, the samples got smaller and smaller indicating a surface erosion degradation mechanism. In fact, if the enzyme cannot diffuse into the hydrogel matrix, the degradation will take place on the surface.[134] This kind of mechanism was confirmed further by the observed decrease in mass loss not associated with a loss of mechanical strength. Even though the external gelatin chains were cleaved, the material maintained its mechanical integrity within the first six hours.

Within the NGs series, NGs_0.5 degraded faster than NGs_1. Sample NGs_0.5, as described in Chapter 4, contains a higher number of dangling chains compared to NGs_1. Therefore, it is likely that collagenase can easily access the gelatin chains

leading to a fast degradation. NGo networks, in general, degraded faster than NGs systems. This behavior could be explained considering the interaction enzyme-substrate. During the enzymatic hydrolysis process, the binding event involves the molecular recognition between the enzyme and the substrate. The use of crosslinker with different structure could potentially affect the ability of enzyme to recognize and attach to the substrate, which will cause an alteration of the degradation rate. Moreover, the use of 4,4'-diazidostilbene-2,2'-disulfonic acid as crosslinker, gave a network with a rigid structure, which could limit the spatial interaction of the enzyme with the substrates.[135]

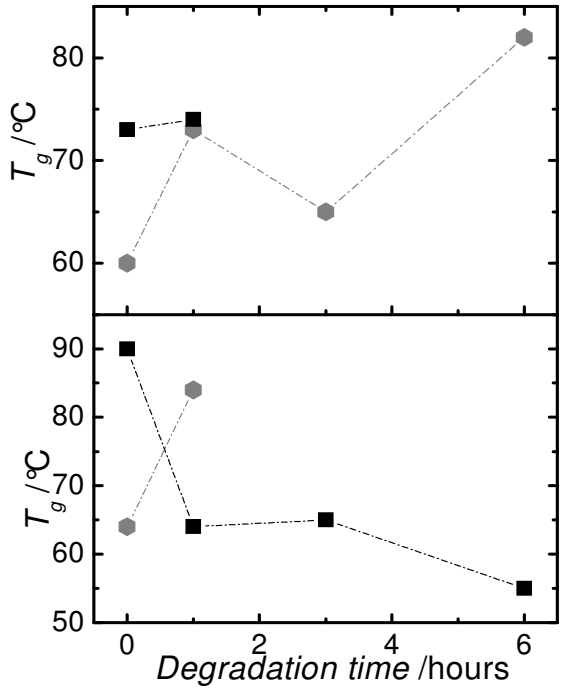

Figure 6.15. Change of thermal properties during enzymatic degradation of NGs (top) and NGo (bottom). (●) NGs_1, (■) NGs_0.5, (●) NGo_1, (■) NGo_0.5

6.2.2 Investigation of molecular organization

The molecular organization of gelatin hydrogels was investigated during the course of enzymatic degradation. Figure 6.16 shows the WAXS spectra of NGs_1 and NGo_0.5. The WAXS spectra of NGs_1 showed at all investigated time points

two diffraction peaks, at 8° and 20°, corresponding to the collagen-like triple helix and the amorphous region, respectively. Sample NGo_5 showed a low peak at 8° corresponding to the triple helix after 1 hour, which disappeared in the next hour leaving only an amorphous peak.

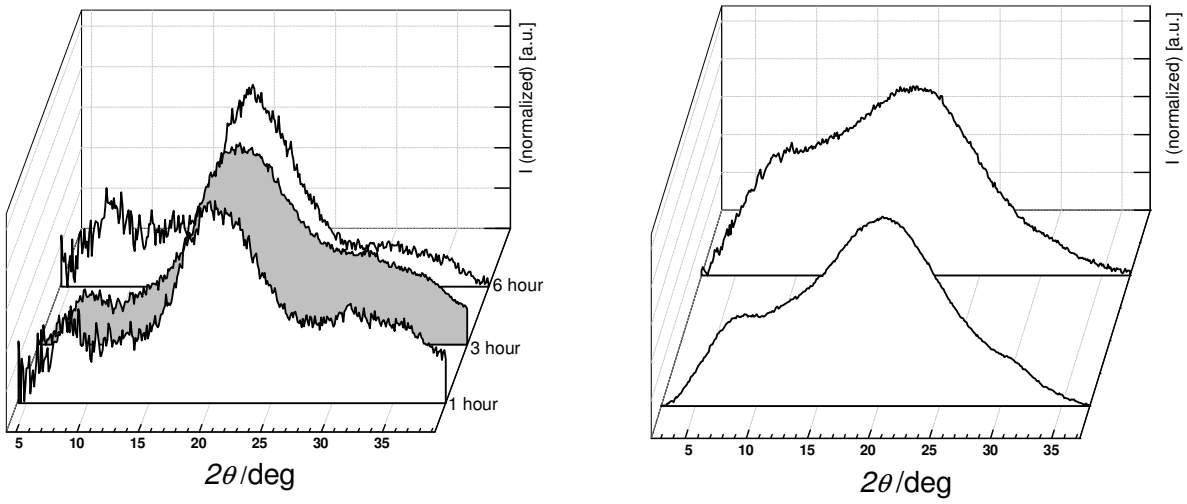

Figure 6.16 WAXS spectra of NGs_1 (left) and NGo_0.5 during enzymatic degradation.

Scheme 6.3 depicts the proposed mechanism for the enzymatic degradation of gelatin-based hydrogels. Enzymatic hydrolysis occurrs on the surface of the hydrogels, resulting in a mass loss while the mechanical integrity is still maintained. When enough chains are cleaved, collagenase can penetrate into the network leading to the complete degradation. The size of the gelatin-based hydrogels decreased during the time, suggesting a surface erosion mechanism of degradation.

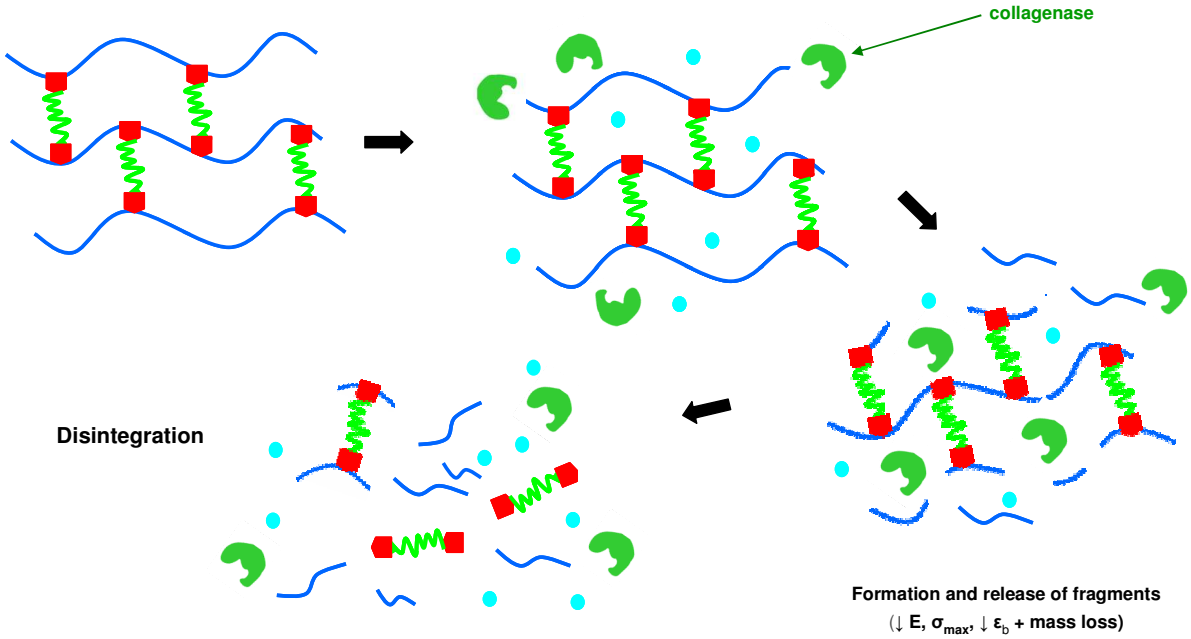

Scheme 6.3 Proposed mechanism for the enzymatic degradation of gelatin based hydrogels.

6.3 Summary

The hydrolytic and enzymatic degradation of the gelatin-based hydrogels NGs and NGo was investigated. The hydrolytic degradation study was carried out at 37 °C in buffered solution at pH 7.4 for six weeks. Changes taking place in water uptake, mass loss, mechanical properties and molecular organization of gelatin-hydrogels were investigated. Since the hydrolytic degradation at 37°C proceeded slowly, a second degradation study was performed at 70 °C which reduced the length of the experiment and allowed to study the difference in material properties over time. At 70 °C also the networks with high crosslinking density are in a rubbery state, which favours the diffusion of water into the system, promoting faster changes in material properties than at 37 °C. In the first stage of hydrolytic degradation an increase in water uptake was observed. During the course of degradation the cleavage of the gelatin amide bonds led to the formation of an increasing number of dangling chains,

detected as a decrease in the mechanical strength. However, no mass loss was observed. This behavior could be likely due to the formation of fragments not small enough to be released from the network. After the scission of a critical number of amide bonds, a decrease of mass was observed. Interestingly, in the last stage of the degradation at 70 °C the renaturation of the triple helix was detected. The hydrolytic degradation was affected by the crosslinking density and crosslinker molecular flexibility. During degradation at 37 °C changes in the material properties could be detected basically for sample with a lower crosslinking density. Moreover, a different behaviour was observed for samples NGs_5 and NGo_5. In sample NGs_5 a mass loss of 11 wt.% was observed after six weeks of degradation, whereas a mass loss of 43 wt.% was observed for NGo_5. The water uptake of NGo_5 increased since the first days of degradation. The different behavior could be due to the molecular flexibility of the crosslinker, which in sample NGo_5 enabled the uptake of more water compared to NGs_5, leading to a fast degradation. During the hydrolytic degradation gelatin hydrogels displayed an increase in the softness, whereas no decrease in the size could be observed. These findings are consistent with a bulk degradation mechanism.

The enzymatic degradation of gelatin hydrogels was performed in PBS buffer using collagenase. The rate of degradation in presence of collagenase was much faster than the hydrolytic process. Samples with low crosslinker amount experienced the fastest degradation and dissolved completely within 1 hour. The rate of degradation was affected by the crosslinker amount and crosslinker type. During the enzymatic hydrolysis process, the binding event involves the molecular recognition between the enzyme and the substrate. The crosslinker structure could potentially affect the ability of enzyme to recognize and attach the substrate, which will cause an alteration of the degradation rate. Moreover, rigid structures are generally much more

resistant than disordered ones, since enzymes need proper spatial interaction with the substrate. During the course of enzymatic degradation, the size of the hydrogel decreased at each data point investigated. This observation suggests a surface erosion mechanism, confirmed also by a decrease of mass loss not associated with changes in mechanical properties.

7. Synthesis and Characterization of Gelatin Fragments Obtained by Controlled Degradation

The data presented in this chapter have been published as: S. Piluso, T. Weigel, A. Lendlein, A. T. Neffe, Synthesis and Characterization of Gelatin Fragments Obtained by Controlled Degradation, *Macromolecular Simposia*, **2011**, *309-310*, 199-204.

In this chapter the synthesis of gelatin fragments by hydroxylamine-mediated cleavage is described. The resulting fragments were characterized by SDS-PAGE, rheological measurements, WAXS and GPC.

7.1 Synthesis of gelatin fragments

The synthesis of gelatin fragments would be advantageous for the preparation of networks based entirely on gelatin. To tailor the material properties fragments with different range of molecular weight need to be prepared. A suitable method for synthesizing gelatin-based telechelics is the hydroxylamine-mediated degradation due to the presence of hydroxylamine sensitive bonds in gelatin.[136,137] Butler[138] and

Bornstein[95] reported that collagen chains were selectively cleaved at the asparyginyl-glycyl bond. The cleavage at this particular bond is due to the tendency of the asparaginyl side chain to cyclize into a substituted succinimide, which is susceptible to nucleophilic attack by hydroxylamine. The sensitivity of Asn-Gly bonds to hydroxylamine compared to other asparaginyl bonds can be likely explained by the ease of cyclization of the asparaginyl side chain in the absence of the steric hindrance imposed by the side chain of the next amino acid.[139] The proposed mechanism of the hydroxylamine cleavage is depicted in Figure 3.2.

Gelatin was reacted with different molar concentration of, specifically 1, 2, and 4 M, at 45 °C or room temperature, for 2 hours and 24 hours respectively. The molecular weight distribution was determined by SDS-PAGE (Figure 7.1). "Gelatin contains α1 and α2 chains (100 kDa) and β chains (200 kDa) as major constituents. These high-molecular weight bands are not visible in any sample treated with hydroxylamine. The treatment of gelatin with hydroxylamine resulted in the formation of smaller fragments compared to the non-treated gelatin.

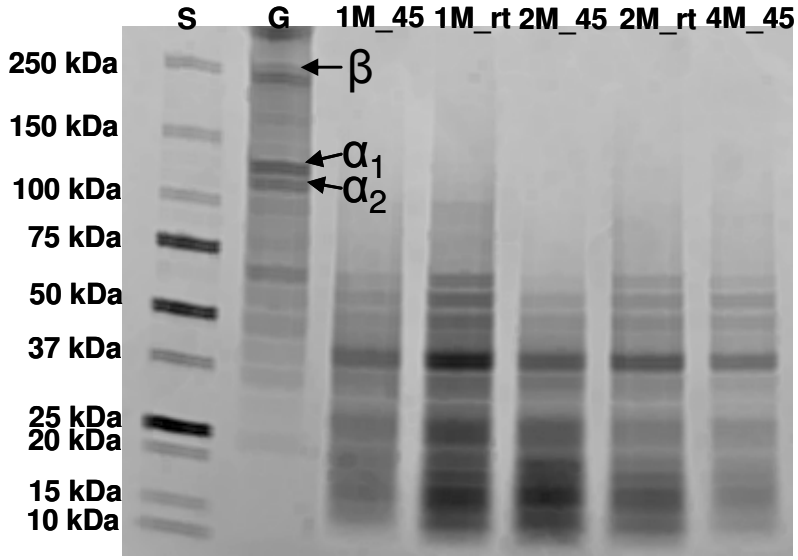

Figure 7.1 SDS-PAGE of gelatin before and after treatment with NH_2OH; S: Standard; G: gelatin; 1M_45, 1M_rt, 2M_45, 2M_rt, 4M_45: Gelatin after NH_2OH mediated cleavage varying the reactions conditions.

Bands at 50 kDa, 37 and 25 and 15 kDa were found in all samples, independent of the reaction time, temperature or hydroxylamine molar concentration, which shows the specificity of the reaction. The fragment mixture was analyzed also by MALDI-TOF mass spectrometry, in which however it was not possible to detect the larger fragments seen in the SDS-PAGE, possibly due to complex spectra because of multiple charges and/or smaller intensities of the larger fragments. However, it was possible to detect fragments of ca. 13.5 and 14.5 kDa, which correspond to the band at 15 kDa in the SDS-PAGE, as well as several peaks below 10 kDa not being resolved in the SDS-PAGE".[140]

The gelatin fragments obtained by hydroxylamine-mediated degradation have aspartyl-hydroxamates and new amino glycine endgroups. The amino content of gelatin before and after treatment with hydroxylamine was determined by the use of a spectrophotometric assay (TNBS, section 4.1). The amino content of gelatin was $27 \cdot 10^{-5}$ mol/ g, and increased to $32 \cdot 10^{-5}$ mol/g for the gelatin fragments. The increase of free amino groups corresponds to the proposed mechanism (Figure 3.2).[96]

7.1.1 Characterization of gelatin fragments

In order to verify wether the hydroxylamine-mediated degradation affected the properties of gelatin (e. g. gel strength, sol-gel transition temperature), the rheological behaviour and the molecular organization were investigated.

To evaluate the strength of the physical gels, frequency sweep measurements of gelatin and fragment mixture solutions (6 wt.%) were carried out at 4, 15 and 25 °C in a frequency range from 0.01 to 1 Hz (Figure 7.1).

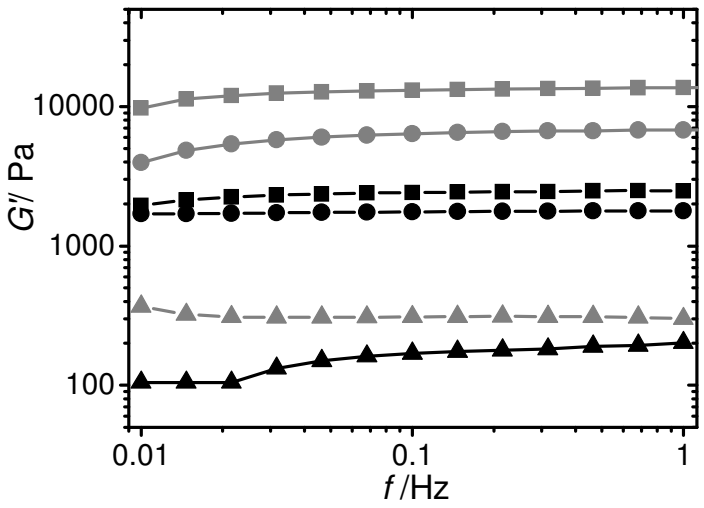

Figure 7.1 frequency sweep measurement of gelatin (■-●-▲) and fragments mixture (■-●-▲) solution (6wt.%) at 4 °C (■) 15 °C (●) and 25 °C (▲).

"At the same weight concentration of gelatin and the fragments mixture, the elastic modulus (G′) of gelatin was higher than the G′ of the fragments mixture at all temperatures investigated and did not depend on the frequency. The viscoelastic behaviour was investigated as a function of the temperature as well (Figure 7.2). The solutions were prepared at 40 °C, placed between the plates and equilibrated at the temperature of the rheometer, forming a physical gel. The gel formed by gelatin was stronger and stable in a wide range of temperature, whereas the elastic modulus of the fragments mixture started to decrease at approximately 10 °C. The sol-gel transition temperature taken as the crossover point between G′ and G", occurred at higher temperature in gelatin gels than in the fragments mixture".[140] The different behaviour could be likely due to the difference in molecular weight and to the relative content of α and β chain components.[141]

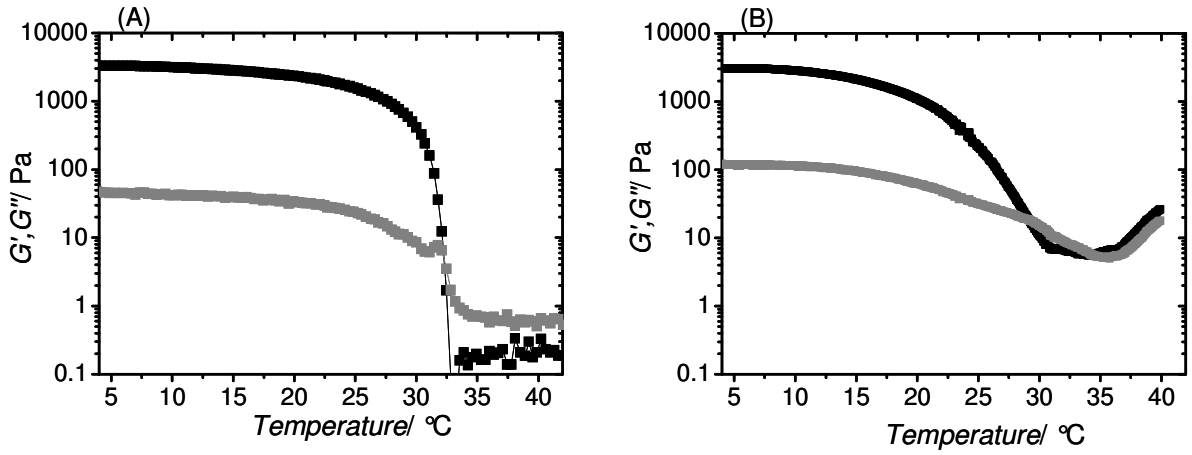

Figure 7.2 Temperature sweep of gelatin (A) and gelatin fragments mixture (B) from 4 to 42 °C, (—) G′ and (—) G".

The molecular organization of gelatin before and after treatment with hydroxylamine was determined by WAXS. The WAXS spectra of gelatin shows three peaks at 2θ = 8°, 20° and 31°, which correspond to the diameter of the triple helix, the amorphous halo, and the amino acids contact along the axis of single helices, repectively.[142] The same molecular organization was observed in gelatin fragments (Figure 7.3-A). "Attempts to separate individual fragments were made by using membrane filtration and GPC; however in both cases no separation was obtained.

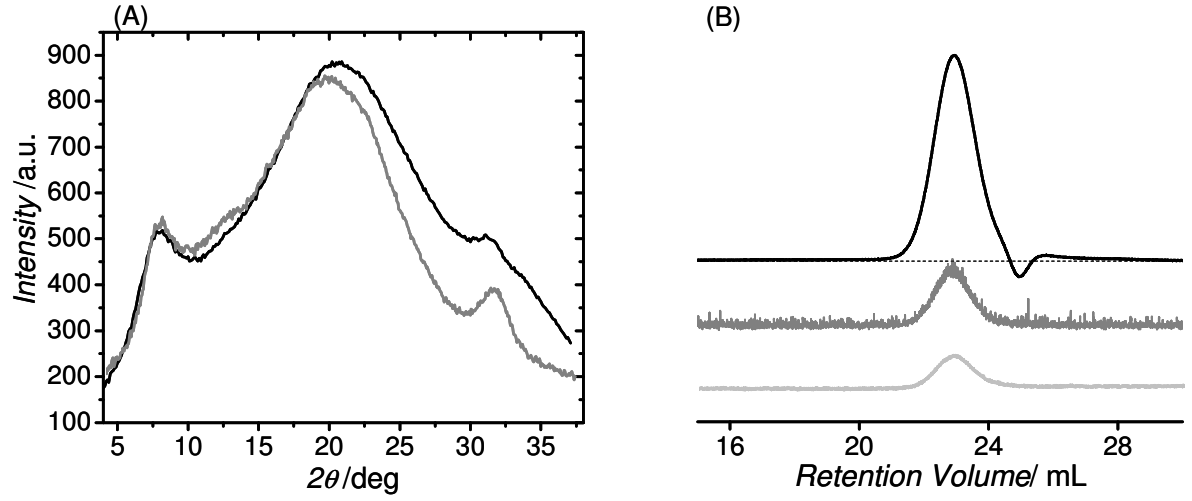

Figure 7.3 (A) WAXS spectra of gelatin (—) and gelatin fragments (—). (B) Gel permeation chromatography of gelatin fragments solution, (—) Refractive Index, (···) Right Angle Light Scattering, (—) Viscometer.

The molecular weight distribution of gelatin and gelatin fragments was analyzed by GPC. The commercial gelatin had a M_n of 45700 and a polydispersity of 3.02, whereas for gelatin fragments a M_n of 25000 and a polydispersity of 1.4 were determined. Even though the separation of the fragments was not possible, the GPC profile showed a more narrow distribution of the gelatin fragments compared to the commercial gelatin".[140]

7.2 Summary

Gelatin-based telechelics with defined molecular weight and endgroups were obtained through hydroxylamine-mediated degradation of gelatin. The degradation of gelatin with hydroxylamine was performed under different conditions and the molecular weight of the fragments mixture was determined by SDS-PAGE, gel permeation chromatography (GPC) and MALDI-TOF MS. The rheological investigation showed lower G′ and G" values for gels from the fragment mixture than from gelatin, and lower gel-sol transitions temperatures, whereas WAXS spectra showed tha same molecular organization for both samples. The method developed here enabled the formation of defined gelatin fragments and would be easy to scale up. The separation of individual fragments would be interesting for the synthesis of fully biopolymer-based networks.

8. Summary and outlook

Biopolymer-based networks with defined mechanical properties were prepared by the use of the chemoselective and high yielding copper(I)-catalyzed azide-alkyne cycloaddition reaction. Gelatin-based hydrogels were prepared by using a two step synthetic route. In the first step, alkyne pendant groups were incorporated into the gelatin backbone. Subsequently, the alkyne-functionalized gelatin was dissolved at 45 °C, above the sol-gel transition, and the crosslinker followed by the catalyst was added. The tailoring of the mechanical and thermal properties was obtained by variation of the crosslinking density and of the length and molecular flexibility of the crosslinker. As crosslinker with rigid structure 4,4'diazido-2,2'-stilbenedisulfonic acid was used, whereas 1,8-diazidooctane, 1,12-diaziododecane and PEG-diazide were selected as crosslinker with flexible structure. The variation of the alkyne:azide ratio and of the crosslinker type affected the renaturation of the collagen-like triple helix. By increasing the crosslinker amount, the renaturation of the triple helix structure was nearly suppressed. However, at the same alkyne:azide ratio, NGo hydrogels displayed a higher content of triple helices compared to the NGs hydrogels. This behaviour could be explained with the flexible structure of the crosslinker in NGo, which cannot completely suppress the renaturation of triple helices, whereas the rigid

structure of crosslinker in NGs are likely to inhibit helix formation due to steric hindrance.

The variation of the described molecular parameters enabled the tailoring of the hydrogels in their mechanical (*E*: 50 kPa - 635 kPa, G': 0.1 kPa - 16 kPa) and swelling (*Q:* 150-470 vol.-%) properties. The crosslinker molecular flexibility and the crosslinking density affected also the thermal properties of the gelatin-based hydrogels. In particular, NGo hydrogels, which contain a flexible crosslinker, displayed higher T_g values compared to hydrogels containing a rigid crosslinker (NGs). This observation could be explained with the physical reorganization of some gelatin chains, which is likely to contribute to the crosslinking density.

In order to elucidate the network structure, a method based on the labeling of free azide (dangling chains) and alkyne (for bioactive molecules attachment) groups with alkyne- and azide-functionalized fluorescent dyes has been described. The hydrogels were then characterized by confocal laser scanning microscopy and fluorescence spectroscopy. Dangling chains were observed at the alkyne:azide ratio of 0.5:1, due to the excess of crosslinker used compared to the alkyne groups. Dangling chains were also observed using an equal molar ratio between alkyne and azide groups. A possible reason might be that when the network is starting to form the movements of the chains are restricted and a further crosslinking is possible only if the crosslinker is flexible and long enough to reach another chain. The highest amount of dangling chains was observed for NGs (0.20 µmol) which contains a rigid crosslinker, whereas a low amount was detected for NGo (0.12 µmol), NGd (0.11 µmol) and NGp (0.044 µmol).

Free alkyne functional groups were observed in all the networks investigated. Unexpected was the low amount of free alkyne groups detected in the networks NGs_5 and NGs_10. Due to the low amount of crosslinker used for synthesizing

NGs_5 and NGs_10, the physical reorganization of the gelatin chains was not completely hindered. Therefore, the azido-functionalized fluorescent dye might not have been able to react with all free alkyne groups available.

The method applied to gelatin enabled also the formation of hyaluronic acid-based hydrogels with defined properties. By variation of the crosslinking density and crosslinker type, the local and bulk mechanical (E: 0.8-26 kPa; *G'*: 0.6-3.7 kPa) properties, and the water uptake (*H*: 4710-6480 wt.-%) of the hydrogels could be tuned.

In order to verify if the method used for synthesizing gelatin-based hydrogels could enable the control of material properties also during degradation, hydrolytic and enzymatic degradation studies were performed. The hydrolytic degradation study was carried out at 37 °C in buffered solution at pH 7.4 for six weeks and at 70 °C for 10 days. Changes taking place in water uptake, mass loss, mechanical properties and molecular organization of gelatin-hydrogels were investigated. During the hydrolytic degradation gelatin hydrogels displayed an increase in the softness, whereas no decrease in the size could be observed. These findings are consistent with a bulk degradation mechanism. The enzymatic degradation of gelatin hydrogels was performed in PBS buffer using collagenase and was much faster than the hydrolytic process. The rate of degradation was affected by the crosslinking density and crosslinker type. Specifically, hydrogels containing the crosslinker with a rigid structure were more resistant against enzymatic degradation than the hydrogel with a flexible linker. During the course of enzymatic degradation, the size of the hydrogel decreased at each data point investigated, suggesting a surface erosion mechanism of degradation.

The hydrogels synthesized in this work, due to the use of small molecules as crosslinker (4,4-diazidostilbenedisulfonic acid, 1,8-diazidooctane and 1,12-

diazidododecane) and to the low amount used (0.002 mol.% → 0.02 mol.% of crosslinker compared to gelatin), can be still considered as biopolymer-based materials. The hydrogels prepared by using PEG-diazide as crosslinker are hybrid materials. However, it would be quite interesting to achieve the synthesis of networks based entirely on biopolymer components. In this case, bifunctional biopolymer-based crosslinkers or telechelics are needed. One possible access to this class of materials would be the synthesis of biopolymer-based telechelics by controlled degradation of gelatin. This was investigated by applying hydroxylamine-mediated degradation of proteins to gelatin. Defined gelatin-based telechelics are formed due to the specific action of hydroxylamine on asparagin-glycine bonds. By the use of this selective method, a mixture of fragments with molecular weight of 15, 25, 37 and 50 kDa (analyzed by SDS-PAGE) was obtained. The fragments were characterized also by GPC. In order to make sure that the cleavage did not altered the properties of gelatin, the molecular organization and the rheological properties of the fragments were investigated. Attempts to separate the individual fragments were made, however no separation was obtained so far. The individual fragments could be used for the preparation of gelatin hydrogels, in order to obtain a fully biopolymer-based networks. The tailoring of the mechanical properties would be obtained by variation of the length and molecular weight of the crosslinker.

In view of potential biomedical applications, the use of the non-toxic copper catalyst for the preparation of the hydrogels would be highly beneficial. In this work has been shown that if copper is properly removed after the reaction no cytotoxic effect can be detected on the cells. However, in presence of living cells, the copper catalyst cannot be use. An alternative could be the use of a strain-promoted cycloaddition between cyclooctynes and azides (Figure 8.1).[143,144,145] The reaction between a cyclooctine and phenyl azide to effort a triazole functionality was reported

already in 1961 by Wittig and Krebs.[146] In 2004, Bertozzi and co-workers[147] demonstrated that the reaction of cyclooctine and azide could be performed under physiological conditions. The reactivity of the first generation of cyclooctines was relatively low compared to the copper-catalyzed process. To improve the reactivity of the cyclooctines with azides, Bertozzi and co-workers[148,149] designed and synthesized a second generation of fluorinated cyclooctynes, introducing fluorine atoms at the propargylic position, generating mono- and difluorinated cyclooctines.

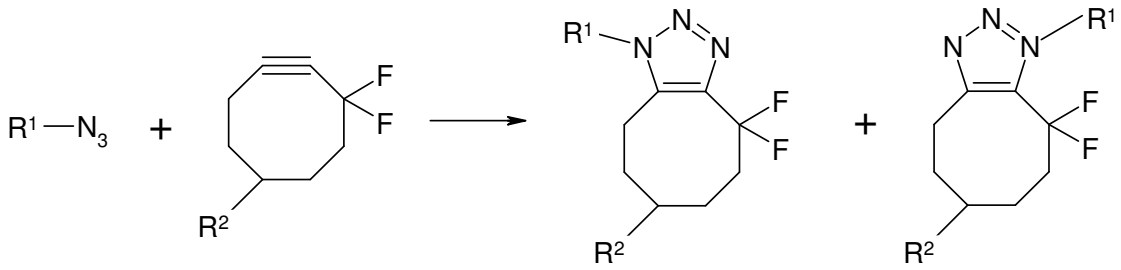

Figure 1.9 Scheme of copper free click chemistry.[75]

These compounds showed a similar reaction kinetic as the copper(I)-catalyzed cycloaddition reaction, even though they are rather difficult to synthesize.[147]

9. Materials and Methods

Gelatin (type A from porcine skin, 300 bloom), propiolic acid, 4-pentynoic acid, *N, N'*-diisopropylcarbodiimide (DIC), 2,4,6-trinitro-benzensulfonic acid (TNBS), N, N-dimethylformamide (DMF anhydrous), copper sulfate pentahydrate ($CuSO_4 \cdot 5H_2O$), sodium ascorbate, propargylamine, 4,4'-diazido-2,2'-stilbenedisulfonic acid, 1,8-dibromooctane,1,12-dibromododecane, PEG-diazide, Ethylenediaminetetraacetic acid (EDTA), fluoresceinamine, were purchased from Sigma Aldrich (Munich, Germany). Tetrahydrofuran (THF, reagent ACS, 99,8%), dimethylsulfoxide (DMSO), sodium azide (NaN_3), borax decahydrate ($Na_2B_4O_7 \cdot 10H_2O$) and hydroxylamine were purchased from Merck (Darmstadt, Germany). Dicloromethane (DCM, anhydrous) and hyaluronic acid were purchased from Acros. 5-azidopentanoic acid was purchased from Bachem. All reagents and solvents were of analytical grade and were used without further purification.

9.1 Synthesis of alkyne-functionalized gelatin

The alkyne-functionalized gelatin was synthesized using a procedure modified from a literature source.[45] One gram of gelatin was added to 20 mL of Borax Buffer (pH 8.5)

and heated at 40 °C while stirring until gelatin was dissolved. Then, the flask was removed from the heating and DMF (40 mL) was added to the stirring mixture at a constant rate of 1 $m \cdot Ls^{-1}$. Separately, in another round bottom flask propiolic acid or 4-pentinoic acid (2 mmol) was dissolved in 4 mL of anhydrous DMF. Then the solution was cooled in an ice bath and treated with 1 mmol of diisopropylcarbodiimide (DIC) at 0 °C for 30 minutes. Afterwards, since the solution became cloudy, anhydrous dichloromethane was added (4 mL) and the solution was left to stir for additional 10 minutes. Consecutively, the activated propiolic acid solution was added to the stirred gelatin solution at a constant rate of 1 $m \cdot Ls^{-1}$ and the reaction was allowed to proceed for 2 h at room temperature. The product was then precipitated by addition of 150 mL THF to the reaction mixture followed by a purification step consisting in the dissolution in PBS buffer (pH 7.4) at 40 °C, mixing with of DMF and re-precipitation with THF. Then functionalized gelatin was dissolved again in 5 mL of PBS buffer at 40 °C and precipitated in 50 mL of THF. This step was repeated two times. Finally the alkyne-functionalized gelatin was rinsed with cold water, methanol, acetone and dried under vacuum. The chemical modification of gelatin was assessed by proton nuclear magnetic resonance (^{1}H NMR) spectroscopy. ^{1}H NMR (500 MHz) spectra were recorded with a Bruker Avance spectrometer (Karlsruhe, Germany).

9.2 Synthesis of alkyl azides

1,8-diazidooctane was synthesized using a procedure reported in the literature.[35] Briefly, 1,8-diazidooctane was synthesized by adding 1, 8-dibromooctane (1 mmol) to a sodium azide (2 mmol) solution in DMSO, stirring the mixture overnight at 25 °C. The crude product was used immediately after the reaction. The same procedure

was used for the synthesis of 1,12-diazidodecane starting from 1,12-dibromododecane. Both samples were characterized by NMR in which the conversion of the bromo group to the azide was confirmed by a shift of the therminal methylene groupf from 3.4→3.3 ppm.

9.3 Synthesis of gelatin-based hydrogels

All hydrogels were prepared by the reaction of the alkyne-functionalized gelatin with a diazide linker in the presence of $CuSO_4 \cdot 5H_2O$/sodium ascorbate in a 1:1 mixture H_2O/EtOH. Alkyne-functionalized gelatin (500 mg) was dissolved in a 1:1 mixture H_2O/EtOH (10 mL) at 45 °C. Then a diazide, specifically 4,4'-diazido-2,2'stilbenedisulfonic acid, 1,8-diazidooctane, 1,12-diazidododecane or PEG-diazide (M_w = 1108 g·mol^{-1}, PD = 1.2) was added to the stirring gelatin solution followed by the addition of 0.01 mmol of sodium ascorbate. Each diazide was used in four different concentrations: 0.1 mmol (ratio 0.5:1), 0.05 mmol (ratio 1:1), 0.02 mmol (ratio 5:1) and 0.01 mmol (ratio 10:1). After copper addition (5 µmol), the solution was stirred vigorously for less than 10 seconds and cast in a Petri dish and left overnight. The hydrogels were swollen in 0.05 M EDTA solution for copper removal and then equilibrated in water. After gelation, hydrogels were punched to obtain samples of equal size (diameter, 1.4 mm). The hydrogels are referred to as NGs_x (network of gelatin with 4,4'-diazidostilbenedisulfonic acid as crosslinker), NGo_x (1,8-diazidoctane as crosslinker), NGd_x (1,12-diazidododecane as crosslinker) and NGp_x (PEG-diazide as crosslinker). The "x" stands for the alkyne:azide ratio: 0.5 (alkyne:azide ratio 0.5:1), 1 (alkyne:azide ratio 1:1), 5 (alkyne:azide ratio 5:1) and 10 (alkyne:azide ratio 10:1).

9.4 Synthesis of 5-(5-azidopentanamido)-2-(3-hydroxy-6-oxo-6*H*-xanthen-9-yl)benzoic acid

To a solution of fluoresceinamine (0.15 g, 0.43 mmol, 1 eq) in pyridine (2 mL) was added EDC (0.083 g, 0.43 mmol, 1 eq) and azidopentanoic acid (0.062 g, 0.43mmol, 1 eq). The reaction was left to proceed overnight at room temperature and under stirring. Then the reaction mixture was poured into cold water (15 mL) and the colour changed suddenly into light orange. The solution was acidified (pH<2) by adding 5M HCl. After stirring for 1 h, the precipitate was filtered off and, washed with 1M HCl (3x3 mL) and dissolved in a small amount of EtOAc (ethyl acetate). The EtOAc solution was dried over Na_2SO_4, filtered and then concentrated. Addition of hexane (150 mL) led to the formation of the product as orange crystals, which were collected and dried under vacuum (90 mg, 44%). FTIR: 3307-2600, 2095, 1735, 1670, 1605, 1385, 1255, 1207, 1170, 1111, 912, 846, 786 cm^{-1}. ^1H NMR (CD_3OD, ppm): δ = 10.13 (br s, 1H, Ar-OH), 8.29 (d, 1H, Ph), 7.74 (t, 1H, Ph), 7.05 (d, 1H, Ph), 6.7-6.47 (m, 6H, Ph), 3.21 (m, 2H, CH_2-N_3), 2.55-2.38 (m, 2H, CH_2C(O)N), 1.61-1.58 (m, 4H, (CH_2)$_2$) ppm. ^{13}C NMR (CD_3OD, ppm): 172.5, 171.0, 160.2, 169.2, 151.8, 147.3, 140.3, 140.2, 128.3, 126.4, 126.6, 116.7-101.6, 52.3, 35.3, 27.6, 21.9 ppm. MS (ESI^+): calculated for $(C_{25}H_{20}N_4O_6+H)^+$: 473.1479, found 473.3828. The NMR of the sample was pure. This compound will be referred to as azido-fluorescein dye.

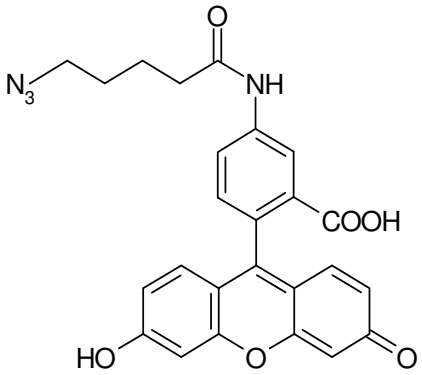

Figure 2.1 Structure of 5-(5-azidopentanamido)-2-(3-hydroxy-6-oxo-6*H*-xanthen-9-yl)benzoic acid.

9.5 Synthesis of 2-(3-hydroxy-6-oxo-6*H*-xanthen-9-yl)-5-pent-4-ynamidobenzoic acid

The alkyne-fluorescein dye was synthesizes using a procedure modified from a literature source.[122] To a solution of fluoresceinamine (0. 5 g, 1.44 mmol, 1 eq) in pyridine (6 mL) was added EDC (0.42 g, 2.17 mmol, 1.5 eq) and 4-pentinoic acid (0.28 g, 2.88 mmol, 2 eq). The suspension was left to proceed overnight at room temperature and under stirring. Then the reaction mixture was poured into cold water (25 mL). The solution was slowly acidified (pH<2) by adding HCl 5N. After stirring overnight the precipitate was filtered off and washed with cold water and dissolved in a small amount of EtOAc (ethyl acetate). The EtOAc solution was dried over Na_2SO_4, filtered and then concentrated. Addition of a large excess of hexane led to the formation of the product as orange crystals, which were collected and dried under vacuum (250 mg, 40%). FTIR: 3500-2400, 2119, 1741, 1673, 1606, 1369, 1253, 1209, 1153, 1111, 850 cm^{-1}. ^1H NMR (CD_3OD, ppm): δ = 10.24 (br s, 1H, Ar-OH), 8.25 (d, 1H, Ph), 7.75 (t, 1H, Ph), 7.04 (d, 1H, Ph), 6.73 (m, 2H, Ph), 6.61-6.42 (m, 4H, Ph), 2.72 (t, 1H, *H*-alkyne), 2,60-2.47 (m, 2H, *CH_2*C(O)N), 2.20 (m, 2H, *CH_2*-

alkyne) ppm. ^{13}C NMR (CD_3OD, ppm): 170.8, 169.1, 159.7, 151.7.2, 147.8, 139.8, 128.3, 126.3, 123.4, 116.3, 114.1, 111.7, 109.5, 101.6, 81.5, 68.7, 34.9, 12.9 ppm. MS (ESI^+): calculated for $(C_{25}H_{17}NO_6+H)^+$: 428.1179, found 428.3010. The NMR of the sample was pure. This compound will be referred to as alkyne-fluorescein dye.

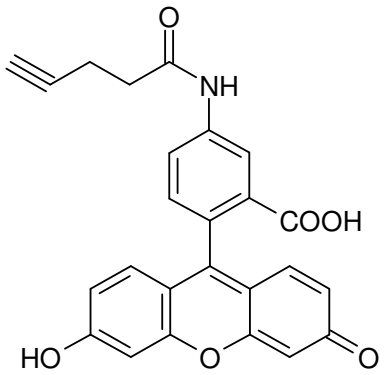

Figure 9.2 Structure of 2-(3-hydroxy-6-oxo-6*H*-xanthen-9-yl)-5-pent-4-ynamidobenzoic acid.

9.6 Labeling of gelatin hydrogels with fluorescent dyes

The gelatin-based hydrogels were dipped into 70 mL of water, then the azido- or alkyne-functionalized fluorescein dissolved in a mixture water/ MeOH (200 µL MeOH + 2 mL H_2O) was added followed by sodium ascorbate and $CuSO_4 \cdot 5H_2O$. The hydrogels were incubated at room temperature, under mild shaking, in the absence of light for three days. Then they were extensively washed with cycles of PBS washing/ MeOH/H_2O (1:1 mixture)/ H_2O, each washing for 15 min. After 3 cycles of washing, the samples were left in water overnight.

9.7 Hydroxylamine cleavage

An aqueous solution of gelatin Type A (pig skin, 300 bloom) (5 mg/mL) was incubated at 45 °C or room temperature with 1 M, 2 M or 4 M aq. hydroxylamine solution. The pH of the mixture was adjusted to 9.5 by adding a 1 M aq. Na_2CO_3 solution. The reaction was performed for 2 or 24 hours. Subsequently, the hydroxylamine was removed by dialysis against water and the product was lyophilized.

9.8 Synthesis of alkyne-functionalized hyaluronic acid

Hyaluronic acid (100mg) was dissolved in 15 ml of MES (2-(N-morpholino)-ethanesulfonic acid buffer) 50 mM, pH=4. Then 2.5 mmol of EDC, 2.5 mmol of NHS and 3.8 mmol of propargylamine were added to the hyaluronic acid solution. The reaction was performed at room temperature under stirring for 24hours. The solution was dialyzed (cutoff = 12 kDa) against a saturated NaCl solution for 1 day and then against distilled water for 5 days. Then the sample was recovered by freeze-drying.

9.9 Synthesis of Hyaluronic acid-based hydrogels

The hydrogels were obtained by dissolving 200 mg of alkyne-functionalized hyaluronic acid in 10 mL of a 2:1 mixture H_2O/EtOH and subsequent addition of a

diazide, specifically 4,4'-diazidostilbenedisulfonic acid, 1,8-diazidooctane, or PEGdiazide (M_W = 1108 g·mol^{-1}, PDI<1.2). Each diazide was used in three different concentrations: 0.1 mmol (ratio 1: 0.5), 0.2 mmol (ratio 1:1) and 0.23 mmol (ratio 1:1.1). Then 0.041 mmol of sodium ascorbate and 20 µmol of $CuSO_4 \cdot 5H_2O$ were added, and the hydrogels formed in less then 10 s at room temperature. The gels were repeatedly washed in 0.05 M EDTA solution for copper removal and then equilibrated in distilled water. The hydrogels are referred to as HAStil (4,4'-diazido-stilbenedisulfonic acid as crosslinker), HAOct (1,8-diazidooctane crosslinker), and HAPEG (PEGdiazide crosslinker).

9.10 TNBS assay procedure

The amount of lysine groups modified on the gelatin backbone was determined by a spectrophotometric method using TNBS as previously described.[46] 11 mg of solid sample were placed in a 50 mL centrifuge tube, followed by addition of 1 mL of 4% $NaHCO_3$ (pH 8.5) and 1 mL of 0.5 % TNBS. The reaction mixture was heated at 40 °C for 4 hours with mild shaking. Then HCl (6M, 3 mL) was added and the mixture was heated at 110 °C for 1 h to hydrolyze and dissolve any insoluble material. The samples were cooled down at room temperature and diluted with 5 mL of water. The hydrolysate dilution was extracted with 20 mL (3x) of anhydrous ethyl ether to remove excess of unreacted TNBS. A 5 mL aliquot of the aqueous phase was removed and heated for 20 min in a hot water bath to evaporate residual ether. The aliquot was diluted with 15 mL of water and the absorbance measured at 346 nm.

All samples were read against a blank, prepared by the same procedure as the samples. However the HCl was added before the addition of TNBS to avoid any

reaction of TNBS with the protein. The amino content was determined by eq 4.1 p. 31.

9.11 Swelling tests

The swelling behavior of gelatin hydrogels was investigated in PBS buffer. Hydrogels disks (1.4 cm) were immersed in 5 mL of buffer at 37 °C, under mild shaking. After 24 h the swollen hydrogels disks were removed from the solutions and gel surfaces were quickly blotted on a filter paper. The equilibrium mass swelling ratio, H, was determined using eq. 4.1 p. 40.

9.12 Wide-angle X-ray Scattering

WAXS measurements were carried out using the X–ray diffractometer Bruker D8 Discover with a two dimensional detector (HIStar) operating in 1024 *1024 pixel mode. The X–ray generator was operated at a voltage of 40kV and a current of 20mA. A copper anode and a graphite monochromator produced Cu Kα radiation with a wavelength (λ) of 0.154 nm. WAXS images were collected from gelatin films in transmission geometry with a collimator-opening of 0.8 mm at a sample-to-detector distance of 15 cm. The exposure time employed was 900s. Integration of the two-dimensional scattering data gave the intensity as a function of the scattering angle 2θ.

9.13 Mechanical Tests

The mechanical properties of gelatin hydrogels were quantified using a mechanical tester (Zwick Z2.5, Zwick GmbH, Germany) equipped with a 200 N cell load in tension mode at 25 °C. Swollen samples were tested with 0.02 N pre-force and 5 mm min^{-1} crosshead speed, until break. Tensile moduli were subsequently calculated from the linear region (around 4-8% strain) of the stress-strain plot.

Rheological behavior was investigated with a stress controlled rheometer MARS (Thermo Haake, Germany) in parallel plate-plate geometry (20 mm), equipped with a solvent trap to minimize solvent evaporation. Preliminary stress-sweep experiments were carried out to determine the linear viscoelastic range. All experiments were performed in oscillation mode at 3 Hz by applying a constant stress of 3 Pa in a frequency range from 0.1-100 Hz. The temperature was kept constant at 37 °C in all experiments except in the temperature sweep where the temperature was varied from 0 to 50 °C for gelatin solutions.

Hydrogel mechanical properties were determined also by microindentation using a micro-force measurements device (Basalt-BT01, Tetra GmbH, Germany). Microindentation tests were performed only for hyaluronic acid-based hydrogels. In microindentation, the recorded force-distance curves were used to calculate the elasticity modulus of the hydrogels and to estimate the adhesion force (retracting process) by using the Johnson-Kendall-Roberts (JKR) model, which considers the surface attraction between two solids. For all hydrogels, elastic moduli were determined from the unloading part of the curve to consider only the elastic behavior and not the plastic deformation of the sample.

9.14 Temperature modulated DSC (TMDSC)

The thermal properties of gelatin films were measured using a Phönix DSC 204 F1 (Netzsch) apparatus. Dry gelatin-network samples were sealed in a hermetic pan during TM-DSC measurements. Two consecutive heating runs from -20 to 150 °C in the first heating run and up to 250 °C in the second heating run were performed with a modulated heating rate with a period of 60 s, amplitude of 0.5 °C, and a heating rate of 5 °C· min^{-1}. Between heating runs, the samples were quickly cooled at a rate of 10 °C· min^{-1}. The melting temperature (T_m) was measured during the first heating, while the glass transition temperature (T_g) was determined during the second heating run.

9.15 Imaging with confocal laser scanning microscope (CLSM)

Gelatin hydrogels labeled with alkyne- and azido-functionalized fluorescein were characterized by using a confocal laser scanning microscope (CLSM 510, Carl Zeiss). The hydrogels were placed between two glass slides excited by using 488 nm laser and imaged in the green channel.

Fluorescence spectroscopy data were acquired on a Varian Cary Fluorescence spectrophotometer. The hydrogels were degraded in an alkaline solution (pH 14) at 50 °C. The solutions were adjusted to pH 10 and the fluorescence was measured. A calibration curve was determined from the measurements of known concentrations of

fluorescein dye and used to quantitatively determine the amount of dye bound to the hydrogels.

9.16 Sodium dodecyl sulfate-poly acrylamide gel electrophoresis (SDS-PAGE)

The molecular weight distribution was determined by SDS-PAGE on 4-20% Ready Gels (Bio-Rad Laboratories) in a Mini-Protean system (Bio-Rad). A pre-stained SDS-PAGE standard was used for the determination of molecular weight. Samples of gelatin were dissolved in distilled water at 40 °C for 30 min at a concentration of 2 mg/mL. All samples were diluted 1:1 with a 2x sample buffer, then heated to 90 °C for 5 min and cooled down. 15 µL of each sample were loaded onto their respective lane in the gel and a current of 120 V was applied for approximately 45 min. Protein bands were visualized after a 60 min staining (0.1 wt.-% Comassie Blue, 10 Vol-% acetic acid and 40 Vol.-% methanol in water) and 60 min treatment in a destaining solution (10 Vol.-% glacial acetic acid, 20 Vol.-% methanol in water). The molecular weight of the gelatin fragments was approximated by measuring the relative mobility of the standard protein molecular weight markers.

9.17 Gel Permeation Chromatography

The molecular weight analysis of gelatin fragments was carried out by multi-detector gel permeation chromatography equipped with a light scattering detector (RALS), differential viscosimetry detector and a refractive index detector. Gelatin solutions were loaded into the column at a concentration of 1.5 mg/mL. The analyses were carried out using two columns (A6000 and A7000, 300 mm x 7.8 ID) connected in series with an A7 guard column, and eluting with aqueous sodium nitrate solution (0.1 M) at a flow rate of 0.7 mL/min. The light scattering detector was calibrated using a dextran standard. The molecular weight of the sample was directly determined with the light scattering detector.

9.18 Determination of copper content

Determination of copper content was performed by inductively coupled plasma-mass spectrometry (ICP-MS). 20-40 mg of the sample was weighed into pre-cleaned PE tubes and 5 mL HNO_3 (65%, suprapur) were added to yield total hydrolysis of the gels (72 h) giving clear or slightly yellow solutions. After dilution with ultrapure water the samples were analysed with collision cell ICP-MS using an external calibration for the Cu determination.

9.19 Cytotoxicity tests

Cytotoxicity tests of hyaluronic acid hydrogel (HAStil, HAOct and HAPEG) eluates were performed. The swollen hydrogel samples were sterilized by steam sterilization. The sterile samples were equilibrated with cell culture medium for three days and the

eluates of the three different hydrogel types were applied to L929 cells. Lactate dehydrogenase concentration and mitochondrial dehydrogenase activitiy were determined. No cytotoxic effect was detected for the HAStil gel (1:1 ratio). Cell incubation with eluates from HAOct and HAPEG gave cytotoxic effects.

.

10. References

[1] A. Lendlein, A. M. Schmidt, R. Langer, *Proceeding of the National Academy of Sciences* **2001**, *98*, 842-847.

[2] A. Göpferich, *Biomaterials* **1996**, *17*, 103-114.

[3] A. T. Neffe, G. Tronci, A. Alteheld and A. Lendlein, *Macromolecular Chemistry and Physics* **2010**, *211*, 182-194.

[4] L. S. Nair, C. Laurencin, *Progress in Polymer Science* **2007**, *32*, 762-798.

[5] Y. Madrid, L. Langer, H. Brem, R. Langer, *Advances in Pharmacology* **1991**, *22*, 299-324.

[6] F. von Burkersroda, L. Schedl, A. Göpferich, *Biomaterials* **2002**, *23*, 4221-4231.

[7] B. D. Ratner, A. S. Hoffman, F. J. Schoen, J. E. Lemons, Biomaterials Science, 2nd Edition, Elsevier Academic Press 2004.

[8] A. Göpferich, R. Langer, *Macromolecules* **1993**, *26*, 4105-4112.

[9] A. K. Burkoth, J. Burdick, K.S. Anseth, *Journal of Biomedical Materials Research* **2000**, *51*, 352-359.

[10] L. S. Nair, C. Laurencin, *Progress in Polymer Science* **2007**, *32*, 762-798.

[11] A. Sisson, M. Schroeter, A. Lendlein, Polyesters, in: Handbook of Biodegradable polymers, Edited by A. Lendlein and A. Sisson, Wiley-VCH, 2010.

[12] A. Lendlein, P. Neuenschwander, U. W. Suter, *Macromolecular Chemistry and Physics* **2000**, *201*, 1067-1076.

[13] J. Kopeček, *Biomaterials* **2007**, *28*, 5185-5192.

[14] N. A. Peppas, J. Z. Hilt, A. Khademhosseini, R. Langer, *Advanced Materials* **2006**, *18*, 1345-1360.

[15] D. A. Evans, A. E. Weber, *Journal of the American Chemical Society* **1987**, *109*, 7151-7157.

[16] G. Tronci, A. T. Neffe, B. F. Pierce and A. Lendlein, *Journal of Materials Chemistry* **2010**, *20*, 8875-8884.

[17] B. V. Slaughter, S. S. Khurshid, O. Z. Fisher, A. Khademhosseini, N. A. Peppas, *Advanced Materials* **2009**, *21*, 3307-3329.

[18] N. A. Peppas, J. Z. Hilt, A. Khademhosseini, R. Langer, *Advanced Materials* **2006**, *18*, 1345-1360.

[19] K. S. Anseth, A. T. Matters, S. J. Bryant, P. J. Martens, J. H. Elisseff, C. N. Bowman, *Journal of Controlled Release* **2002**, *78*, 199-209.

[20] A. Sawhney, C. Pathak, J. Hubbell, *Macromolecules* **1993**, *26*, 581-587.

[21] J. F. Mano, G. A. Silva, H. S. Azevedo, P. B. Malafaya, R. A. Sousa. SS. Silva, L.F. Boesel, J. M. Oliveira, T. C. Santos, A. P. Marques, N. M. Neves, R. L. Reis, *Journal of Royal Society Interface* **2007**, *4*, 999-1030.

[22] B. Alberts, A. Johnson, J. Lewis et al., Molecular Biology of the Cell 4th edition, New York: Garland Science, 2002.

[23] M. P. Lutolf, F. E. Weber, H. G. Schmoekel, J. C. Schense, T. Kohler, R. Müller, J.A. Hubell, *Nature Biotechnology* **2003**, *21*, 513-518.

[24] W. Friess, *European Journal of Pharmaceutics and Biopharmaceutics* **1998**, *45*, 113-136.

[25] J. L. Gornall, E.M. Terentjev, *Soft Matter* **2008**, *4*, 544-549.

[26] K. Reiser, R. J. McCormick, R. B. Rucker, *Journal of the Federation of American Societies for Experimental Biology* **1992**, *6*, 2439-2449.

[27] S. Young, M. Wong, Y. Tabata, A. G. Mikos, *Journal of Controlled Release* **2005**, *109*, 256-274.

[28] A. G. Ward, A. Courts, *The Science and Technology of Gelatin*, London, Academic Press,

London, 1977.

[29] A. K. Lynn, I. V. Yannas, W. Bonfield, *Journal of Biomedical Materials Research Part B Applied Biomaterial* **2004**, *71*, 343-354.

[30] S. T. Khew, Q. J. Yang and Y. W. Tong, *Biomaterials* **2008**, *29*, 3034-3045.

[31] S. Z. Yow, C. H. Quek, E. K. F. Yim, C. T. Lim, K. W. Leong, *Biomaterials* **2009**, *30*, 1133-1142.

[32] Y. Liu, M. B. Chan-Park, *Biomaterials* **2009**, *30*, 196-207.

[33] C. L. Tseng, S. Y. H. Wu, W. H. Wang, C. L. Peng, F. H. Lin, C. C. Lin, T. H. Young, M. J. Shieh, *Biomaterials* **2008**, ***29***, 3014-3022.

[34] Y. Tabata, Y. Ikada, *Advanced Drug Delivery Reviews* **1998**, *31*, 287-301

[35] Cell biology of extracellular matrix, second edition edited by Elizabeth D. Hay, Springer 1991, pp 14.

[36] M. J. Zohuriaan-Mehr, A. Pourjavadi, H. Salimi and M. Kurdtabar, *Polymers for Advanced Technologies* **2009**, *20*, 655-671.

[37] A. Bigi, S. Panzavolta, K. Rubini, *Biomaterials* **2004**, *25*, 5675-5680.

[38] Y. Otani, Y. Tabata, Y. Ikada, *Biomaterials* **1998**, *19*, 2091-2098.

[39] A.J. Kuijpers, G. H. M. Engbers, J. Fejen, *Macromolecules* **1999**, *32*, 3325-3333.

[40] I. Pezron, M. Djabourov, L. Bosio, J. Leblond, *Journal of Polymer Science Part B: Polymer Physics* **1990**, *28*, 1823-1839.

[41] I. Pezron, T. Herning, M. Djabourov, J. Leblond. In: W.E. Burchard, S. B. Ross-Murphy, editors. Physical Networks. Amsterdam: Elsevier; 1990, p. 231.

[42] M. Djabourov, N. Bonnet, H. Kaplan, N. Favard, P. Favard, *Journal de Physique II* **1993**, *3*, 611-624.

[43] H. Bohidar, S. J. Sidharta, *Journal of Chemical Physics* **1993**, *98*, 8970-8977.

[44] L. Guo, R. H. Colby, C. P. Lusignan, T. H. Witesides, *Macromolecules* **2003**, *36*, 9999-10008.

[45] S. Piluso, B. Hiebl, S. N. Gorb, A. Kovalev, A. Lendelin, A. T. Neffe, *International Journal of Artificial Organs*, **2011**, *34*, 192-197.

[46] J. A. Burdick, G. D. Prestwich, *Advanced Materials* **2011**, *23*, H41-H46.

[47] A. Borzacchiello, L. Ambrosio, *Journal of Biomaterial Science Polymer Edition* **2001**, *12*, 307-316.

[48] D. A. Gibbs, E. W. Merrill, K. A. Smith, E. A. Balazs, *Biopolymers* **1968**, *6*, 777-791.

[49] S. J. Falcone, D.M. Palmeri, R. A. Berg, *Journal of Biomedical Materials Research Part A* **2006**, *76*, 721-728.

[50] G. Kogan, L. Šoltés, R. Stern, P. Gemeneir, *Biotechnology Letters* **2007**, *29*, 17-25.

[51] A. Jayakrishnan, S. R. Jameela, *Biomaterials* **1996**, *17*, 471-484.

[52] A. Bigi, G. Cojazzi, S. Panzavolta, K. Rubini and N. Roveri, *Biomaterials* **2001**, *22*, 763-768.

[53] A. Bigi, B. Bracci, G. Cojazzi, S. Panzavolta and N. Roveri, *Biomaterials* **1998**, *19*, 2335-2340.

[54] Y. Marois, N. Chakfé, X. Deng, M. Marois, T. How, M. W. King, R. Guidoin, *Biomaterials* **1995**, *16*, 1131-1139.

[55] M. Bertoldo, S. Bronco, T. Gragnoli and F. Ciardelli, WILEY-VCH Verlag, 2007, pp. 328-338.

[56] H. Petite, I. Rault, A. Huc, P. Menasche and D. Herbage, John Wiley & Sons, Inc., 1990, pp. 179-187.

[57] H. W. Sung, H. L. Hsu, C. C. Shih, D. S. Lin, *Biomaterials* **1996**, *17*, 1405-1410.

[58] T. Abete, E. Del Gado, D. Hellio Serughetti, L. de Arcangelis, M. Djabourov, A. Coniglio, *Journal of Chemical Physics* **2006**, *125*, 174903.

[59] M. T. Nickerson, J. Patel, D. V. Heyd, D. Rousseau and A. T. Paulson, *International Journal of Biological Macromolecules* **2006**, *39*, 298-302.

[60] A. Abbasi, M. Eslamian and D. Rousseau, *Drug Delivery* **2008**, *15*, 455-463.

[61] M. K. McDermott, T. Chen, C. M. Williams, K. M. Markley and G. F. Payne, *Biomacromolecules* **2004**, *5*, 1270-1279.

[62] T. Chen, D. A. Small, M. K. McDermott, W. E. Bentley and G. F. Payne, *Biomacromolecules* **2003**, *4*, 1558-1563.

[63] V. Crescenzi, A. Francescangeli and A. Taglienti, *Biomacromolecules* **2002**, *3*, 1384-1391.

[64] J. Yeom, S. H. Bhang, B. S. Kim, M. S. Seo, E. J. Hwang, I. J. Hwang, I. H. Cho, J. K. Park, S. K. Hahn, *Bioconjugate Chemistry* **2010**, *21*, 240-247.

[65] K. Tomihata, Y. Ikada, *Journal of Polymer Science Part A: Polymer chemistry* **1997**, *35*, 3553-3559.

[66] S. K. Masters, D. N. Shah, L. A. Leinwand, K. S. Anseth, *Biomaterials* **2005**, *26*, 2517-2525.

[67] A. Ramamurthy, I. Vesely, *Journal of Biomedical Materials Research* 2002, 60, 195-205.

[68] C. M. Nimmo, S. C. Owen, M. S. Shoichet *Biomacromolecules* **2011**, *12*, 824-830.

[69] P. L. Golas, K. Matyjaszewski, *Chemical Society Reviews* **2010**, *39*, 1338-1354.

[70] V. V. Rostovtsev, L. G. Green, V. V. Fokin, K. B. Sharpless, *Angewandte Chemie International Edition* **2002**, *41*, 2596-2599.

[71] H. Durmaz, A. Dag, O. Altintas, T. Erdogan, G. Hizal, U. Tunca, *Macromolecules* **2007**, *40*, 191-198.

[72] C. R. Becer, R. Hoogenboom, U. S. Schubert, *Angewandte Chemie International Edition* **2009**, *48*, 4900-4908.

[73] N. V. Tsarevsky, K. V. Bernaerts, B. Dufour, F. E. Du Prez and K. Matyjaszewski, *Macromolecules* **2004**, *37*, 9308-9313.

[74] R. Huisgen, *Angewandte Chemie International Edition* in *English* **1963**, *2*, 565-598; R. Huisgen, *Angewandte Chemie* **1963**, *2*, 604-637.

[75] J.F. Lutz, *Angewandte Chemie International Edition* **2008**, *47*, 2182-2184.

[76] G. C. Tron, T. Pirali, R. A. Billington, P. L. Canonico, G. Sorba, A. A. Genazzani, *Medicinal Reserch Review* **2008**, *28*, 278-308.

[77] F. Himo, T. Lovell, R. Hilgraf, V. V. Rostovtsev, L. Noodleman, K. B. Sharpless, V. V. Fokin, *Journal of the American Chemical Society* **2005**, *127*, 210-216.

[78] V. D. Bock, H. Hiemstra, J. H. van Maarseveen, *European Journal of Organic Chemistry* **2006**, 51-68.

[79] P. L. Golas, N. V. Tsarevsky, B.S. Sumerlin, K. Matyjaszewski, *Macromolecules* **2006**, *39*, 6451-6457.

[80] J. W. Lee, J. H. Kim, W. S. Shin, S. H. Jin, *Tetrahedron* **2006**, *62*, 894-900.

[81] P. Wu, M. Malkoch, J. N. Hunt, R. Vestberg, E. Kaltgrad, M. G. Finn, V. V. Fokin, K. B. Sharpless, C. J. Hawker, *Chemical Communications* **2005**, 5775-5777.

[82] B. Helmes, J. L. Mynar, C. J. Hawker, J. M. J. Frenchet, *Journal of the American Chemical Society* **2004**, *126*, 15020-15021.

[83] P. Lecomte, R. Riva, C. Jerome, R. Jerome, *Macromolecular Rapid Commununications* **2008**, *29*, 982-997.

[84] P. L. Golas, N. V. Tsarevsky, B.S. Sumerlin, K. Matyjaszewski, *Macromolecules* **2006**, *39*, 6451-6457.

[85] D. J. V. C. Van Steenis, O. R. P. David, G. P. F. Van Strijdonck, J. H. Van Maaeseveen, J. N. H. Reek, *Chemical Communications* **2005**, 4333-4335.

[86] G. Lu, S. Lam, K. Burgess, *Chemical Communications* **2006**, 1652-1654.

[87] Q. Liu, P. Zhao, Y. Chen, *Journal of Polymer Science* **2007**, *45*, 3330-3341.

[88] T. D. Hirt, P. Neuenschwander, U. W. Suter, *Macromolecular Chemistry and Physics* **1996**,

197, 1609-1614.

[89] S. Kelch, N. Y. Choi, Z. Wang, A. Lendlein, *Advanced Engineering Materials* **2008**, *10*, 494-502.

[90] M. S. Reeve, S. P. McCarthy, R. A. Gross, *Macromolecules* **1993**, *26*, 888-894.

[91] C. Lauzier, J. F. Revol, E. M. Debzi, R. H. Marchessault, *Polymer* **1994**, *35*, 4156-4162.

[92] Y. Doi, Y. Kanesawa, M. Kunioka, T. Saito, *Macromolecules* **1990**, *23*, 26-31.

[93] K. Okuyama, H. Narita, T. Kawaguchi, K. Noguchi, Y. Tanaka, N. Nishino, *Biopolymers* **2007**, *86*, 212-221.

[94] D. Hofmann, M. Entrialgo-Castaño, K. Kratz, A. Lendlein, *Advanced Materials* **2009**, *21*, 3237-3245.

[95] P. Bornstein, *Biochemical and Biophysical Research Communications* **1969**, *36*, 957.

[96] W. T. Butler, *J. Biol Chem.* **1969**, *244*, 3415.

[97] S. Van Vlierberghe, P. Dubruel, E. Schacht, *Biomacromolecules* **2011**, *12*, 1387-1408.

[98] K. M. Gattas-Asfura, E. Weisman, F. M. Andreopoulos, M. Micic, B. Muller, S. Sirpal, S. M. Pham, R. M. Leblanc, *Biomacromolecules* **2005**, *6*, 1503-1509.

[99] W. A. Bubnis and C. M. Ofner, *Analytical Biochemistry* 1992, **207**, 129-133.

[100] M. A. Viswamitra, R. Radhakrishnan, J. Bandekar, G. R. Desiraju, *Journal of the American Chemical Society* **1993**, *115*, 4868-4869.

[101] E. Galoppini, R. Gilardi, *Chemical Communications* **1999**, 173-174.

[102] I. Pezron, M. Djabourov, L. Bosio and J. Leblond, *Journal of Polymer Science Part B: Polymer Physics* **1990**, *28*, 1823-1839.

[103] J. Crespo, M. A. Satorre and J. A. Quintana, *Journal of Material Science* **1995**, *30*, 6145-6150.

[104] K. Kacprzak, *SYNLETT*, **2005**, *6*, 943-946.

[105] E. F. V. Scriven, K. Turnbull, *Chemical Review* **1988**, *88*, 297-368.

[106] F. D. Marsh, *Journal of Organic Chemistry* **1972**, *37*, 2966-2969.

[107] D. A. Evans, A. E. Weber, *Journal of the American Chemical Society* **1987**, *109*, 7151-7157.

[108] A. K. Feldman, B. Colasson, V. V. Fokin, *Organic Letters* **2004**, *6*, 3897-3899.

[109] M. Catalina, G. E. Attenburrow, J. Cot, A. D. Covington and A. P. M. Antunes, *Journal of Applied Polymer Science*, **2011**, *119*, 2105.

[110] C. Joly-Duhamel, D. Hellio and M. Djabourov, *Langmuir* **2002**, *18*, 7208-7217.

[111] S. b. Giraudier, D. Hellio, M. Djabourov and V. r. Larreta-Garde, *Biomacromolecules* **2004**, *5*, 1662-1666.

[112] D. Hellio-Serughetti and M. Djabourov, *Langmuir* **2006**, *22*, 8516-8522.

[113] M. Itoh, Y. Okawa, H. Kobayashi, T. Ohno, Y. Okamoto, T. Katoh, *Journal of Photographic Science* **1994**, *42*, 14-

[114] K. Watanabe, J. Nakagawa, T. Ebihara and Y. Okamoto, *Polymer* **1996**, *37*, 1285-1288.

[115] N. A. Peppas, J. Z. Hilt, A. Khademhosseini, R. Langer, *Advanced Materials* **2006**, *18*, 1345-1360.

[116]J. Y. Lai, P. L. Lu, K. H. Chan, Y. Tabata, G. H. Hsiue, *Biomacromolecules* **2006**, *7*, 1836-

[117] M. P. Lutolf, J. A. Hubbell, *Biomacromolecules*, **2003**, *4*, 713-722.

[118] R. D. Patil, J. E. Mark, A. Apostolov, E. Vassileva, S. Fakirov, *European Polymer Journal* **2000**, *36*, 1055-1061.

[119] H. A. Khonakdar, S. H. Jafari, H. Hassler, *Journal of Applied Polymer Science* **2007**, *104*, 1654.

[120] F. D. Marsh, *Journal of Organic Chemistry* **1972**, *37*, 2966-2969.

[121] M. Taki, M. Shiota and K. Taira, *Protein Engineering Design and Selection* **2004**, *17*, 119-126.

[122] R. K. O'Reilly, M. J. Joralemon, K. L. Wooley and C. J. Hawker, *Chemistry of Materials* **2005**, *17*, 5976-5988.

[123] C. Munkholm, D. R. Parkinson, D. R. Walt, *Journal of the American Chemical Society* **1990**, *112*, 2608-2612.

[124] N. Le Baut, D.D. Diaz, S. Punna, M.G. Finn, H. R. Brown, *Polymer* **2007**, *48*, 239-244.

[125] S. Gorb, Y. Jiao, M. Scherge, *Journal of Comparative Physiology A* **2000**, *186*, 821-831.

[126] K. Johnson, K. Kendall, A. D. Roberts, *Proceedings of the Royal Society of London A* **1971**, *324*, 301-313.

[127] J. Solon, I. Levental, K. Sengputa, P. C. Georges, P. A. Jamney, *Biophysical Journal* **2007**, *93*, 4453-4461.

[128] A. T. Metters, K.S. Anseth, C. N. Bowman, *Polymer* **2000**, *41*, 3993-4004.

[129] A. Lendlein, J. Zotzmann, Y. Feng, A. Alteheld, S. Kelch, *Biomacromolecules* **2009**, *10*, 975-982.

[130] A. Lendlein, M. Colussi, P. Neuenschwander, U. W. Suter, *Macromolecular Chemistry and Physics* **2001**, *202*, 2702-2711.

[131] G. B. Fields, *Journal of Theoretical Biology* **1991**, *153*, 585-602.

[132] K. N. Riley, I. M. Herman, *Journal of Burns and Wounds* **2005**, 4, e8.

[133] Seifter, S. and Harper,E.; The Collagenases in: The Enzymes Bd. III, 1971,649.

[134] K. Ulbricht, J. Strohalm, J. Kopeček, *Biomaterials* **1982**, *3*,150-154.

[135] Yu Cheng, R. K. Prud'homme, *Biomacromolecules* **2000**, *1*, 782-788.

[136] O. O. Blumenfeld, M. Rojkind, P. M. Gallop, *Biochemistry* **1965**, *4*, 1780-1788.

[137] P. Bornstein, *Biochemistry* **1970**, *9*, 2408-2421.

[138]W. T. Butler, *Journal of Biological Chemistry* **1969**, *244*, 3415-3417.

[139] P. Bornstein, G. Balian, *Methods in Enzymology* **1977**, *47*, 132-145.

[140] S. Piluso, T. Weigel, A. Lendlein, A. T. Neffe, *Macromolecular Simposia*, accepted on 06.09.2011, DOI: 10.1002/masy.201100054.

[141] S. S. Choi, J. M. Regenstein, *Journal of Food Science* **2000**, *65*, 194-199.

[142] J. Crespo, M. A. Satorre, J. A. Quintana, F. Ania, *Journal of Material Science* **1995**, *30*, 6145-6150.

[143] J. M. Baskin, J. A. Prescher, S. T. Laughlin, N. J. Agard, P. V. Chang, I. A. Miller, A. Lo, J. A. Codelli and C. R. Bertozzi, *Proceedings of the National Academy of Sciences* **2007**, *104*, 16793-16797.

[144] P. V. Chang, J. A. Prescher, E. M. Sletten, J. M. Baskin, I. A. Miller, N. J. Agard, A. Lo and C. R. Bertozzi, *Proceedings of the National Academy of Sciences* **2010**, *107*, 1821-1826.

[145] S. T. Laughlin, J. M. Baskin, S. L. Amacher and C. R. Bertozzi, *Science* **2008**, *320*, 664-667.

[146] G. Wittig, A. Krebs, *Chemische Berichte* **1961**, *94*, 3260-3275.

[147] N. J. Agard, J. A. Prescher, C. R. Bertozzi, *Journal of the American Chemical Society* **2004**, *126*, 15046-15047.

[148] J. A. Codelli, J. M. Baskin, N. J. Agard, C.R. Bertozzi, *Journal of the American Chemical Society* **2008**, *130*, 11486-11493.

[149] E. M. Sletten, C.R. Bertozzi, *Organic Letters* **2008**, *10*, 3097-3099.